Synthesis and Evaluation of Tri-cyclic Alkaloid-like Compounds as Anticancer Agents

Xixi Xu

Supervisor: Assoc. Prof. Alison T. Ung

Co-supervisor: Dr. Tristan Rawling

School of Mathematical and Physical Sciences

April 2018

Xi Xi Xu

Declaration / Certificate of authorship and originality

I certify that the work in this thesis has not previously been submitted for a degree nor has it been submitted as part of the requirements for a degree except as fully acknowledged within the text.

I also certify that the thesis has been written by me. Any help that I have received in my research work and the preparation of the thesis itself has been acknowledged. In addition, I certify that all the information sources and literature used are indicated in the thesis.

Production Note:
Signature removed
prior to publication.

Xixi Xu

April 2018

Dedication

I dedicate this thesis to my late beautiful Aunty, Wendy Xu, who was battling cancer. Her resilience and courage to fight this disease has set new standards for me and she continues to inspire me every day. Every day I go into the laboratory hoping that one day we can eradicate this disease.

Acknowledgements

It is my pleasure to thank the following people for their contribution and hard work in this thesis. Without their efforts this work would never have been completed. I would like to express my gratitude to my supervisor Assoc. Prof. Alison Ung, thank you for all your help and guidance on this project. To my co-supervisor Dr. Tristan Rawling, thank you for dedicating your time to this project, especially for the biological discussions. Thanks Tristan, and keep rocking that cauliflower shirt!

My sincere thanks go to our level 5 laboratory manager Dr. Ronald Shimmon, scientific officer Verena Taudte, Dr. Linda Xiao, and technical support officer Alexander Angeloski. Nothing has been too much trouble for you guys; you guys were always there helping with NMR, GC/MS, and other technical issues. For that, I am always grateful for your time.

To my family, thank you mum and dad, my two little cousins Caesar and Louis, and my eternal cheerleaders Aunty Wendy and Grandma Lucy. Thank you all for the emotional and financial support throughout my studies, you guys make it possible for me to do what I do. I love you all!

With a special mention to my two office buddies big Matt (aka Doctor in training), and Dr. Steven Williams. We never did get that office puppy, and I will hold it against you guys forever!

I would like to thank my colleagues in the level 5 research labs, thank you, Curtis, for all your encouragement when it came coffee breaks, and little Matt, for eating dumplings with me all the time.

Moreover, last but not least, to the Ung's research group, especially Ariane, it has been a pleasure to work together over the past few years. The people I have worked with comprise the best memories of my studies.

TABLE OF CONTENTS

List of Figures

List of Schemes

List of Tables

List of Abbreviations

Å	Angstrom
δ	Delta (Chemical shift in parts per million)
μM	micro-molar
V_{max}	Maximum absorbance
$[\alpha]_D^T$	Specific rotation for a Na lamp at 589nm
$[M+H]^+$	Protonated molecular ion
$CDCl_3$	Deuterated chloroform
$CHCl_3$	Chloroform
br s	Broad singlet
d	Doublet
ºC	Degrees Celsius
Da	Dalton
DCM	Dichloromethane
dd	Doublet of doublets
ddd	Doublet of doublet of doublets
DMAD	Dimethyl acetylenedicarboxylate
DMEM	Dulbecco's modified eagle's medium
DMSO	Dimethyl sulfoxide
dq	Doublet of quartets
dt	Doublet of triplets
EDTA	Ethylenediaminetetra acetic acid
ER	Oestrogen receptor
EtOAc	Ethyl acetate
Equiv.	Equivalents

FTIR	Fourier transform infrared spectroscopy
g	gram
HER2	Human epidermal growth factor receptor 2
HSQC	Heteronuclear single quantum coherence
HRMS	High resolution mass spectrometry
Hz	Hertz
IC_{50}	The half maximal inhibitory concentration
J	Coupling constant (NMR)
MeOH	Methanol
m	Multiplet
mL	millilitre
mmol	milli mole
m.p	Melting point
MS	Mass spectrometry
$NaBH_4$	Sodium borohydride
$NaHCO_3$	Sodium hydrogen carbonate
NaOH	Sodium hydroxide
$Na(OAc)_3BH$	Sodium triacetoxyborohydride
^1H NMR	Proton nuclear magnetic resonance
^{13}C NMR	Carbon nuclear magnetic resonance
NOE	Nuclear overhauser effect
NOESY	Nuclear overhauser effect spectroscopy
PBS	Phosphate buffered saline
PI	Propidium iodide
ppm	Parts per million

PR	Progesterone receptor
PSA	Polar surface area
q	Quartet
R_f	Retention factor
RPMI	Roswell park memorial institute medium
r.t.	Room temperature
s	Singlet
t	Triplet
td	Triplet of doublet
TLC	Thin layer chromatography

Publications from this Thesis

X. Xu, T. Rawling, A. Roseblade, R. Bishop and A. T. Ung, Med. Chem. Commun.

Published on 25 October 2017.

Abstract

As part of our ongoing research for anticancer agents, the synthesis of a library of tricyclic compounds using the Bridging Ritter reaction has been described in Chapter 2. Tricyclic imines **82a-c** and amines (**90a-b, 91a-b**) were synthesised in good yields (> 70%). Eleven alkaloid-like compounds were successfully synthesised.

Encouraged by the synthetic success described in Chapter 2, preparation of tricyclic caryophyllene derived alkaloid-like compounds was undertaken to provide new leads as described in Chapter 3. The synthesis focused on the use of β-caryophyllene **96** and caryophyllene monoepoxide **117** as key starting materials in the Ritter reaction. Treating **96** and **117** with various nitriles under strong acidic conditions afforded optically active tricyclic amides of caryolane **119a-i** and clovane **120a-d** skeletons. The formation of these skeletons proceeded *via* the acid catalysed Wagner-Meerwein rearrangement. The rations of the two structures depended on the reactivity of the nitriles that led to the more kinetically stable of the two skeletons. Caryolane **119c** and clovane **120c** and **126c** were further used to generate complex alkaloid-like compounds through sequential amide cleavage and reductive alkylation. A total of 30 caryophyllene derived alkaloid-like compounds were successfully obtained and subjected to antiproliferative assays.

Chapter 4 describes the biological activities of the synthesised compounds described in Chapter 2 and 3. In-house *in vitro* biological assays were used to assess the cytotoxicities of the synthesised compounds on breast cancer cell lines MCF-7 (ER+) as well as MDA-MB-231 (triple negative). Compound **63** was selected by the US National Cancer Institute (NCI) for their standard cytotoxicity screening program. It was shown to have significant anti-cancer activities with IC_{50} in the μM range, across seven cancer types. The anti-cancer activities of **82c** were found to be selective towards the aggressive and more challenging to treat triple negative (MDA-MB-231) cell line while exhibiting no antiproliferative activities towards the

MCF-7 cells at the highest concentration tested (50 µM). The IC$_{50}$ of compound **82c** was determined to be 7.9 µM for the MDA-MB-231 cell line. Furthermore, **82c** arrested cell cycle at the G$_2$/M phase and induced apoptosis in a dose-dependent manner. Cytotoxicities of compounds **63** and **82c** were tested against noncancerous mammalian cells (Vero cell line) and found to be approximately eight folds more selective towards MDA-MB-231 than the Vero cell line.

From caryophyllene-derived compounds, eight compounds effectively decreased the proliferation and viability of MDA-MB-231, with observed IC$_{50}$ values ranging from $3.0 - 55.3$ µM. Amongst the eight, **119c**, **120c**, and **126a** were most active and selective towards the more aggressive triple negative (MDA-MB-231) over the MCF-7 cells. Furthermore, compounds **119c**, **120c**, and **126a** also altered the distribution of cells throughout the cell cycle, as well as the ability to induce apoptosis in the MDA-MB-231 cells. This observed selectivity towards the harder to treat triple negative breast cancer cells make these compounds more ideal drug candidates for further development.

Chapter 1   Introduction

1.1 Alkaloids

1.1.1 Natural alkaloids and alkaloid-like compounds

Alkaloids are a naturally occurring and structurally diverse group of compounds found in bacteria, fungi, plants and animals. The roles of these alkaloids were thought to be for self-preservation, inhibition of competitors, or communication between organisms.[1-2] They are also historically known for their medicinal benefits as well as their harmful effects as poisons in humans.[3] Alkaloids are categorised by their structural diversity according to the amino acids that give rise to both the nitrogen atom and the alkaloid skeleton. These organic nitrogenous bases can come in the form of primary (RNH_2), secondary (R_2NH), or tertiary amines (R_3N), as well as unsaturated and saturated heterocyclic ring systems.[4]

Isoquinoline **1**, Quinoline **2**, Imidazole **3**, Indole **4**, Indolizidine **5**, Piperidine **6**, and Pyridine **7** are examples of nitrogen-containing cyclic structures that are often found in natural alkaloids (Figure 1.1).
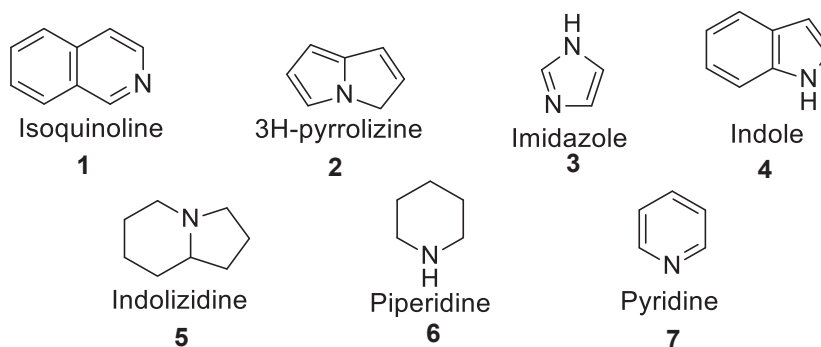
Figure 1.1: Core structures of heterocyclic alkaloid classes.

Archaeological and historical records show that natural alkaloids and the organisms they are derived from were used in medicine across Asia, Europe, and Africa as much as 4000 years

ago.[5-6] In the early 19th century Fredrich Sertürner successfully isolated and characterised morphine **8**. Further discoveries and isolations of other alkaloids such as xanthine **9**, strychnine **10**, atropine **11**, quinine **12**, and caffeine **13** marked a breakthrough in the process of drug discovery (Figure 1.2).[7-8]
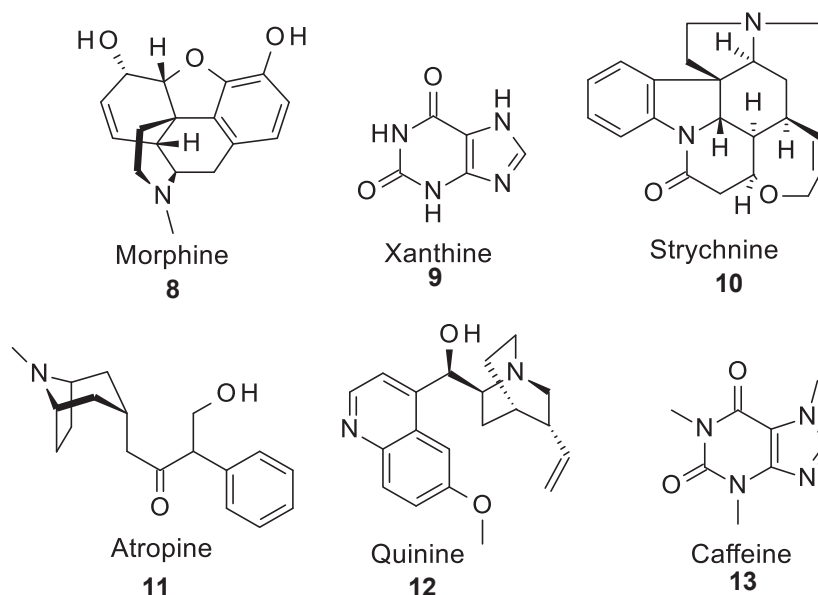
Figure 1.2: Representative structures of alkaloids isolated in the early 19th century.

According to the Dictionary of Natural Products (DNP), there are now over 27,000 alkaloids, and the Dictionary of Alkaloids lists 53 alkaloids currently being used pharmaceutically for a diverse range of applications including analgesia **14**, cancer treatment **15**, and Alzheimer's disease **16** (Figure 1.3).[9-10]
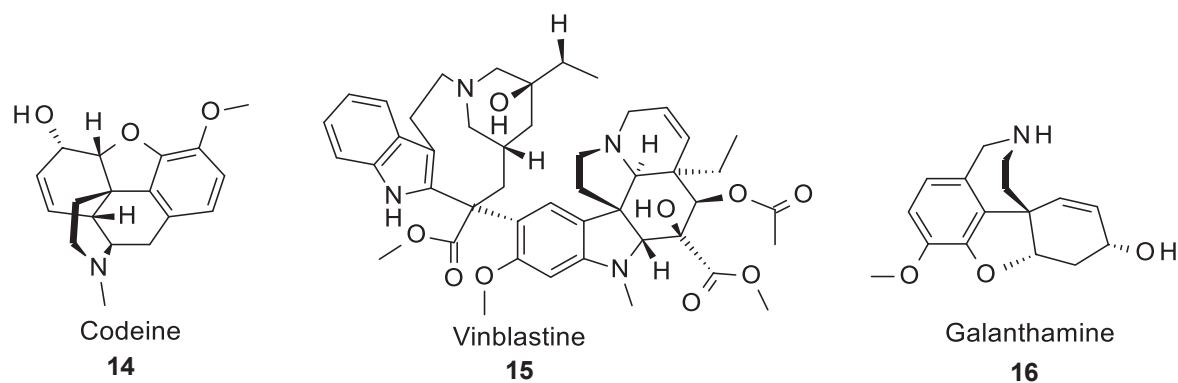
Figure 1.3: Representative of Codeine **14**, Vinblastine **15** and galanthamine **16**.

Throughout history, the discovery of natural alkaloids has played a significant role in drug development. The early 1980s saw a move towards more readily manipulated semisynthetic or synthetic compound libraries. Drug discovery has since been more focused on derivatisation of natural alkaloids, as well as the synthesis of natural-alkaloid-like compounds using well known natural product scaffolds.[11]

1.1.2 Alkaloid compounds targeting cancer

Natural alkaloids and the analogues derived from them are to date the most successful anti-cancer drugs on the market, and alkaloid derived drugs continue to play a major role in the discovery of new anti-cancer agents. Pharmaceutical companies have embraced many plant-derived anticancer compounds such as vinca alkaloids, epipodophyllotoxin lignans, *taxane* diterpenoids and camptothecin quinolone alkaloid derivatives.

1.1.2.1 Vinca alkaloids

Found in the Madagascar periwinkle *Catharanthus roseus* G. Don (Apocynaceae) (Figure 1.4), vinblastine **17** and vincristine **18** (Figure 1.5) have proven to be amongst the most valuable drugs used in clinical oncology for over 50 years and are on the World Health Organisation's

List of Essential Medicines. These alkaloids and their analogues bind to the tubulin and inhibit microtubule polymerisation, which leads to cell cycle arrest and apoptotic cell death in actively dividing cells.[12-14]
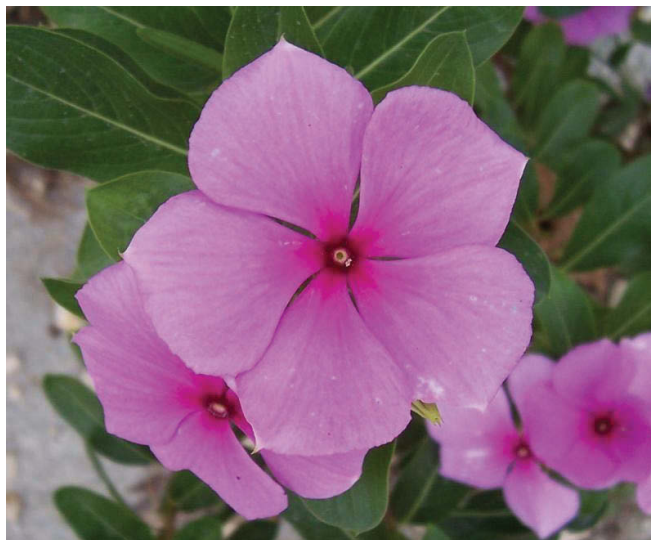
Figure 1.4: Madagascar periwinkle, *Catharanthus roseus* G. Don (Apocynaceae).

Since the discovery of vinblastine **17** and vincristine **18**, a series of alkaloid analogues including vindesine **19**, vinorelbine **20**, and vinflunine **21** have been developed and approved for human clinical trials (Figure 1.5).[15-19] Vindesine **19** was the first alkaloid analogue from the vinca family to enter human clinical trials. Its main use is for treatment of acute lymphocytic leukemia but is also used as a broad spectrum anti-cancer drug.[15]

In 1989, vinorelbine **20** was first approved in France for the treatment of non-small cell lung cancer, under the brand name Navelbine. It was later approved for the treatment of metastatic breast cancer in 1991and 1994, in France and the US, respectively.[17]

Vinflunine **21** has been shown to have broad *in vitro* and *in vivo* activities against a range of malignant cell lines and is currently in phase I/II trials evaluating its efficacy in advanced solid tumours.[20]

Vinblastine
17

Vincristine
18

Vindesine
19

Vinorelbine
20

Vinflunine
21
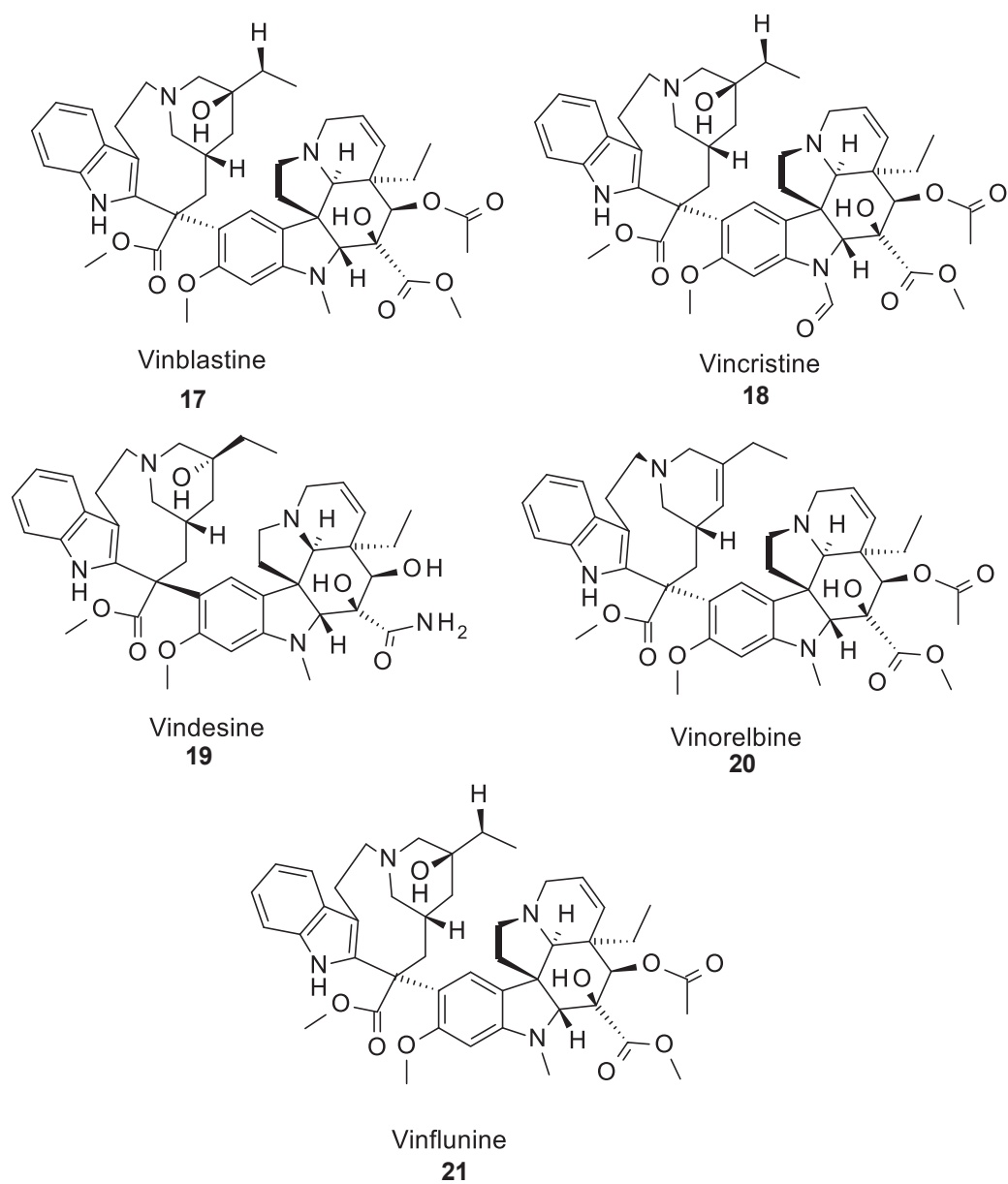
Figure 1.5: Vinca alkaloid series derived from *Catharanthus roseus*.

1.1.2.2 Taxol alkaloids

Paclitaxel **22** was found in the bark of the Pacific Yew; *Taxus brevifolia Nutt* (Taxacaesae) (Figure 1.6). It is a frontline chemotherapy drug in the treatment of ovarian and breast cancer and works by interfering with microtubule formation.[21]

Figure 1.6: *Taxus brevifolia* (Pacific yew).

Analogues such as docetaxel **23** and cabazitaxel **24** were developed in the late 1990's and early 2000's (Figure 1.7). Docetaxel **23** was the first to reach clinical trials showing an improved toxicity level to the parent compound. Cabazitaxel **24** was approved by the Food and Drug Administration (FDA) and launched into the market in 2010 for use in combination with prednisone for the treatment of prostate and hormone-refractory prostate cancers. However, the limitation of compounds **22** and **23** is their inability to diffuse across the blood-brain barrier.[22-23] Unlike other taxane analogues, cabazitaxel **24** was found to penetrate the blood-brain barrier and is thus used to treat brain cancer.[24]
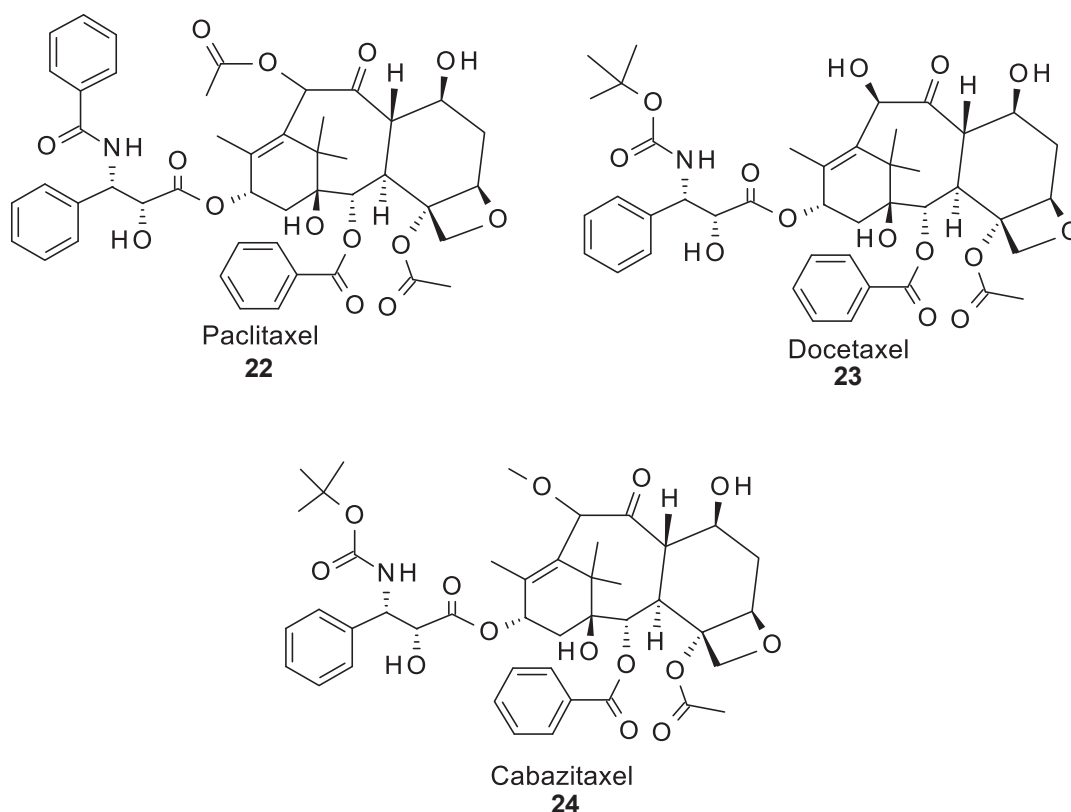
Figure 1.7: Representatives of three taxol alkaloids **22 – 24**.

With the intention of improving the tolerability of taxol alkaloids and reducing clinical resistance, medicinal chemists are focusing on developing new taxane formulations such as albumin, nanoparticles, emulsions, liposomes, or new analogues. Later developed compounds such as Abraxane, CT-2103, docosahexenoic acid and (DHA)-paclitaxel have all shown greater activity than paclitaxel with safer toxicological profiles.[25]

1.1.2.3 Camptothecin alkaloids

Camptothecin **25** (Figure 1.9) is an anticancer alkaloid derived from the bark of *Camptotheca acuminate* (Figure 1.8). Camptothecin is a quinoline alkaloid that exerts its anti-cancer activity by inhibiting the enzyme topoisomerase, resulting in DNA damage and cell death.[26] However, due to its toxicity and low solubility, camptothecin was withdrawn from a clinical trial. To

improve clinical performance, three promising analogues were developed; topotecan **26**, irinotecan **27**, and belotecan **28** (Figure 1.9). These analogues effectively inhibit topoisomerase-I and offer improved solubility and better pharmacokinetics for the treatment of ovarian and lung cancer.[27]

Figure 1.8: *Camptotheca acuminate*, United States Botanic Garden.

Figure 1.9: Representatives of alkaloid camptothecin and analogues.

1.1.2.4 Pyrrolizine alkaloids

Over 660 alkaloids, isolated from a range of plants and animals possess a similar structural moiety to pyrrolizine.[28-29] These alkaloids are known to cause hepatotoxicity and genotoxicity by the formation of pyrrolic metabolites that bind to DNA to form DNA-protein-cross-links.[30-31] Analogues of pyrrolizine possess unique biological and pharmacological activities and are therefore of great interest to the medicinal chemist.

Alkaloids **29 – 31** containing the pyrrolizine core structure were found to exhibit excellent anticancer activities (Figure 1.10). It was demonstrated that these pyrrollizines containing compounds (clazamycin A **30** and clazamycin B **31**) could cross-link the exocyclic amino groups of deoxyguanosine residues at the sequence 5'-d(CG) in duplex DNA.[30, 32]

Figure 1.10: Mitomycin C **29**, clazamycin A **30** and clazamycin B **31**.

In 2002 more compounds of pyrrolizine core structure **32 – 35** shown in Figure 1.11, were synthesised as anticancer compounds and were tested against the MCF-7 human breast cancer cell line, and cytotoxicity assessed against human KB cells. Out of all the compounds synthesised, **33** was found to be the most active with (IC_{50} =16 nM), while compound **35** was found to be the most toxic (IC_{50} = 70 nM).[33-34]
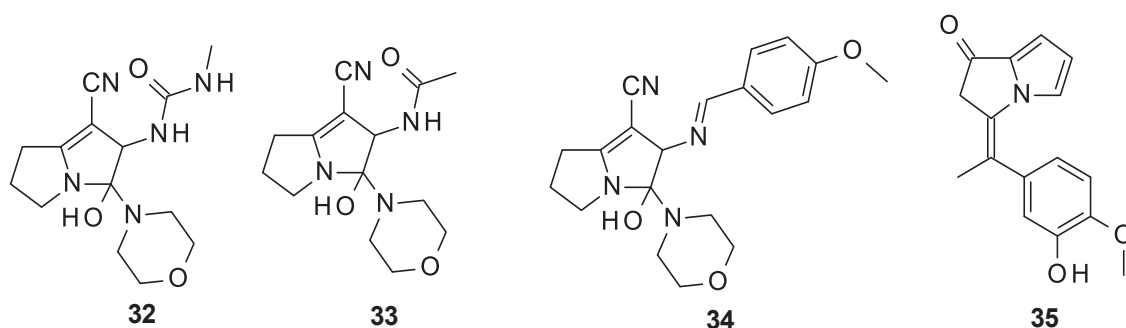
Figure 1.11: Analogues of pyrrolizine **32 – 35**.

The pyrrolizine containing licofelone **36** (Figure 1.12), which was first developed as an anti-inflammatory drug, shows promising antitumor activity towards prostate cancer cells as well as HCA-7 colon cancer cell line. Gust and co-workers developed novel derivatives (**37, 38a-f, 39** and **40**) of licofelone and reported their cytotoxicity against MCF-7 and MDA-MB-231 breast cancer cell lines (Figure 1.12). Licofelone **36** and compound **37** showed good activity

against MCF-7 cells, but poor activity against MDA-MB-231 cells. Compounds **38a-d** inhibited the growth of both cell lines with a similar potency to that of cisplatin, while compounds **38e-f** showed high selectivity for MCF-7 cells. Results from this study suggest that changing the substituent at C-5 of licofelone analogues can enhance efficacy and selectivity.[35]

38a) R = H
38b) R = OCOH
38c) R = OCOCH$_3$
38d) R = OCH$_2$CH$_3$
38e) R = OCO-*p*-C$_6$H$_4$Cl
38f) R = OCO-*m*-C$_6$H$_4$CH$_3$
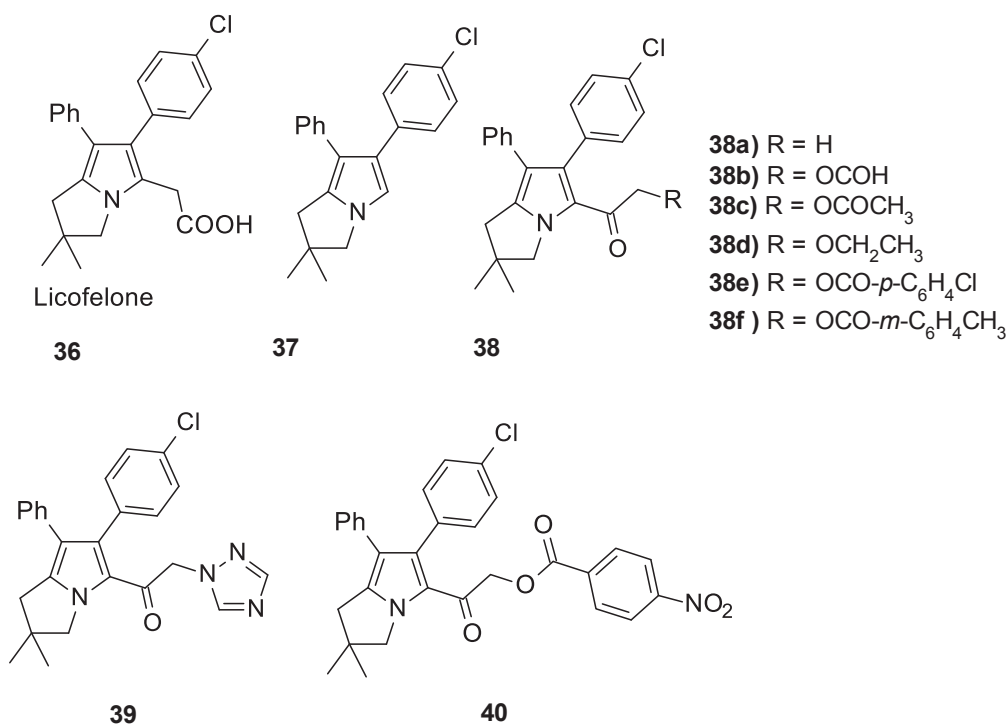
Figure 1.12: Novel derivatives **37**, **38a-f**, **39** and **40** of licofelone.

Gong and co-workers reported the anti-tumour activities of a series of novel pyrrolizine compounds *in vitro* against BEL-7402 (human liver cancer) and HT-1080 (human fibrous sarcoma) cell lines. The most outstanding compound was **41** which showed anti-proliferative activity up to 3.3 fold greater than that of cisplatin (IC$_{50}$ = 18.2 μM and 8.2 μM against BEL-740 and HT-1080 cell lines, respectively).[36] Further investigation by the same group found compound **42** to be the most potent and superior to cisplatin across all tested cell lines (Figure 1.13).[37]
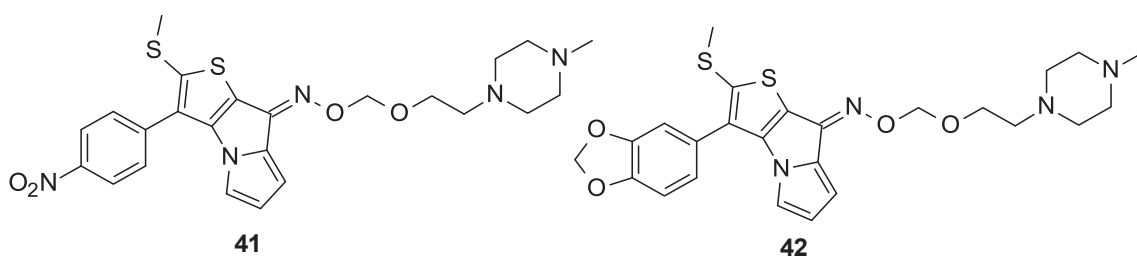
Figure 1.13: Methylthio-8H-thieno[2,3-b]pyrrolizin-8-oximino derivatives **41** and **42**.

Rault and co-workers prepared several compounds containing a thieno[2,3-*b*]pyrrolizin-8-one scaffold (Figure 1.14). One of the first members of the series showed promising antiproliferative activity, compound MR22388 **43** inhibited growth of the L1210 leukemia cell line with an IC_{50} of 15 nM.[38] Further testing against nine tumor cell lines confirmed the cytotoxic activity of MR22388 **43**, including activity against the epidermoid carcinoma doxorubicin-resistant KBA1 cell line (IC_{50} = 2.9 nM).[39-40] Further investigation revealed compound MR22388 **43** to be an active inhibitor of a mutated form of tyrosine kinase (FLT3-ITD) that exists in about 25% of normal karyotype acute myeloid leukaemia (NK-AML) and linked to an adverse prognosis.[38]

Structure-activity relationship studies of this series of thieno pyrrolizine compounds revealed some structural features required for anticancer activity. For example, the thiophene ring and phenyl substituent at C-3 are crucial for activity. Replacement of the phenyl ring with a small alkyl group **44** diminishes the activity. The activity was also very sensitive to changes made to the ether substituent at the phenyl. Altering the ether substituent to ethyl **45a**, propyl **45b**, isopropyl **45c**, or butyl **45d** in all cases reduced the activity by at least 10 fold (relative to **43**) (Figure 1.14).[41]
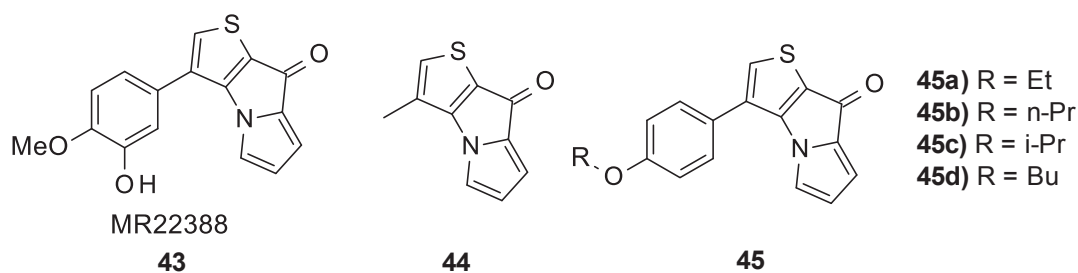
Figure 1.14: Thieno[2,3-*b*]pyrrolizin-8-ones compounds **43 – 45**.

1.1.2.5 Berberine alkaloids

Berberine **46**, an isoquinoline alkaloid, is found in the roots and stem bark from a range of medicinal plants such as *Berberis vulgaris, Hydrastis canadensis, Copis chinensis* and *Arcangelisia flava* (Figure 1.15). This alkaloid exhibits anti-cancer activity both *in vitro* and *in vivo* through inhibition of various tumorigenic microorganisms and viruses such as Helicobacter pylori and hepatitis B virus.[42-43] Recent studies revealed that berberine increases the activity of AMP-activated protein kinase, resulting in phosphorylation of tumour suppressor gene (*p53*), and subsequent inhibition of platelet-derived growth factor (PDGF) induced angiogenesis (the formation of blood vessels to feed growing tumours).[44]

Studies determined berberine effectively inhibits cyclooxygenase-2 (COX-2) transcription in a dose-dependent and time-dependent manner in colon cancer cells, oral cancer cell line OC2, KB cells, and breast cancer MCF-7 cells. As increased COX-2 activity supports tumour development, berberine's COX-2 inhibitory activity underlies its potential for treatment of multiple cancers.[45-47]
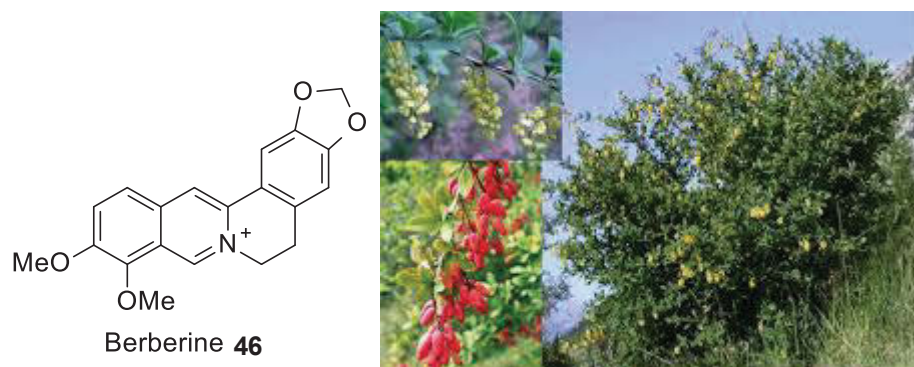
Figure 1.15: Berberine **46** and *Berberis vulgaris*.

Accumulated evidence revealed berberine to have proapoptotic effects to many cancer cell lines by increasing Fas protein expression. Fas is a prototypic death receptor expressed on the surface of a number of cell types and triggers apoptosis by binding its ligand FasL.[48-51] Although berberine displays promising anticancer activity, its therapeutic utility may be limited by its efflux from cancer cells by ABC transporter proteins.[52] These proteins include P-glycoprotein (ABCB1 or P-gp), MRP1 (ABCC1), and ABCG2 (breast cancer resistance protein), all of which confer drug resistance by actively pumping drugs from cancer cells. Studies suggest berberine up-regulates P-gp expression in oral (KB, OC2), gastric (SC-M1, NUGC-3), colon (COLO205, CT26), and HepG2, Hep3B, HA22T/VGH cancer cell-lines.[53-54]

1.2 Current breast cancer therapies

1.2.1 Breast cancer

The oldest description recorded for cancer dates back to early 3000 BC in Egypt. It described eight different types of tumours of the breast.[55] Despite its early discovery, breast cancer remains the most common cancer in women worldwide. The overall 5-year survival rate is currently at 90% which can be attributed to early diagnosis and improvements in the treatment regimens. Sadly for patients diagnosed with advanced breast cancer, the 5-year survival rate

remains at a low 26%.[56] Current prognosis relies on histologic, clinical and biologic factors such as hormone receptors and human epidermal growth factor receptor 2 (HER-2).[57] Breast cancer is comprised of biologically and clinically distinct subtypes based on specific gene expression patterns.[58-59] Studies have shown that breast cancer can be divided into two main groups: oestrogen receptor positive (ER+) and oestrogen receptor negative (ER-). ER+ tumour types are generally referred to as the luminal A and B groups, whereas ER- types can be subdivided into a further two groups: HER2+ and basal (triple negative).[60] Breast cancer cell lines can mimic biological subtypes and pathways in tumours, which suggest that treating certain breast cancer cell lines with potential drug candidates can help guide the drug designing process.[58]

1.2.1.1 Luminal A and B subtype

In general, hormone-receptor positive patients have a more favourable prognosis followed by a more optimal survival rate compared to other breast cancer subtypes. Luminal subtypes compromise of ER-responsive genes as well as other genes that are characteristic proteins of luminal epithelial cells. This subtype can be subdivided into luminal A and luminal B tumours depending on the expression of certain proliferation genes and/or HER2.[61] Luminal-type breast cancer usually responds to hormone and chemotherapy, and is sometimes responsive to HER2 antibody therapy. Luminal cell lines can be characterised by their immuno-profiles which usually consists of the high or low expression of ER, progesterone receptors (PR), HER2 and proliferation marker Ki67. Luminal A breast cancers are generally ER+ and/or PR+, HER2- with low levels of protein Ki-67. Whereas luminal B breast cancers are generally defined as ER+, HER2-, and either Ki-67 high or PR low.[62]

1.2.1.2 HER-2 subtype

The HER2 amplified subtype has a high expression of HER2 and Ki67 markers and often is responsive to HER2 antibody therapies as well as chemotherapy agents.[62] In healthy tissue HER2 functions as a co-receptor that transduce growth signals through dimerisation with other HER receptors, hence leads to activation of signalling pathways which promotes cell growth.[60] In malignant tissue, HER2 is amplified on the cell membrane surface and hence resulting in constitutive signalling which induce tumorigenic growth.[63] This subtype generally will not be responsive to hormone therapy as they do not express hormone receptors such as ER or PR on the surface of the cells.[62]

1.2.1.3 Basal-like (triple negative) subtype

It should be noted that there is still no internationally accepted definition of basal-like breast cancer, and there is still ongoing debate on how best to describe this particular subtype, whether it is through microarray-based expression profiling or immunohistochemical markers. In literature there is a lack of comparisons between the two techniques of identification.[64] The highly metastatic triple negative breast cancer subtype is considered to be the most aggressive breast cancer due to its high risk of recurrence and there is currently no targeted therapy available.[65] Histologically, basal-like breast cancer is characterised by morphological features such as mitotic indices, the presence of central necrotic or fibrotic zones and lymphocytic infiltrate (Figure 1.16).[66-67] Current literature suggests that the main characteristics of the triple negative subtype, is their negativity for ER, PR and HER2 markers while observing high expressions of Ki67 and epidermal growth factor receptor (EGFR).[68]
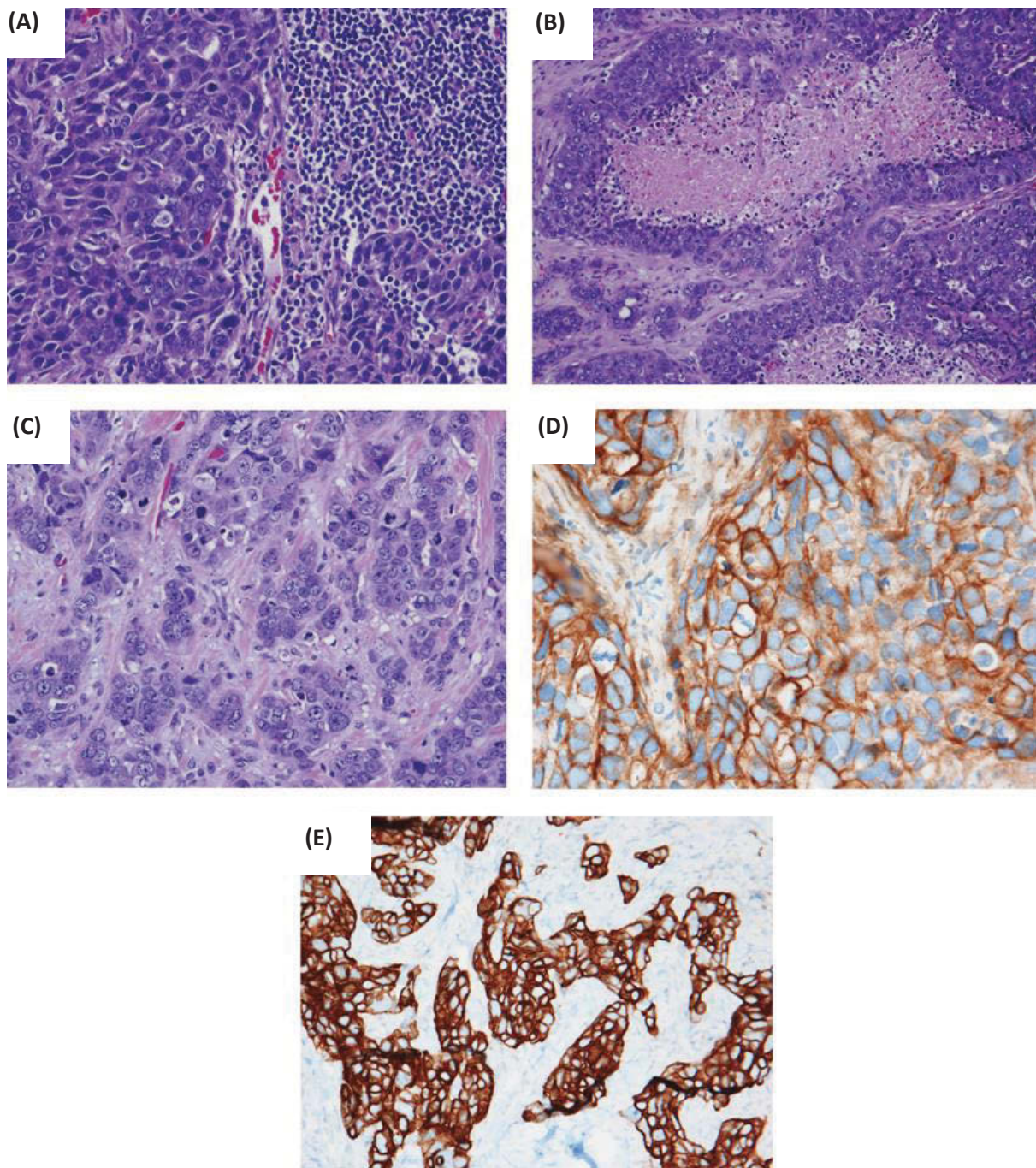
Figure 1.16: The typical morphological features of the triple-negative/basal-like cancer are those of a high-grade ductal carcinoma (Nottingham grade 3) associated with prominent lymphoid aggregates (A). It is not uncommon to observe extensive areas of necrosis (B). Cells show marked areas of pleomorphism and conspicuous mitotic activity (C). Prominent membranous expression of EGFR (D) and CD5 (E).[69]

1.2.2 Current therapeutic challenges

Advancements in the field of cancer research in the past two decades have led to remarkable progress in areas such as cancer prevention, early detection, and treatment. Current treatments include surgery, hormone therapy, radiation, chemotherapy, immunotherapy, and targeted therapy. From a drug discovery view, the focus will be on the evolution of hormone therapy, chemotherapy, and targeted therapy.

Breast cancer is the most common tumour amongst women, and 1 in 8 women have the risk of developing such disease.[70] Many breast cancer types express higher levels of oestrogen receptors (ER) and progesterone receptors (PR) than normal breast tissue. Therefore most hormone therapy drugs are oestrogen receptor inhibitors. These drugs and/or their metabolites binds to the oestrogen receptor, which then undergoes conformational change, hence reducing DNA polymerase activity, blocking oestradiol uptake and ultimately diminishing the oestrogen response.[71] Hormone therapy has evolved since the 19th century with the release of new classes of inhibitors such as aromatase inhibitors to treat breast cancers.

In recent years cancer drug discovery has taken a shift away from cytotoxic agents and towards a more targeted therapy. Target therapy uses more selective drugs that target dysregulated pathways in cancer cells such as certain tyrosine and kinases.[72] In general, these targeted therapy agents exhibit fewer side effects than most chemotherapy agents and can sometimes be used in combination with other treatments. However, the development of targeted therapy drugs for the treatment of highly metastatic triple negative breast cancer subtype has been held back due to lack of understanding of its molecular nature.[73-74]

Over the years conventional chemotherapy drugs were used to treat and in some cases even cure patients with ER and PR negative breast cancer. Despite using a combination of hormone

therapy, targeted therapy, and chemotherapy, most malignant breast tumours will eventually become resistant to such treatments. Chemotherapy agents generally inhibits microtubule function, protein function, or DNA synthesis, hence causing cell death or preventing cell growth. These cytotoxic agents' mechanisms of action can be cell cycle dependent, for example arresting cancer cell growth at different cell cycles, or induction of apoptosis.[73] Multidrug resistance in cancer plays a contributing factor in the battle against cancer. Similar to antibiotic resistance, cancer cells can grow resistance either due to the nature and genetic background of the cancer cell or as a result of genetic changes following chemotherapy treatments.[75]

At the start of the 20th Century, people began to see the advantages of new therapies such as combination, and adjuvant therapies as well as new delivery techniques to improve the activity of current chemotherapy agents. Recent novel approaches to cancer therapy include drugs that specifically target the cancer cell such as liposomal and monoclonal antibody therapies.[76] Currently, there is an urgent need to develop new drug candidates to improve activity, selectivity, and combat multidrug resistance as well as to reduce some of the toxic side effects of current chemotherapy drugs.

1.3 The Ritter reaction

Diversity-oriented synthesis of alkaloid-like molecules has shown considerable potential as a means of discovering new and novel chemotherapeutic agents. The non-planar ring systems of most alkaloid-like compounds can be readily substituted to improve drug-like properties, bioactivity and selectivity, making them attractive building blocks for chemotherapy drugs. The bridging Ritter reaction has enabled the synthesis of alkaloid-like compounds of novel structures. In this section, the Ritter reaction is reviewed, with an emphasis on its application in drug discovery.

1.3.1 The classical Ritter reaction

The Ritter reaction was first described by John Ritter and co-workers in 1948.[77-79] This versatile reaction has provided a new means of preparing a variety of chemical compounds. Many articles have described the Ritter reaction as an efficient one-flask process yielding an amide as the final product.[79-85] Even though the potential of the classical Ritter reaction has been considerably explored by many; it is not surprising due to its versatility that the many other Ritter-type reactions have subsequently been reported.[86-90]

The classical Ritter reaction comprises of the nucleophilic addition of a nitrile to a carbenium ion which is commonly generated *in situ* from an organic substrate in the presence of a strong acid. Water is then added to the one-flask reaction to afford the amide. The mechanism for the conversion of *tert*-butanol to *N-tert*-butylacetamide is illustrated in Scheme 1.1. The reaction proceeds *via* the formation of a carbenium ion **47** as the first intermediate under strong acidic conditions, which then undergoes nucleophilic attack on the nitrile to form a resonance stabilised nitrilium ion **48**, which is then converted to the imidate **49**. This is followed by hydrolysis affording the amide as the final product.
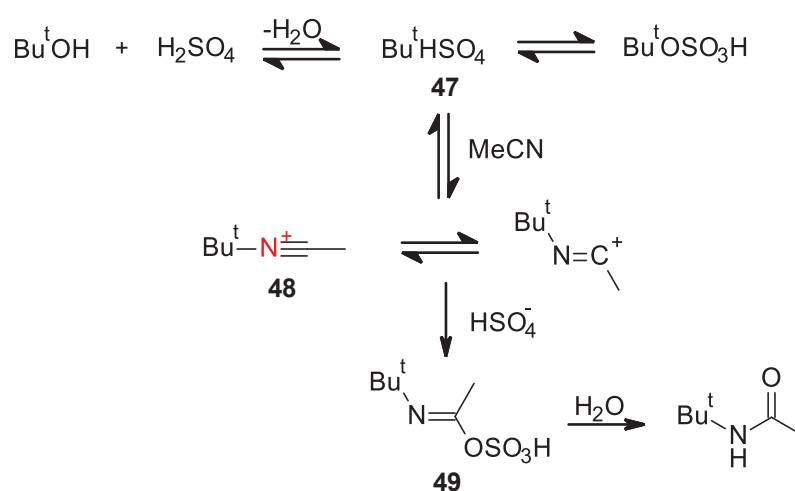
Scheme 1.1: Proposed mechanism of classical Ritter reaction.[84]

Ritter reactions can be carried out with a range of different acids, giving rise to a range of carbenium ions or their equivalents. Most nitriles that contain acid-stable functional groups can undergo Ritter reactions; however, the yields of the products can vary considerably. For example, nitriles having electron donating groups are most desirable, as the added electron density makes the nitrile a stronger nucleophile. Scheme 1.2 illustrates a wide range of nitrile containing compounds that can participate in Ritter reactions and offer significant yields of the desired products.[91-92]
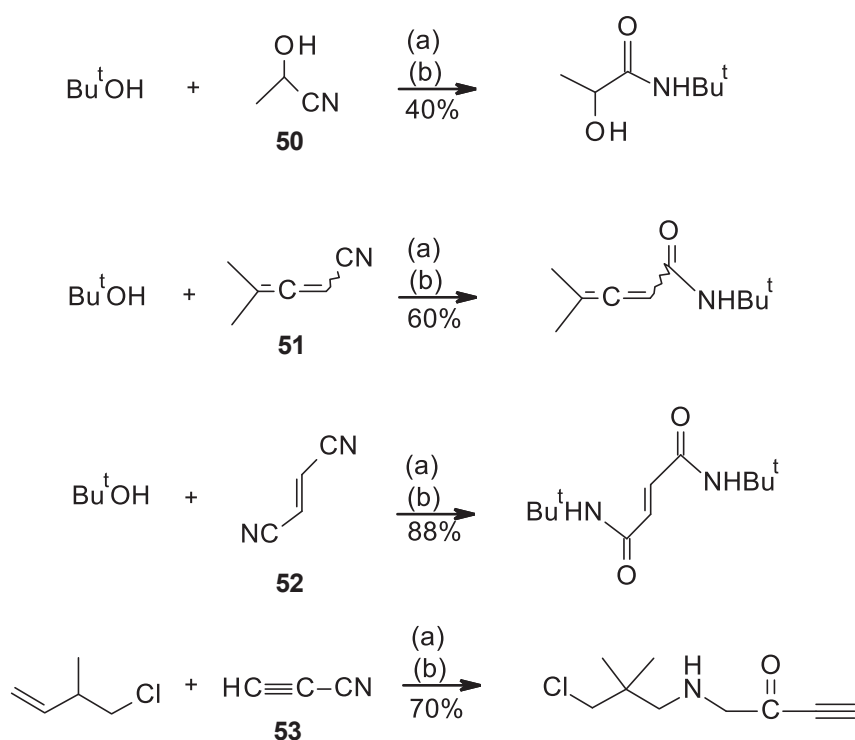
Scheme 1.2: Ritter reaction using a variety of nitriles.[93] Reaction conditions: (a) H_2SO_4, AcOH. (b) H_2O.

Furthermore, in 1965 Holmes *et al.* reported significant yields for the application of the Ritter reaction to petroselinic acid using hydrogen cyanide, acetonitrile, propionitrile, acrylonitrile, benzonitrile, and dinitrile Table 1.1.[94]

Table 1.1: Yield of Ritter product using different nitriles.[94]

Nitriles	Yield of Crude product (%)
Hydrogen cyanide	82
Acetonitrile	94
Propionitrile	99
Acrylonitrile	99
Benzonitrile	contaminated with benzonitrile

Since the discovery of the Ritter reaction, a number of review articles have been published documenting the precise experimental conditions. Amongst all, the most comprehensive surveys are the articles by Krimen and Cota in 1969, as well as by Roger Bishop in 1991.[81, 84] Optimum experimental conditions are crucial for the efficiency of the Ritter reaction. Significant yields have been documented for reactions at 20-50℃ and the reaction typically goes to completion by 24 hrs. In most cases the acid of choice was 85-90% sulphuric in order to produce comparative studies. Generally the Ritter reaction has been to known to proceed using only the acid and nitrile as solvent, however in many cases it has been observed that the use of slightly polar solvents such as glacial acetic acid or nitrobenzene can polarise the nitrile group and increase its nucleophilicity.[95-98]

In addition to optimum reaction conditions, an overwhelming number of carbenium ion sources have also been reported in the literature. Despite the wide range of sources available, the most commonly used precursors are alcohols and alkenes. However, functional groups such as alkyl halides, dienes, aldehydes, alkanes, carboxylic acids, esters, epoxides, ketones, oximes, and glycols are all capable of producing carbenium ions under strong acidic conditions. Therefore, all are possible candidates for the Ritter reaction. Examples of employing alkene **54**, oxime **55**, ester **56**, and *N*-methylolamide **57**, and other functional groups as precursors for the Ritter reaction, are shown in Scheme 1.3.[99-102]
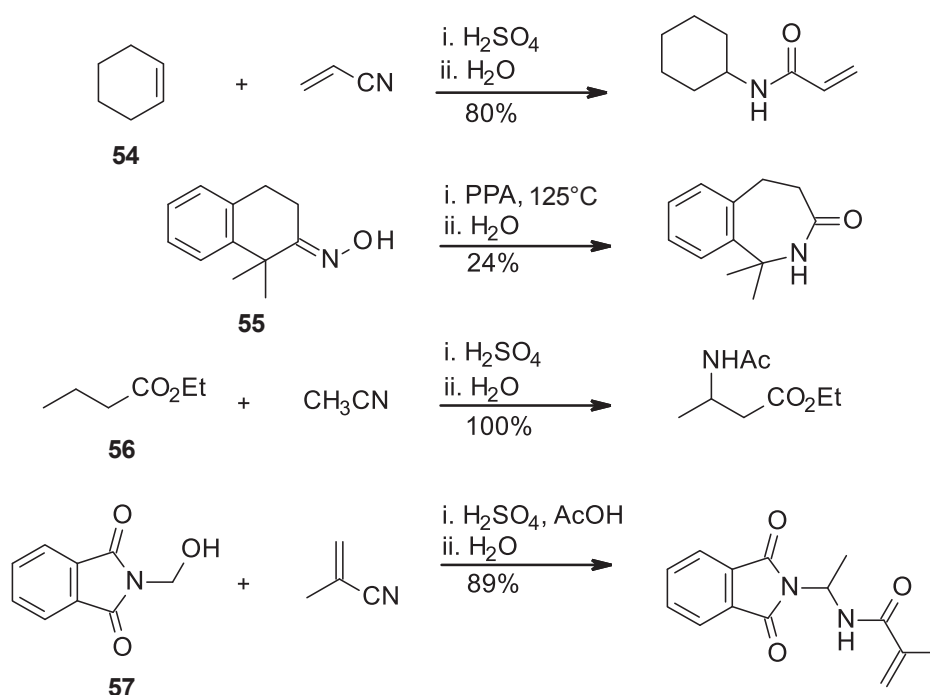
Scheme 1.3: Ritter reaction using alkene **54**, oxime **55**, ester **56**, and *N*-methylolamide **57**.[84]

1.3.2 Heterocyclic Ritter reactions

In 1952 Ritter and Murphy first reported an intramolecular variation of the classical Ritter reaction when they obtained a heterocycle product **58** with an imine functional group (Scheme 1.4, equation A).[103] Examples of this process were later demonstrated by Sasaki *et al. via* the reaction of aryl imidoyl chloride **59** under Lewis acid conditions (Scheme 1.4, equation B), as well as Meerwein *et al. via* the cyclisation of the compound **60** (Scheme 1.4, equation C).[104-105]
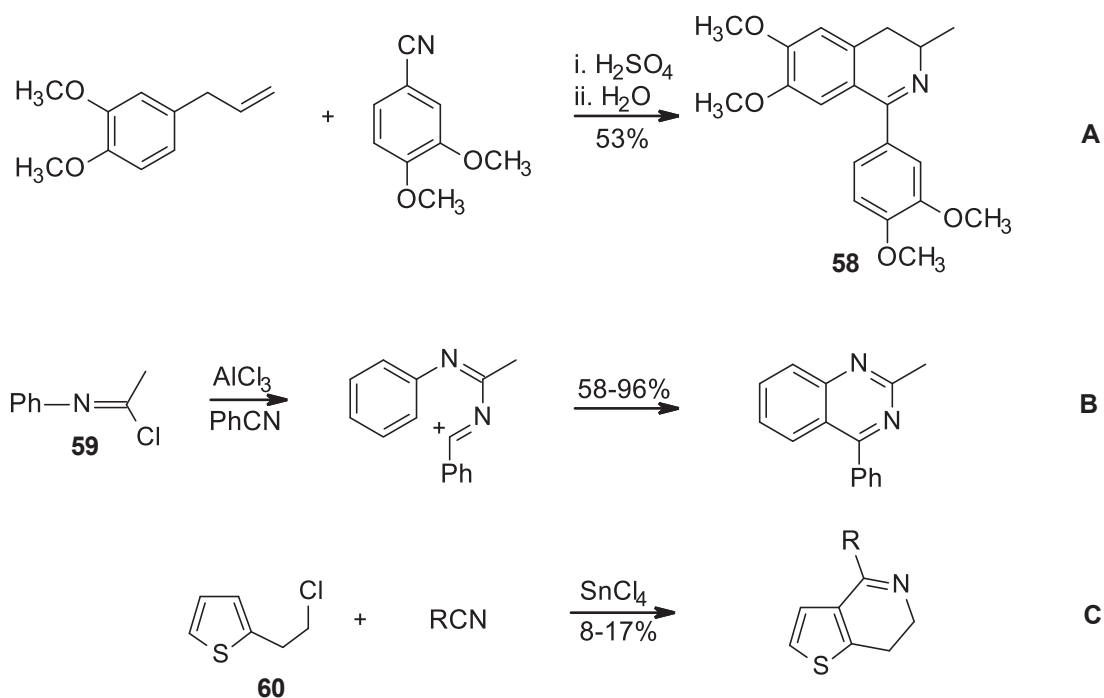
Scheme 1.4 A/B/C: Representatives of the intramolecular variant of the Ritter reaction by Sasaki *et al*. and Meerwein *et al*.

In 1970 Meyers and Sircar described the application of Ritter reactions to yield a wide range of heterocyclic products containing an imine functional group.[85] This intramolecular variant of the classical Ritter reaction can be divided into two distinct processes based on the different mechanistic pathways the reaction can undergo. The more common pathway is demonstrated in Scheme 1.5A. The reaction proceeds *via* the attack of the carbenium ion by the nitrile to generate the nitrilium ion, which then undergoes an intramolecular cyclisation with a nucleophilic group on the same molecule giving compound **61**. Alternatively, in Scheme 1.5, equation B illustrates the less common pathway involving the intramolecular formation of a cyclic nitrilium ion which is then attacked by an external nucleophile giving compound **62**. It is worth noting that both methods are constrained by ring sizes due to the intramolecular ring formation.
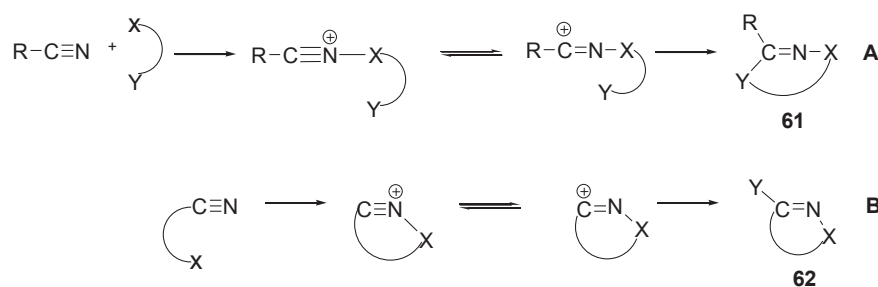
Scheme 1.5 A/B: Representatives of both pathways of the intramolecular variant of the Ritter reaction.

1.4 Project aims

As previously mentioned, natural alkaloids have represented a rich reservoir of potential small molecules with anticancer properties. For decades medicinal chemists have focused on studying their structural activity relationships, their biological activities and using their scaffolding as a foundation to develop large libraries of alkaloid-like analogues with improved anticancer properties. With cancer mortality rates still currently on the rise, the search for more effective anti-cancer agents with less toxic side effects and greater efficacy is a continuous battle.

Our alkaloid-like compound **63** (Scheme 1.6), derived from a 1-azacyclohexene scaffold, was selected by the US National Cancer Institute as a candidate for their standard anti-cancer screening program against 60 cancer cell lines (Appendix 7.1). Compound **63** is an active anticancer agent with $IC_{50} < 10$ μM on selective groups of tumour types such as leukaemia, colon, melanoma and breast cancer. The proliferation of most of these cell lines was potently inhibited by **3**. The aggressive and highly metastatic MDA-MB-231 cell line was the least active ($IC_{50} = 38.9$ μM), however, this finding has provided a starting point of the discovery.

These results further indicated that the series of alkaloid-like compounds synthesised could be biologically active compounds, in particular against cancerous cells.

Significant anti-cancer activity was observed in all 48 cancer cell lines and particularly against the aggressive and highly metastatic MDA-MB-231 cell line provide a clear indication of the anticancer potential of the tricyclic alkaloid-like scaffold and their derivatives against breast cancer cell lines is worth pursuing.

1.4.1 Approach and methodology

1.4.1.1 Chemistry

This project will focus on the synthesis of a range of tricyclic alkaloid-like compounds from 2,6-dimethylenebicyclo[3.3.1]nonane **72**, caryophyllene **96** and its monoepoxide **117** (Scheme 1.6). The anticancer activity of newly synthesised compounds will be assessed against the aggressive triple-negative MDA-MB-231 breast cancer cell line. This cell line has been chosen because it is the triple-negative subtype which is unresponsive to many currently used chemotherapeutic agents. Cell testing will consist of an initial screening assay to evaluate the effects of test compounds on cell viability. The cytostatic and cytotoxic effects of active compounds will be further characterised by assessing effects on cell cycle progression and apoptotic cell death, respectively.

Some hit compounds have been identified *via* this screening procedure based on their activity and IC_{50} values.
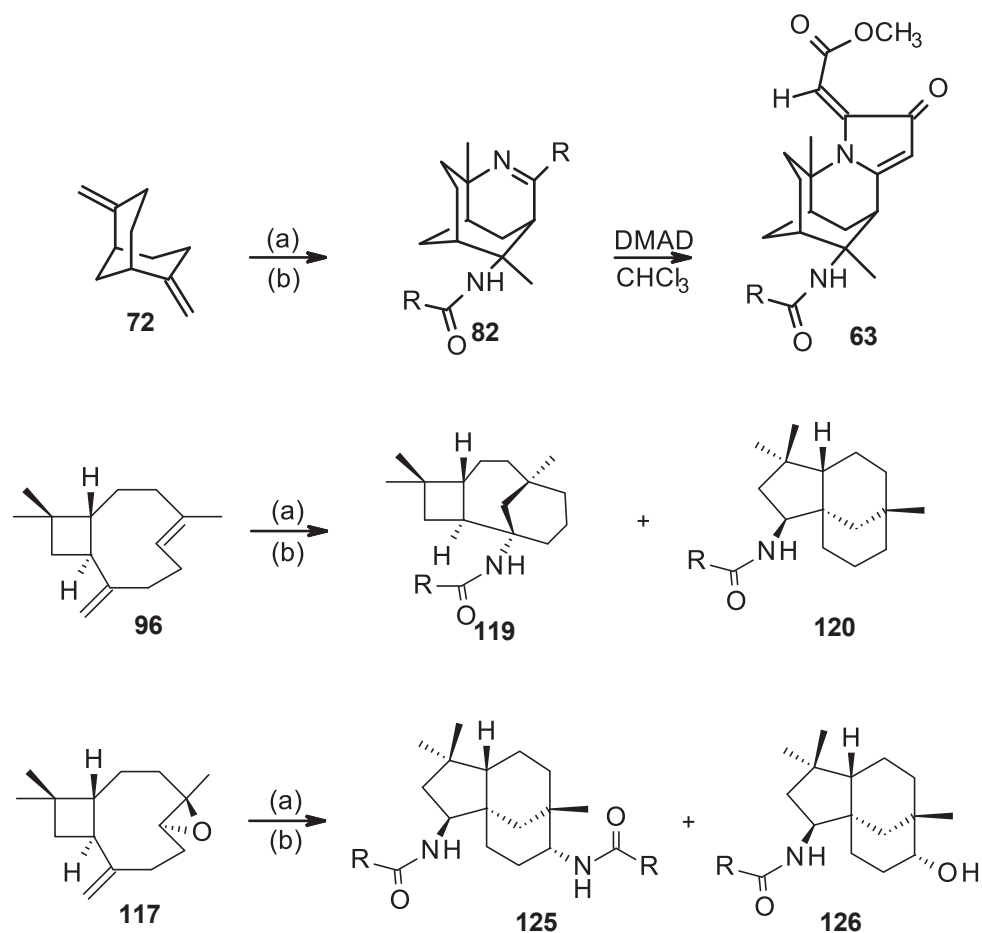
Scheme 1.6: Synthesis of Tricyclic alkaloid-like compounds. Reaction conditions: (a) H_2SO_4, RCN. (b) H_2O.

1.4.1.2 Biological evaluation

Cell viability assay

Effects of the synthesised drugs on cell viability will be analysed using a standard 3-(4,5-dimethylthiazol-2-yl)-5-(3-carboxymethoxyphenyl)-2-(4-sulfophenyl)-2H-tetrazolium (MTS) assay. MTS is a well-established quantitative colourmetric assay for the determination of cell viability and cytostaticity. MTS assay uses an indirect staining technique and is used for adherent cell lines such as MDA-MB-231 breast cancer cells.

Cell Cycle Study

All cells divide from an existing cell in which the genome and organelles are duplicated. In non-cancerous cells, this process is tightly regulated but in cancer cells becomes out of control, leading to uncontrolled cell proliferation, a hallmark of cancer.[106] The human cell cycle consists of two main phases: the interphase which contains G_1, S and G_2 sub-phases, and the mitosis phases (M-phase) as shown in Figure 1.17. During the cell cycle, DNA is replicated in the S-phase (interphase) before it divides into two daughter cells in the M-phase. Checkpoints exist in all phases of this cycle to ensure the proper completion of each phase before progression to the next. Non-dividing cells enter the G_0 phase from G_1; it can stay viable for a certain amount of time without participating in cell division or exit the cycle by apoptosis (programmed cell death).
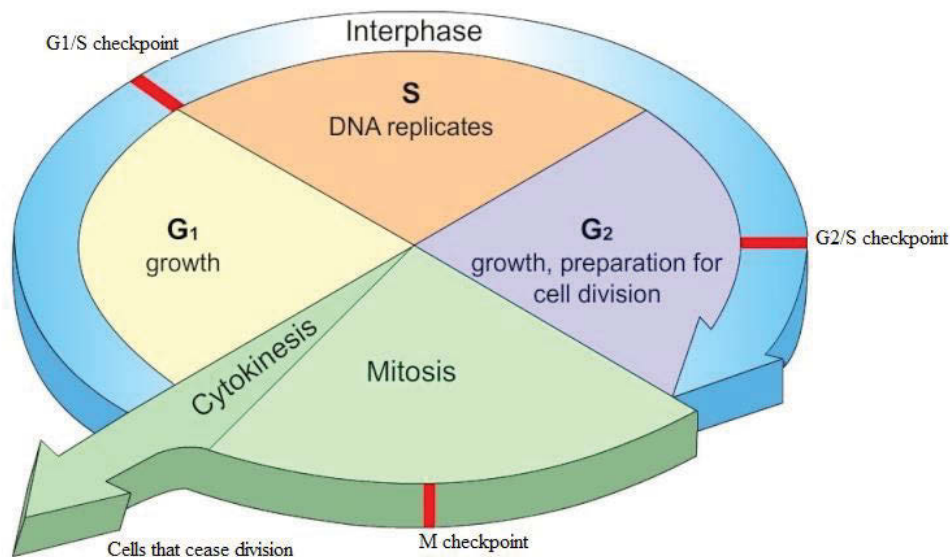
Figure 1.17: Different phases of the eukaryotic cell cycle.[107]

Cell cycle analysis will be performed using the propidium iodide (PI) stain and flow cytometry. The DNA of mammalian cells can be stained by DNA binding dyes (PI). These dyes bind in proportion to the amount of DNA present in the cell, for example, cells in the S-phase will have

29

more DNA than cells in the G_1 phase, whereas the cells in the G_2 phase will have approximately double the DNA as the cells in G_1 phase.

Apoptosis assay

Cell death can proceed by two different processes, called apoptosis and necrosis. Necrotic cell death occurs as a result of trauma or toxic agents and involves an uncontrolled drop in ATP concentrations so that the Na^+/K^+ ATPase no longer operates which results in a drop of ion concentrations, and eventually, the cell swells up and bursts. The second process is apoptosis, or programmed cell death, and involves the shrinkage of the cell and its contents followed by its contents being packaged into blebs (membrane-bound packets), and then engulfed by macrophages.[106] When a cell is going through the first stage of apoptosis the cell membrane phospholipid phosphatidylserine (PS) is translocated from the inner to the outer leaflet of the plasma membrane. This inversion exposes the PS for binding with Annexin V (phospholipid binding protein). Annexin V has a high affinity for PS and acts as a sensitive probe for flow cytometry analysis and thus can be used to determine if the cell is undergoing apoptosis.

Chapter 2 Synthesis of the 3-azatricyclo[5.3.1.0^{4,9}]undec-2-ene system using the Bridging Ritter reaction

2.1 The Bridging Ritter reaction

In addition to the intramolecular Ritter reaction mentioned in Chapter one, the procedure can also be used to form bridged bicyclic structures, in a variant known as the Bridging Ritter reaction. This bridging cyclisation proceeds *via* the formation of the nitrilium ion that undergoes an intramolecular nucleophilic attack by an alkene group to produce a 1-azocyclohexene intermediate carbenium ion. The carbenium ion is then subjected to a conventional Ritter reaction to produce an amide. The nitrile reagent is most likely to attack the carbenium ion from the least hindered face, which typically imparts a high degree of stereoselectivity to the reaction. However, it is also possible to produce racemic mixtures since the bridging process can occur on either face of the carbenium ion. For example, Bridging Ritter reactions using the diaryl compounds suberenol **64** produced the bridged imine product **65** as a racemic mixture (Scheme 2.1).[108] The same group later further investigated the Bridging Ritter reaction and documented the behaviour of 5-methyl-5*H*-dibenzo[a,d]cyclohepten-5-ol under Ritter conditions.[109]
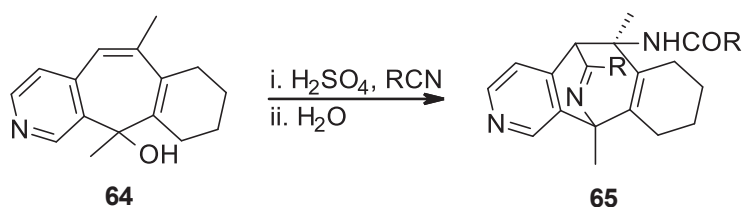
Scheme 2.1: Bridging Ritter reaction of diaryl subernol **64** resulting in a racemic mixture **65**.[108]

In 1994 Samaniego *et al.* demonstrated that a stereospecific conversion of (*R*)-(+)-limonene **66** and (*1S*)-(-)-β-pinene **67** to bicyclic amides **68** and **69**, respectively, could be carried out *via* the Bridging Ritter reaction (Scheme 2.2).[110] The first carbenium ion generated was from a chiral molecule. Similar examples of this process can be found in later publications by Rodriguez *et al.* utilising a broad range of substrates.[111]
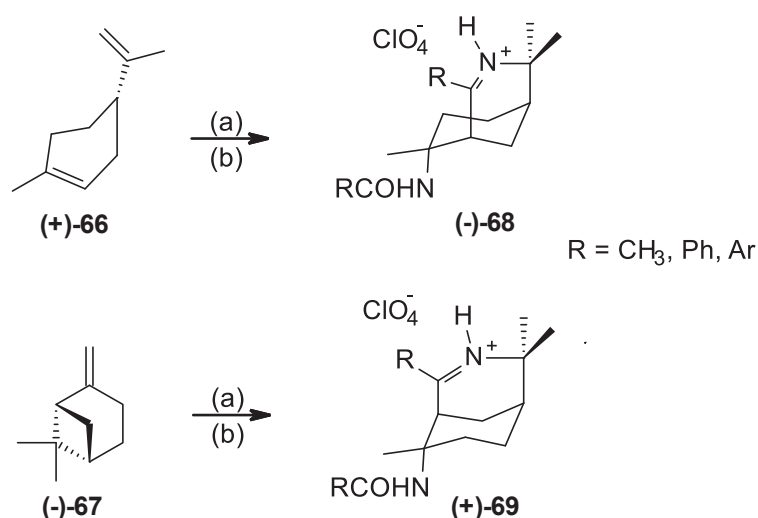
Scheme 2.2: The typical representative reaction of (*R*)-(+)-limonene **66** and (*1S*)-(-)-β-pinene **67** with acetonitrile *via* the Bridging Ritter reaction. Reaction conditions: (a) HClO, RCN. (b) H₂O.

Furthermore, in 1979 Hassner *et al.* reported the reduction of a bromo nitrile compound *via* an intramolecular allylic halide displacement resulting in a tricyclic compound **71** (Scheme 2.3).[112]
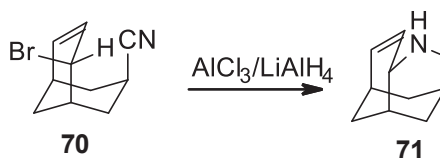
Scheme 2.3: Reduction of the bromonitrile compound to yield compound **71**.

Fascinated by the 3-azatricyclo-[5.1.3.0^{4,9}]undecane structure, Bishop *et al.* later reported a simple and effective method of synthesising derivatives of this particular ring system using the Ritter Reaction.[113] Reaction of 2,6-dimethylenenicyclo[3.3.1]nonane **72** with acetonitrile under Ritter conditions, provided the compound **72** as its monohydrate (Scheme 2.4).
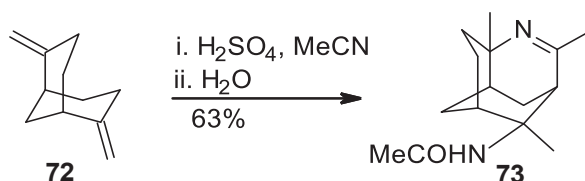
Scheme 2.4: Bridging Ritter reaction with 2,6-dimethylenenbicyclo[3.3.1]nonane **72**, affording tricyclic imine product **73**.

In contrast, the same diene **72** undergoes the same Bridging Ritter reaction conditions with benzyl nitrile to produce product **74** due to unexpected air autoxidation of the X-PhCH$_2$ side chain as shown in Scheme 2.5.[114]

a) X = H, 33 %
b) X = Br, 35 %
c) X = Cl, 32 %
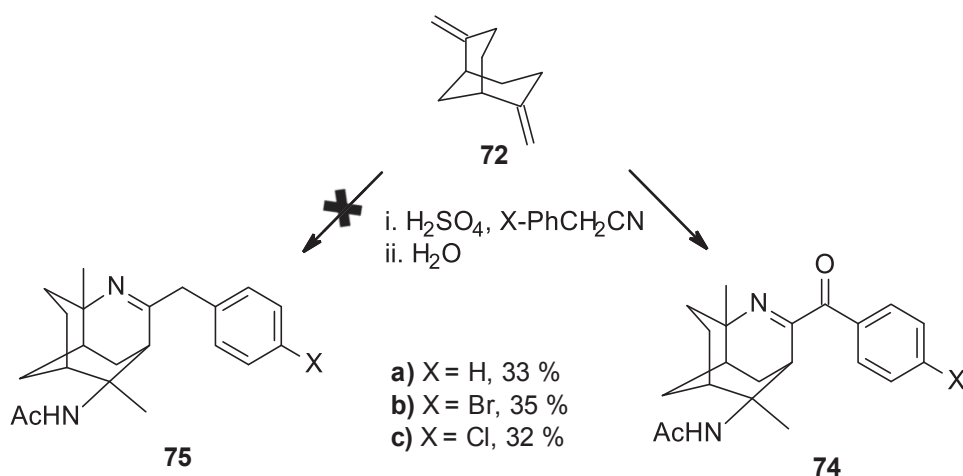
Scheme 2.5: Bridging Ritter reaction with 2,6-dimethylenenicyclo[3.3.1]nonane **72**, affording the tricyclic imine product **74**.

As shown in the examples above, the Bridging Ritter reaction is a versatile reaction for the development of novel bridged imine products as interesting scaffoldings. These scaffolds can be used to generate alkaloid-like compounds *via* reactions with DMAD, nucleophilic additions, reductions, and reductive alkylations.

2.1.1 Synthesis of 2,6-dimethylenebicyclo[3.3.1]nonane

As part of our ongoing research for alkaloid-like compounds as anti-cancer agents,[115-116] a library of tricyclic compounds has been synthesised using the Bridging Ritter reaction as the key reaction. Various nitriles were used, and subsequent reactions such as reduction, reductive alkylation and DMAD cycloaddition were used to derivatise these small molecules to heterocyclic alkaloid-like compounds.[117] The synthesis of cyclic alkene precursor **72** required Meerwein's ester as the starting material (Scheme 2.6). The synthesis of the ester proceeded *via* an aldol condensation, Michael addition and Dickmann condensation. This was followed by an acid hydrolysis to produce the diketone **77** that then reacts with two moles equivalent of Wittig reagent to yield the diene **72**.
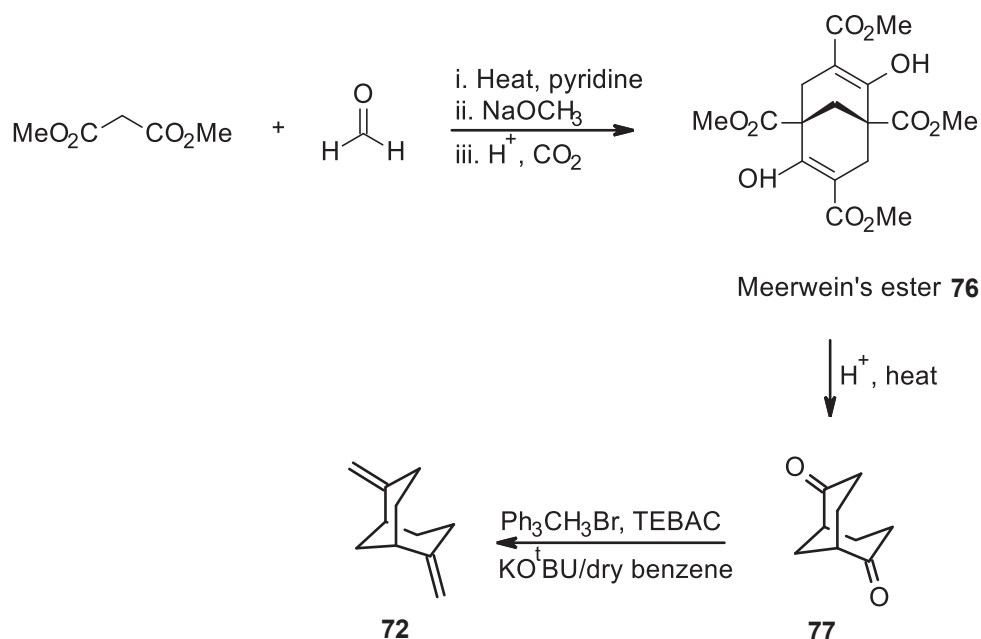
Scheme 2.6: Synthetic pathway of precursor diene **72**.

2.1.1.1 Formation of ketone alkene

The cyclic diene **72** was previously prepared by Ung *et al.* as the precursor for generating the tricyclic imine scaffold.[86, 113-114, 118] The reaction proceeds *via* the Wittig reaction from the corresponding diketone **77** (Scheme 2.7) and phosphonium ylide, in the ratio of 1:2.

This reaction was repeated but with a slightly lower molar ratio of ylide (1:1.5). Under these conditions formation of a ketone-alkene compound **78** as the major product (55% yield) was observed. Compound **78** was characterised by spectroscopy, where the ^{13}C NMR spectrum showed the presence of both alkene and ketone peaks at 109 and 216 ppm respectively. The ^{1}H NMR spectrum also supported the presence of only one terminal alkene functional group at 4.75 and 4.69 ppm as two singlets. HRMS analysis confirmed the exact mass of **79** to be 151.1094 which is corresponding to $C_{16}H_{28}N_2O$ required 150.1123.
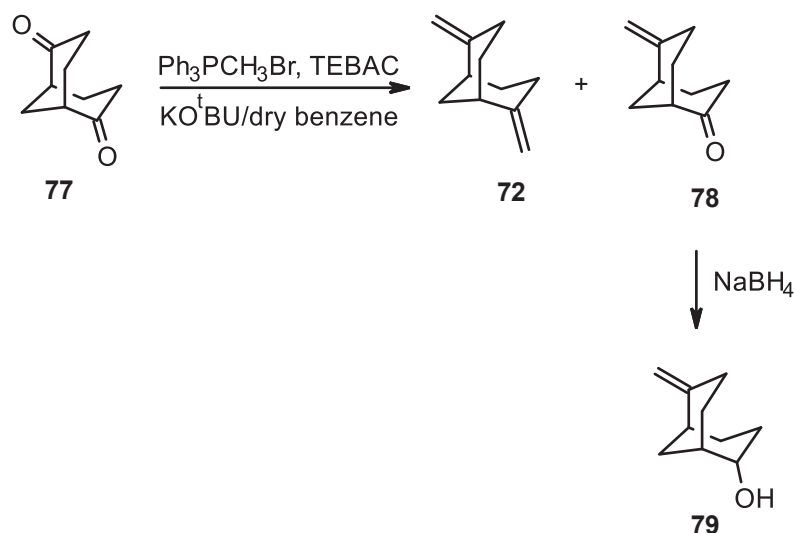
Scheme 2.7: A proposed synthetic pathway for the synthesis of cyclic alkene **72** and alkene

alcohol **79**.

Compound **78** was selectively reduced to yield the alcohol **79** in 77% yield (Scheme 2.7) which

was further reacted with acetonitrile under the Bridging Ritter reaction conditions in an attempt

to investigate the tricyclic imine scaffold with an alcohol functional group at the C-6 position.

However, this reaction was unsuccessful, and no bridging product was observed. GC-MS

analysis determined the mass of the reaction product to be $m/z = 214$ which suggests that is the

alcohol **80**. The possible side product should be **80** and not **81** (Figure 2.1).
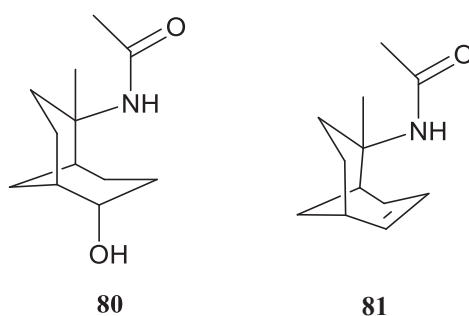
Figure 2.1: Proposed side products **80** and **81**.

Previous studies have demonstrated that the Bridging Ritter products can be obtained from the

alcohol-alkene starting material. It is feasible under the provision that the alcohol functional

group will be first to undergo dehydration to generate the carbocation. Subsequent addition of the nitrile to the carbocation should produce the nitrilium ion. The intramolecular cyclisation can then take place *via* a subsequent alkene nucleophilic attack on the nitrilium ion. In the case of **79**, if the carbocation at C-OH formed first and reacted with CH_3CN to generate carbenium then bridging is possible. However, if the carbocation firstly formed at the alkene, then the reaction would not favour the formation of the desired bridging product, *via* the OH nucleophilic addition. The expected product would be a dihydro-1,3-oxazine derivative.[119-120]

2.1.2 Synthesis of 3-azatricyclo[5.3.1.0^{4,9}]undec-2-ene

Tricyclic imines **82b-c** were synthesised *via* the Bridging Ritter reaction in benzene under strongly acidic conditions according to literature (Scheme 2.8). Compound **82a** was previously synthsised by Ung *et.al.*[116, 121] The nitriles used in the Bridging Ritter reaction were chosen to provide a variety of substituents at the C-2 position which in turn can alter the reactivity of the respective imine at the C-2 position. The Bridging Ritter reaction proceeds *via* the formation of the nitrilium ion which then undergoes an intramolecular nucleophilic attack by the alkene group to produce an 1-azocyclohexene moiety and hence resulting in a new carbenium ion (Scheme 2.9). This carbenium ion is then subjected to a standard Ritter reaction to produce an amide (Scheme 2.9). The nitrile reagents attack the carbenium ion from the least hindered face, hence making the series of conversions stereospecific.[86, 118]
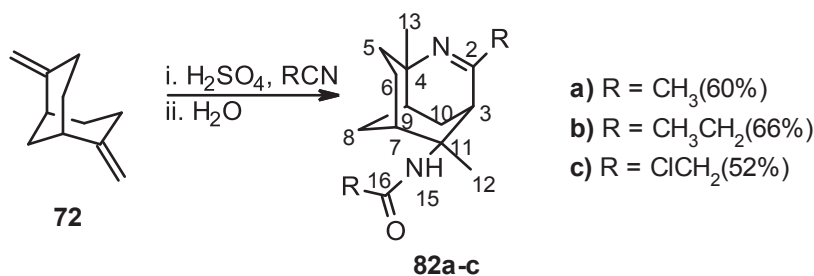
Scheme 2.8: Proposed synthetic pathway for tricyclic imines **82a-c**.
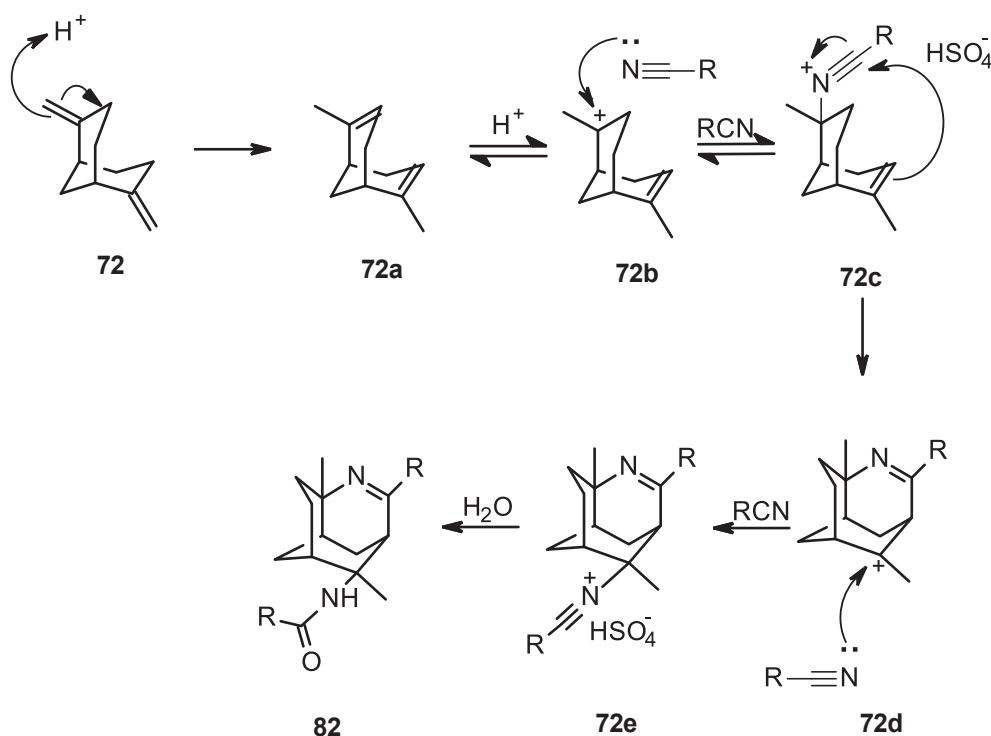
Scheme 2.9: Proposed mechanism of the Bridging Ritter reaction.

The structures of **82a-c** were confirmed by extensive NMR studies. Figure 2.2 shows the ^{1}H NMR spectrum of **82b**, in which proton resonances from the newly formed bridgehead (H-3) appear at δ 3.35 ppm. The cyclisation of the nitrogen-containing ring system for compound **82a** can be further confirmed by the newly formed N=C peak at 172 ppm identified in the ^{13}C NMR spectrum. The NMR spectral data for compounds **82a** and **82c** also displayed these resonances.

The electron withdrawing nature of ClCH$_2$CN has resulted in the decrease in the percentage yield of **82c** in comparison to **82a** and **82b**. Bulkier nitriles such as cinnamonitrile and benzonitrile observed no bridged products. This phenomenon has also been observed in our earlier work, where outcomes of the bridging reactions were significantly influenced by the nitrile used.[115]
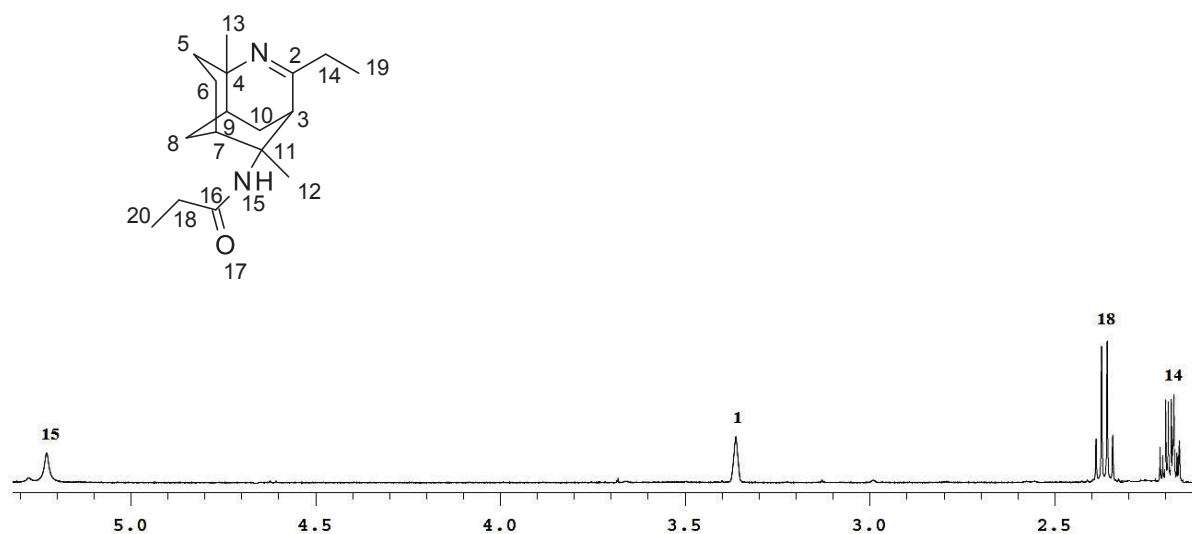
Figure 2.2: ^{1}H NMR spectrum of compound **82b**, showing region 2.1 – 5.3 ppm.

2.1.3 Derivatisation of 3-azatricyclo[5.3.1.0^{4,9}]undec-2-ene

The Bridging Ritter reaction results in the formation of a reactive imine compound which sets the foundation for a variety of reactions such as reduction, reductive alkylation, nucleophilic addition, and the addition of dimethyl acetylenedicarboxylate (DMAD). Reactions with DMAD can produce complex products, some of which are similar to that of plant alkaloids that exhibit a variety of biological activities including anticancer.

2.1.3.1 Cycloaddition of DMAD to 3-azatricyclo[5.3.1.0^{4,9}]undec-2-ene

Reactions with DMAD have proven to be very versatile. This reagent is often used in Michael reactions as the Michael acceptor to a number of nucleophiles such as sulphur, nitrogen and oxygen.

Reactions between imines and DMAD are well known in the literature and can produce unpredictable reaction products.[122-126] This type of cycloaddition of DMAD is complicated by the many pathways it can undergo. It was apparent through the studies carried out by Bishop

and co-workers that the reaction between certain bridged imines and DMAD can lead to a variety of both cyclised and uncyclised products.

In 1992, Bishop and co-workers found that the reaction between imine **82a** and DMAD initially produced the 1:2 adduct **83**, which further cyclised in the presence of SiO$_2$ to provide compound **63** as an orange solid (Scheme 2.10).[90]
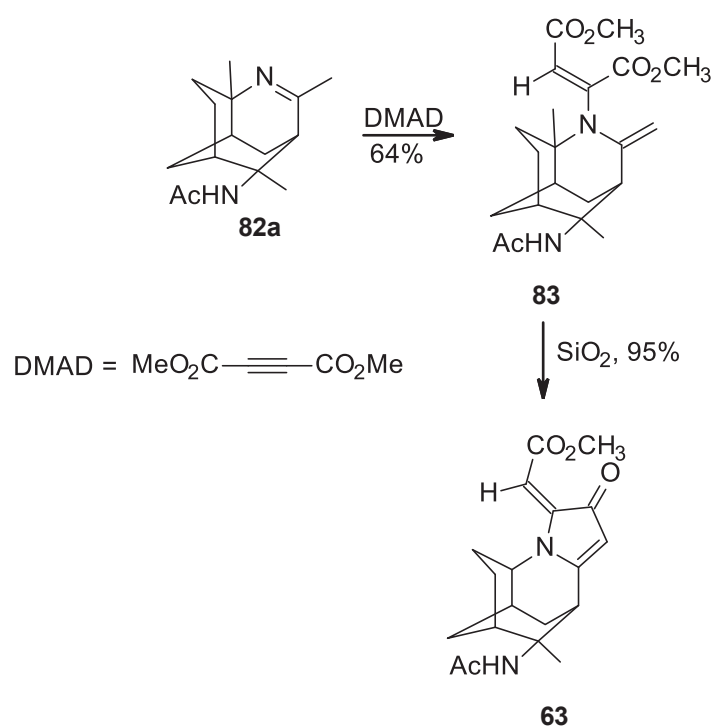
Scheme 2.10: DMAD reaction with bridged imine **82a** affording the final cyclised product **63**.

This project cyclic amide **63** was synthesised in 40% yield from a one-pot reaction in chloroform with acetylenedicarboxylate (DMAD) and tricyclic imine **82a**, according to the method that was previously reported.[86] Compound **63** was found to display anticancer activities as well as cytotoxicity against Vero cells. It was found that compound **63** reduced Vero cell viability by 77% of control at the maximum concentration tested (139 μM). The presence of

the α,β-unsaturated carbonyl system at C-12, C-21 is a Michael acceptor which is commonly to contribute to toxicity. The α,β-unsaturated carbonyl can form covent bonds via addition with nucleophilic groups such as OH of serine, the SH of cysteine and the ω-NH_2 of lysine residues. Therefore it was selectively reduced with $NaBH_4$ in the presence of $NiCl_2 \cdot 6H_2O$ to yield compound **84** in 70% yield, which observed less cytotoxicity against Vero cells (Scheme 2.11).[127]
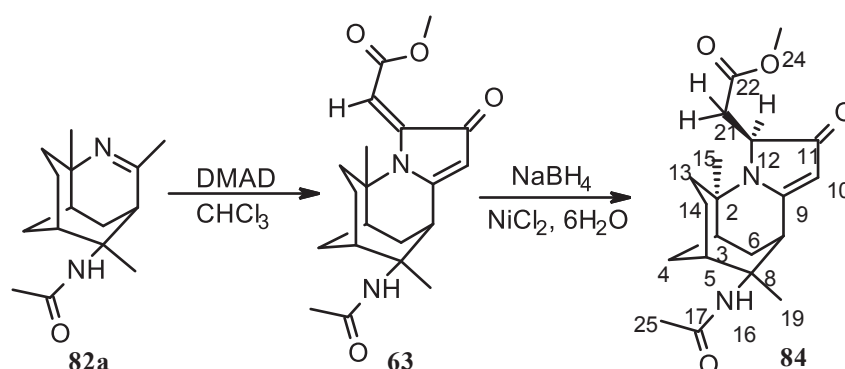
Scheme 2.11: Derivatisation of tricyclic imine scaffold **82a**.

The ^{1}H NMR spectrum of the compound **84** showed the disappearance of a proton resonance at δ 5.86 ppm which corresponds to the loss of the alkene proton at the C-21 position. A newly formed doublet of doublets at 2.85 ppm arises from the two protons on C-21, which is consistent with the structure of **84** being reduced at C-12 and C-21 positions. The ^{13}C NMR spectrum further confirmed the presence of HC-12 and H_2C-21 at 61.6 and 40.9 ppm, respectively, which indicates a shift from an alkene to an alkane. Furthermore, two-dimensional Nuclear Overhauser Effect Spectroscopy (2D NOESY) experiments were carried out to ascertain the relative stereochemistry at C-12. There were significant cross-peaks between H-12 & H-15 and between H-13 & H-21. The lowest-energy conformation of **84** was calculated using Spartan 10 molecular modelling software (WAVEFUNCTION, INC). The calculation was carried out using the setup menu in Spartan, with the specification of equilibrium

conformation, at ground states, Semi-Empirical Model at AM1 level. This calculation revealed that the (*S*)-configuration had the lowest energy and predicted the distances between H-12 & H-15, and between H-13 & H-21 to be 2.61 and 2.37 Å, respectively (Figure 2.3). 2D NOSY NMR showed significant interaction between these protons and supported the *(S)*-configuration at C-12, which further indicates that the hydride attacked the C-12 position from the less hindered backside of the heterocyclic ring structure. HRMS analysis revealed the exact mass of 361.2104, $C_{20}H_{28}N_2O_4$ required 361.2127.
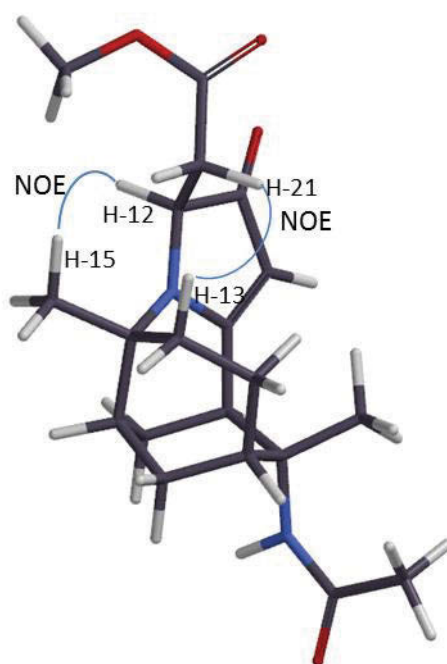
Figure 2.3: Molecular model of compound **84** (Spartan 10, generated structure), showing NOE correlations between H-12 and H-15, and H-13 and H-21.

2.1.3.2 Reductive alkylation, reduction and hydrogenation

In 1978 Delpech and Khong-Huu synthesised the bridged imine **85** from (-)-α-pinene which was later reduced to the amine **86**. This compound was then reacted with formaldehyde to afford in 88% yield the azaadamantane derivative **87** (Scheme 2.12).[128]
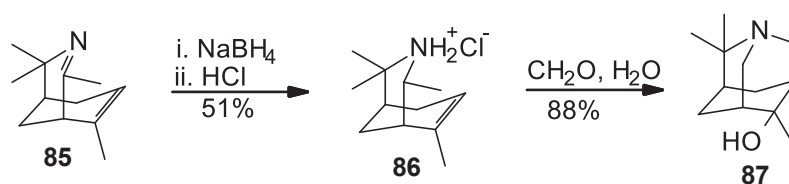
Scheme 2.12: Delpech and Khong-Huu's synthesis of compound **87** from bridged imine **85**.

A similar reduction process can be observed in Stevens and Kenney's approach to (+)-makomakine **89a** and (+)-aristoteline **89b** as shown in Scheme 2.13.[129]
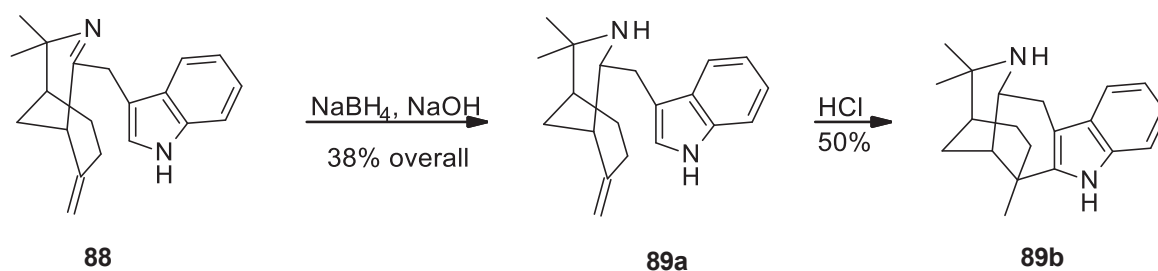
Scheme 2.13: Stevens and Kenney's approach to (+)-makomakine **89a** and (+)-aristoteline **89b**.

The reactivity of these bridged imine products can act as the basis for the further synthesis of additional novel alkaloid-like molecules and hence was used as a stepping-stone for the synthesis of novel compounds (Scheme 2.14).
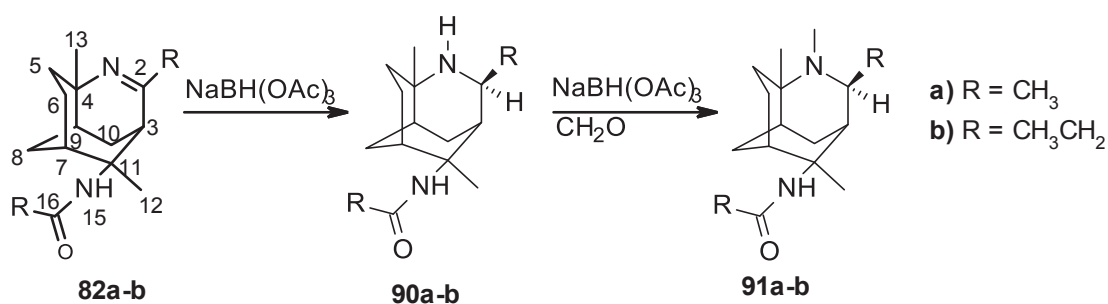
Scheme 2.14: Subsequent reactions following the Bridging Ritter reaction.

Reduction of **82a-b** was carried out under mild reduction conditions with $NaBH(OAc)_3$ in dry methanol (Scheme 2.14). The hydride reduces exclusively at the C-2 site of the imine from the less hindered face of the tricyclic ring structure to yield compounds **90a-b** in 71%, and 97% yields, respectively.

Structures of **90a-b** were confirmed by NMR analysis. The ^{1}H NMR spectra showed the newly formed H-2 resonances at δ 3.50 (quintet, J = 7.50 Hz), and δ 3.12 ppm (quintet, J = 5.50 Hz), for **90a** and **90b** respectively. The rest of the proton resonances remained similar to that of their corresponding imines, with slight upfield shifts of H-3. HRMS analysis further confirmed the identities of **90a-b**. The stereochemistry of C-2 was evident in 1D NOESY NMR studies where cross peaks were observed for H-14 and H-6 (Figure 2.4). This stereoselectivity results from the front face of the cyclic ring system being hindered by the bicyclic hexane rings.
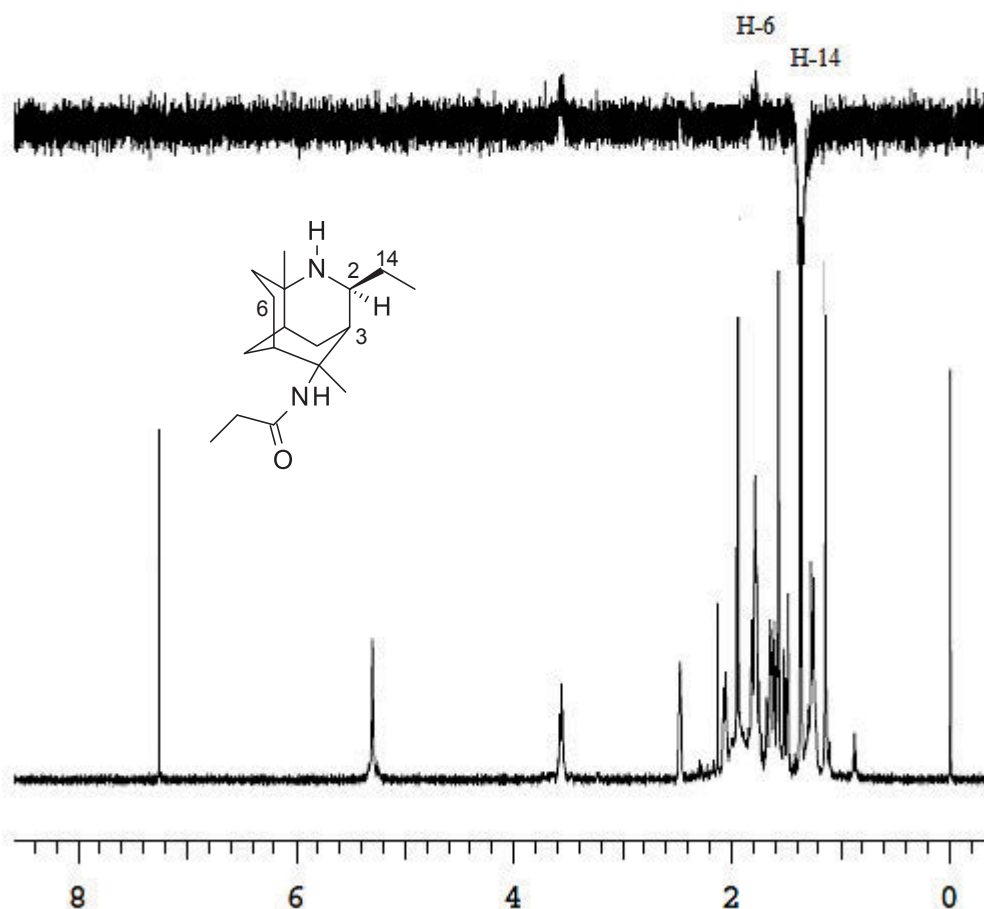
Figure 2.4: 1D NOESY NMR of compound **90b**, showing region 0.00 – 8.00 ppm.

Compounds **90a-b** were then subjected to reductive alkylation with 28% formaldehyde to yield compounds **91a** and **91b** in 49% and 26% yield, respectively. The experimental yields of **91a-b** highlight the significance of steric hindrance of the substituents at the C-2 position, making the amine less accessible by the formaldehyde.

Structures of **91a-b** were confirmed by NMR analysis; the ^{1}H NMR showed the newly formed –NCH$_3$ resonances at δ 2.29 and 2.42 ppm, respectively. While the ^{13}C NMR confirmed the presence of two –NCH$_3$ peaks at δ 35.97 and 39.16 ppm corresponding to the structure of **91a** and **91b** respectively, the rest of the spectral features remained relatively similar to that of their corresponding amines. Identities of **91a** and **91b** were further confirmed by HRMS analysis.

The chemistry used to produce **91a-b** from **82a-b** was also performed on the chloro-substituted compound **82c**. The reduction of **82c** using either NaBH(OAc)$_3$ or NaBH$_4$ failed to provide the desired product. The ^{1}H NMR analysis of the crude product revealed a mixture of unidentified compounds. In the attempt to reduce **82c** by hydrogenation in the presence of 5% Pd/C, an unexpected product **92** was isolated in 79% yield (Scheme 2.15). The formation of **92** can be explained *via* the palladium catalysed dehalogenation of α-haloamides.[130-131] Compound **92** was then subjected to reduction using NaBH$_4$ to give **93** in 72% yield. The structure of **93** was confirmed by NMR analysis; the ^{1}H NMR spectrum showed the newly formed H-2 (quintet, δ 3.61 ppm, J = 7.00 Hz) resonance. The rest of the spectrum remained similar to that of reduced imines **90a-b**.
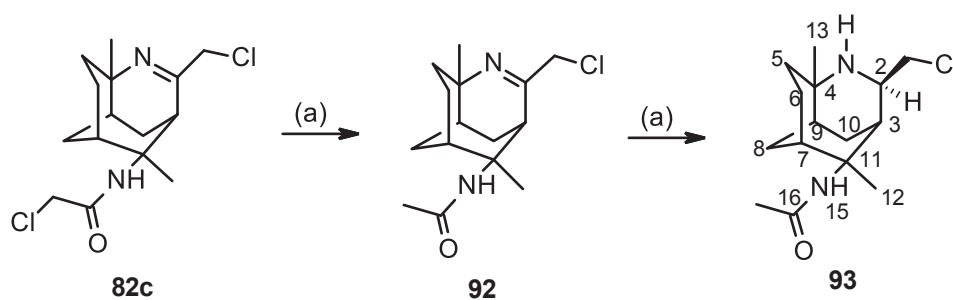
Scheme 2.15: Hydrogenation of compound **82c**. Reaction conditions: (a) Pd/C, H$_2$ in dichloromethane.

2.2 Drug-like properties of synthesised compounds

Molecular modelling programs such as Discovery Studio (DS) 4.5 can help visualise, build and analyse complex molecular models as well as interpret and predict the drug-like properties of compounds *via* ADMET (absorption, distribution, metabolism, excretion, and toxicity) and QSAR studies (quantitative structural activity relationship).[132] QSAR studies can be a powerful tool for medicinal chemists to gain a better insight into the structural activity relationship (SAR), to help suggest new molecules to synthesise with the desired biological activities.

The term drug-likeness is often used in drug design; it is a qualitative concept used to determine how "drug-like" a compound is. Factors such as bioavailability, solubility in both water and fat (LogP value), potency (IC_{50} value), molecular weight, and substructures with known pharmacological properties can all affect the drug-likeness of a compound. Lipinski's rule of five is a traditional method used to evaluate the drug-likeness of compounds. The rules describe the pharmacokinetics of a drug in an organism which includes their absorption, distribution, metabolism, and excretion (ADME). However, it does not predict a compound's toxicity or if the compounds pharmacologically active. Based on the rule of five, an orally active drug has no more than one violation of the following rules:

- LogP is not greater than 5

- Molecular mass is less than 500 Daltons

- No more than 5 hydrogen bond donors

- No more than 10 hydrogen bond acceptors

Despite the predictive power of the rule of five, many use this as more of a guideline, as 16% of oral drugs violate at least one of the criteria, and 6% of the natural product-derived drugs violates two or more. Known drugs such as Atorvastatin (Lipitor) **94** and Montelukast (Singulair) **95** violate more than one of Lipinski's rules (Figure 2.5).[133]

94   **95**
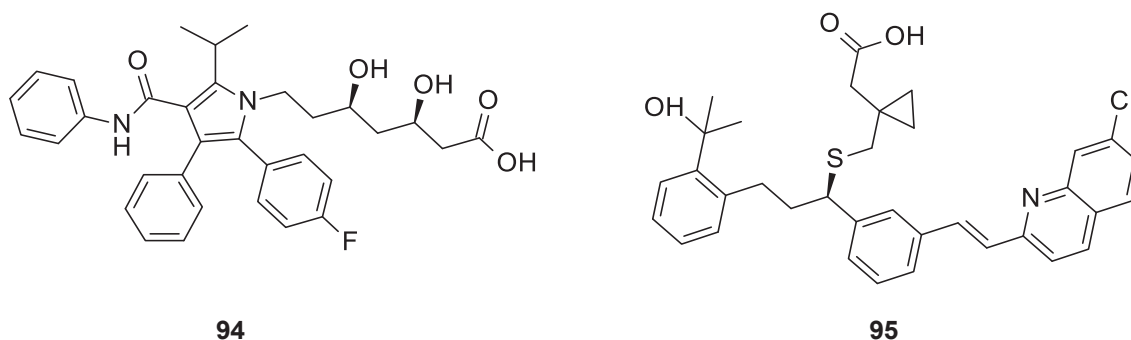
Figure 2.5: Drugs used to treat cardiovascular disease and asthma that violate Lipinski's rule, Lipitor **94**, and Singulair **95** respectively.

Modern methods such as a quantitative estimate of drug-likeness (QED) implemented by modelling software such as Discovery Studio provides a quantitative metric system for assessing the drug-likeness of compounds in early-stage drug discovery. QED values can range from zero (all properties unfavourable) to one (all properties favourable).[133] Based on the molecular properties calculated by Discovery Studio all of the synthesised compounds obeyed Lipinski's rules of five, as well as scoring highly (closest to 1, 0 − 1 scale) on the concept of drug-likeness (QED) (Table 2.1). This indicated that all compounds would make ideal drug candidates for further development.

Table 2.1: Drug-likeness and predicted molecular properties of synthesised compounds, as calculated in Discovery Studio.

Compound	MW[a]	LogP[b]	Solubility	HA[c]	HD[d]	Fractional PSA[e]	QED
82a	248.189	1.167	-3.729	2	1	0.150	0.756
82b	276.220	2.500	-4.450	2	1	0.133	0.860
82c	316.111	2.232	-4.983	2	1	0.134	0.811
63	358.189	1.079	-3.280	4	1	0.206	0.603
84	360.205	0.935	-2.954	4	1	0.204	0.755
90a	250.205	1.105	-3.310	1	2	0.149	0.732
90b	278.236	2.295	-4.061	1	2	0.132	0.831
91a	264.220	1.641	-2.861	1	1	0.107	0.781
91b	292.251	2.831	-3.598	1	1	0.096	0.867
92	282.150	1.699	-4.396	2	1	0.141	0.783
93	284.166	1.421	-3.990	1	2	0.140	0.753

[a]MW: molecular weight
[b]LogP: logarithm of partition coefficient between *n*-octanol and water
[c]H-acceptors: hydrogen bond acceptors
[d]H-donors: hydrogen bond donors
[e]Fractional PSA: the ratio of polar surface area divided by the total surface area

2.3 ADMET studies

Molecular modelling programs can be applied to find ligands that will specifically interact with a receptor in a hydrophobic, electrostatic and/or hydrogen bonding manner. However, sometimes the best docking score does not always guarantee the desired activity or minimise undesirable side effects. Therefore, during the early stages of drug design one should also take into consideration the pharmacokinetics of the drug from the point of administration to the point that the drug is excreted from the organism. DS 4.5 took into account the ADMET descriptors of ligands and calculated the following absorption, distribution, metabolism, excretion, and toxicity properties:

Absorption level predicts human intestinal absorption (HIA) after oral administration.

- Zero indicates good absorption; one indicates moderate, two means low absorption

Blood-brain barrier penetration predicts blood-brain barrier (BBB) penetration after oral administration.

- Zero indicates very high penetrant, one indicates high, two indicates medium, three indicates low penetrant

Cytochrome P450 2D6 (CYP2D6) inhibition predicts CYP2D6 inhibition (inhibition can cause drug-drug interaction).

- True/False – classification whether a compound is a CYP2D6 inhibitor

Hepatotoxicity predicts potential organ toxicity.

- True/False – classification whether a compound is hepatotoxic

Plasma protein binding predicts whether a compound is likely to be bound to carrier proteins in the blood. Plasma protein binding of a drug can affect the efficiency of the drug.

- True/False – classification whether a compound is highly bounded ($\geq$ 90% bound) to plasma proteins.

Aqueous solubility predicts the solubility of each compound in water at 25 ºC

- One indicates very low solubility; two indicates low, three indicates good solubility.

Based on the ADMET predictions calculated by Discovery Studios (Table 2.2), all of the synthesised compounds observed good human intestinal absorption scores, as well as highly unlikely to cause drug-drug interactions due to liver metabolism, which suggests the good bioavailabilities of these synthesised compounds. As expected, most of the compounds were predicted to have medium to low blood-brain barrier penetration abilities due to their predicted aqueous solubility and logP values.

Furthermore, three of the eleven compounds were predicted to observe hepatotoxicity, while two were predicted to bind to the plasma protein. It is worth noting that these two calculations do not take into account the IC_{50} of the compounds; to determine a compound's toxicity the IC_{50} of the compound would need to considered. Furthermore, the ADMET plot seen in Figure 2.6 showed all the calculated compounds fall within the 95 – 99% confidence eclipses, which indicates that the predictions are mathematically valid.

Table 2.2: ADMET properties of synthesised compounds, as calculated in Discovery Studio.

Compound	HIA level[a]	BBB[b]	CYP2D6[c]	Hepatotoxicity	Plasma protein binding	Aqueous solubility
82a	0	2	False	True	False	3
82b	0	2	False	False	True	3
82c	0	2	False	True	True	3
63	0	3	False	False	False	3
84	0	3	False	False	False	3
90a	0	2	False	False	False	3
90b	0	2	False	False	False	3
91a	0	2	False	False	False	3
91b	0	1	False	False	False	2
92	0	2	False	True	False	3
93	0	2	False	False	False	3

[a]HIA level: human intestinal absorption level (inside 95% confidence level)
[b]BBB: blood brain barrier penetration levels
[c]CYP2D6: classification whether a compound is a CYP2D6 inhibitor using the cut-off Bayesian score of 0.161
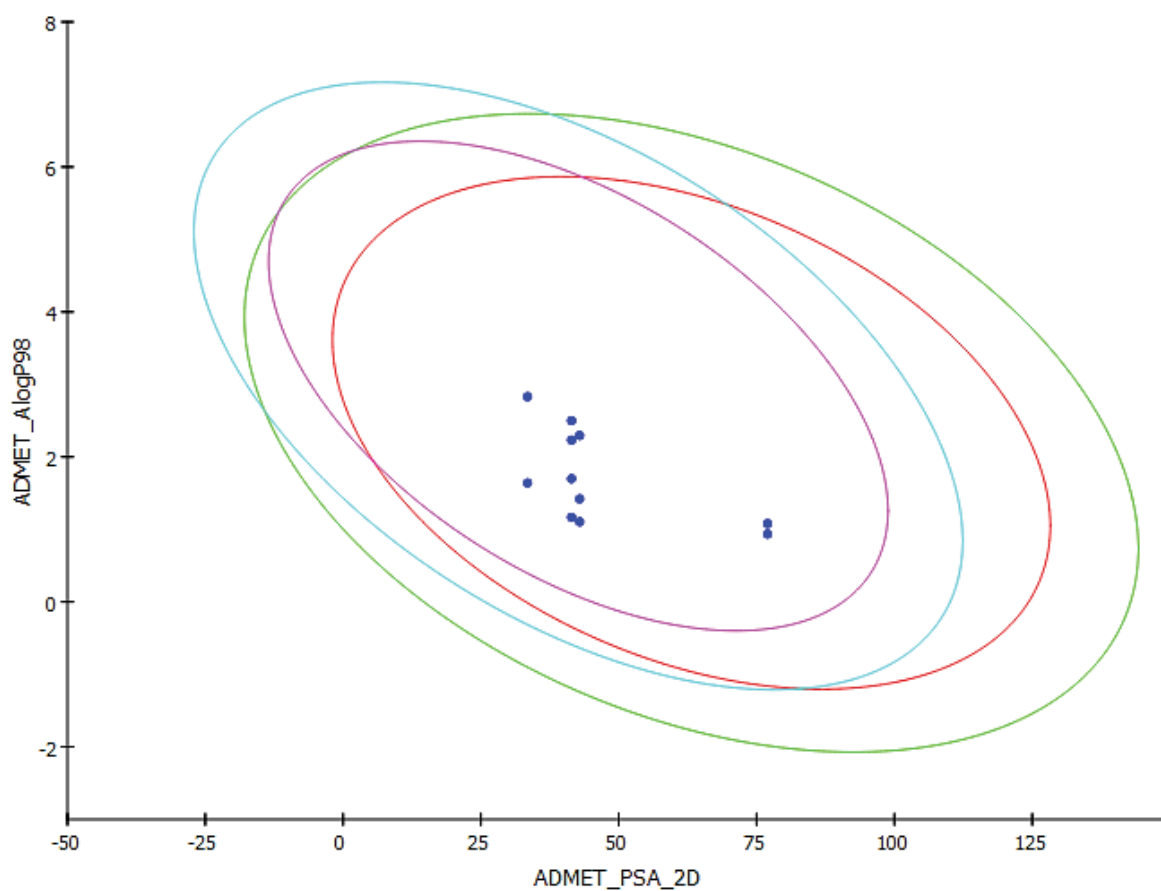
Figure 2.6: ADMET pot of synthesised compounds, as plotted in Discovery Studio.

This study has determined that the Bridging Ritter reaction can be used to synthesise structurally unique alkaloid-like compounds with desirable calculated drug-like properties. For this reason, the nature of these alkaloid-like molecules will be explored in more detail through the synthesis and derivatisation of tri-cyclic alkaloids using caryophyllene **96** and monoepoxy **117**, as described in Chapter 3.

Chapter 3 Synthesis of tricyclic alkaloids using Caryophyllene and Monoepoxy

3.1 Introduction

Alkaloids are a well-established drug source *via* semi-synthesis to provide libraries of compounds that have drug-like properties.[134] These caryophyllene derived alkaloid-like libraries of compounds can provide a new class of leads for current drug discovery programs. As part of our ongoing research for alkaloid-like compounds as anti-cancer agents,[115-116] a library of tricyclic caryophyllene derivatives has been developed and described in this chapter. The synthesis of the library will be described using the Ritter reaction as the key reaction.

Caryophyllene **96** can be found most abundantly in the stems and flowers of the clove tree *Eugenia caryophyllata*; in its unusual *trans*-fused ring structure. The complete stereochemistry of *trans*-caryophyllene and its *cis* isomer (isocaryophyllene) have been previously determined.[135-137] The first total synthesis of *trans*-caryophyllene and isocaryophyllene conducted by Corey *et al.* reinforced the *endo*-double bond arrangements in *trans*-caryophyllene and isocaryophyllene are indeed *trans* and *cis*, respectively.[138]

In the early 1950s, Aebi *et al.* wrote a series of papers documenting the absolute configuration of caryophyllene and its derivatives.[135, 137, 139-140] The unusual molecular geometry of caryophyllene had led Corey *et al*. to choose it as the target for their synthesis. Corey also reported the total synthesis of caryophyllene and isocaryophyllene. The reaction proceeds *via* the synthesis of a fused four and six-membered rings **98** by a photochemical cycloaddition process, followed by the addition of the five-membered ring **103** *via* series of reactions (methoxycarbonylation, alkylation, carbonyl addition and Dieckmann condensation). The nine-membered ring was then formed by removing the common carbon bond between the six and five-membered rings (Scheme 3.1).[138] Other groups subsequently reported other methods,

however, due to its complicated multi-step synthesis, it is more feasible to obtain caryophyllene from the plant.[141-144]
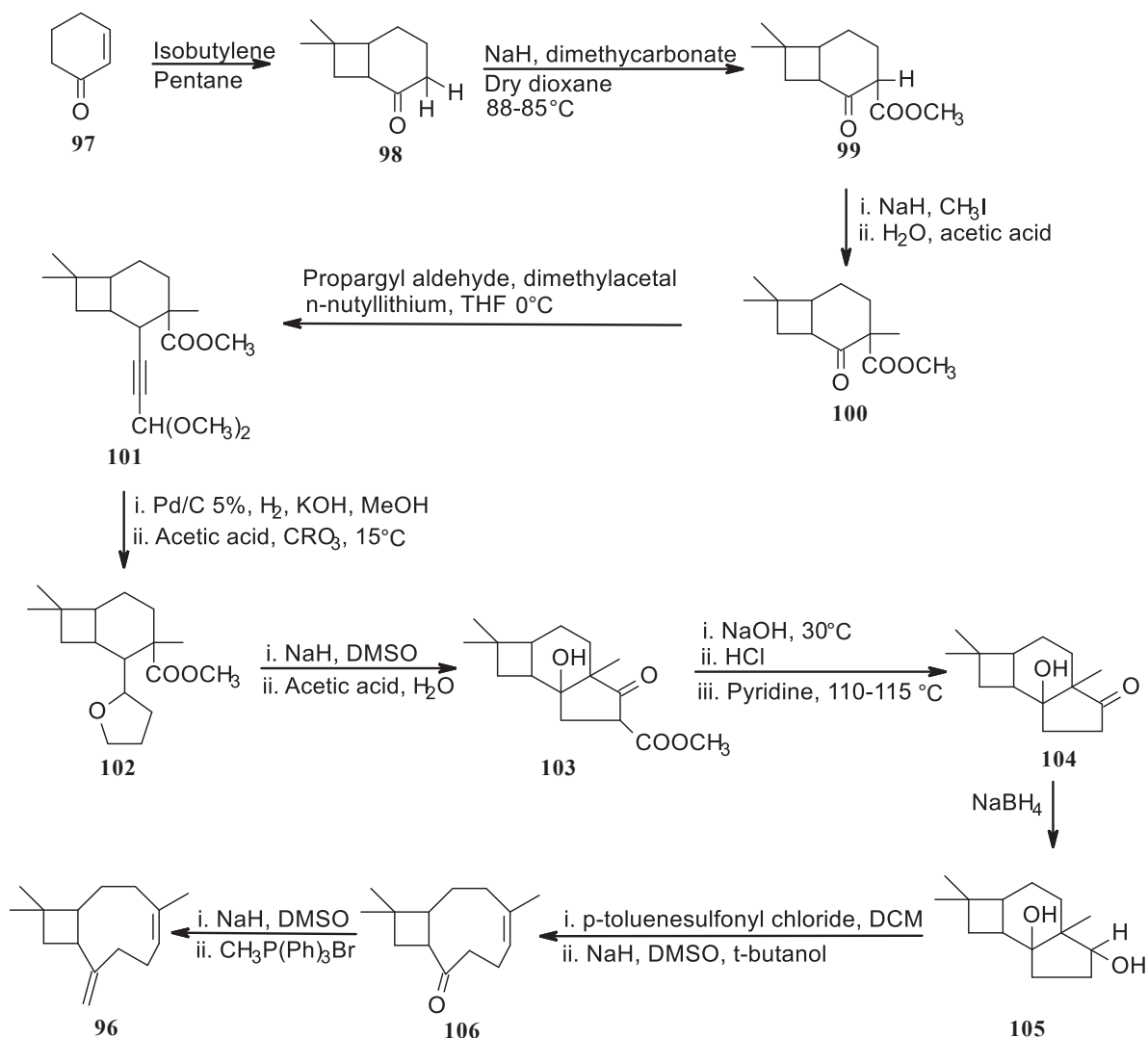
Scheme 3.1: Proposed synthesis of caryophyllene by Corey *et al.*[138]

Several reports have indicated that caryophyllene can exhibit a range of biological activities such as anti-inflammatory, antibiotic, antioxidant, and anti-carcinogenic effects.[138, 145] Caryophyllene is commercially available, low-cost, optically active, and already exhibits

therapeutic biological activities. It is, therefore, an attractive building block to generate a variety of tricyclic alkaloid-like compounds.

3.1.1 Cyclisation and Wagner-Meerwein Rearrangements

Acid catalysed Wagner-Meerwein rearrangement studies of caryophyllene have been well documented since the 1920s to understand the carbocations formation and transformation to the final products **107**, **108**, and **109**.

The rearrangement of caryophyllene in acidic media was demonstrated by multiple acid-catalysed studies.[135-137, 146-148] It was observed that when caryophyllene was treated with concentrated sulphuric acid in diethyl ether for 30 min, a product mixture of 14 hydrocarbons and four alcohols had formed. After three days the reaction mixture was simplified, and the major products isolated were mainly caryolane-1-ol **107**, clov-2-ene **108** and α-neoclovene **109** (Figure 3.1).[135]

107   **108**   **109**
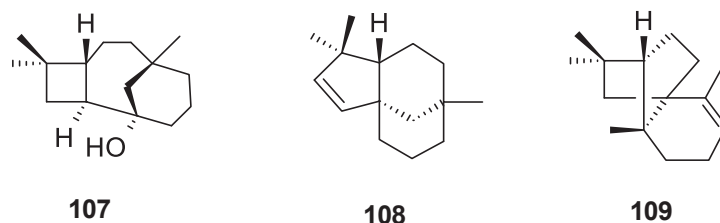
Figure 3.1: Structures of caryolane-1-ol **107**, clov-2-ene **108** and α-neoclovene **109**.

As mentioned earlier when caryophyllene was reacted under strong acidic conditions the sum of the products include the four-membered tricyclic caryolane (**107**, **110**) the five-membered tricyclic clovane (**108**, **111**).[149] Caryolane **110** and clovane **111** arose from the two major conformers of caryophyllene, ββ **112a** and αα **113a** respectively (Scheme 3.2). The internal double bonds in **112a** and **113a** selectively reacted first to generated **112b** and **113b** respectively. The internal bonds were more reactive than their corresponding external because

of the higher accumulation of sp^2 electrons than that of the externals. These cyclisations and rearrangements were reversible and led to the most stable isomers, product ratio could also depend on the reactivity and the size of the nitriles used.[150] The clovane **111** skeleton was formed *via* a cyclisation on the lower face of the molecule after the expansion of the four-membered ring (Scheme 3.2). Since the formation of the clovane skeleton **111** required an extra expansion step, it was, therefore, the kinetically unfavoured of the two skeletons.[150-151]
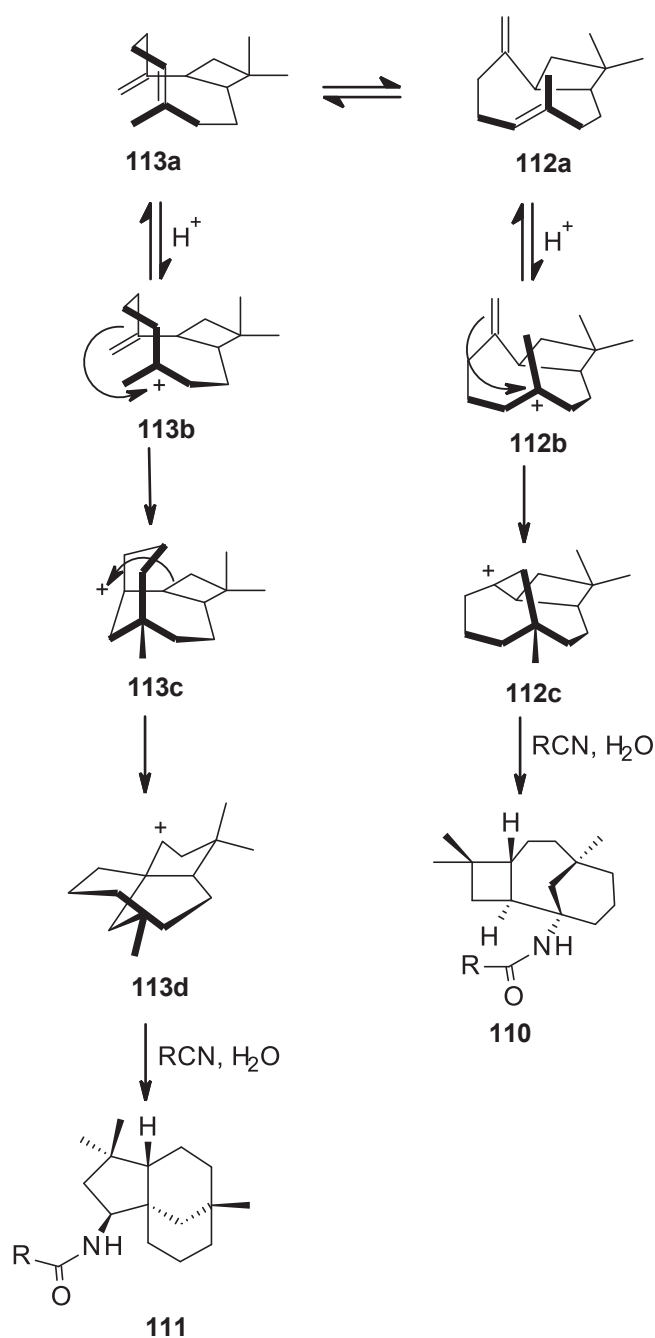
Scheme 3.2: Formation of caryolane **110** and clovane **111** skeletons.

3.1.2 Ritter reaction of caryophyllene with various nitriles

The transformations of *trans*-caryophyllene and its isomers, as well as their multistage rearrangements, were well documented *via* methods of acid catalysed rearrangements[149] followed by the nucleophilic addition of nitrile.[151-152] The unique cyclobutane fused to a nine-membered ring structure of trans-caryophyllene **96** has provided the basis for the synthesis of a variety of tricyclic alkaloid-like molecules. Further acid catalysed cyclisation studies of caryophyllene, and its monoepoxide will form the base of this chapter discussion.

Acid catalysed cyclisation studies of caryophyllene, and its monoepoxide revealed the formation of two tricyclic products, compounds **114** and **115** (Figure 3.2).[151]
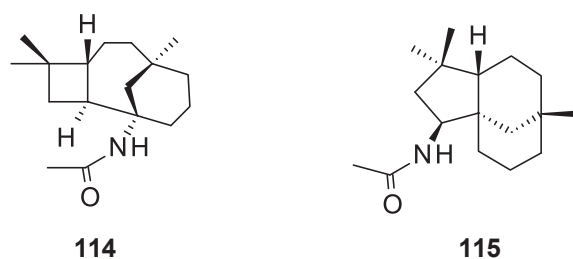
Figure 3.2: Structures of **114**, and **115**.

It was not until the early 2000s that chemists started exploring the chemistry of caryophyllene and the range of structurally unique compounds it can form.[150, 152] In light of this, Yarovaya *et al.* investigated the reactions of caryophyllene and its derivatives with acetonitrile under Ritter reaction conditions to yield optically active amides **114** $[\alpha]_D^{20}97.0^\circ$, and **115** $[\alpha]_D^{20}$-38.0° with tricyclic skeletons.[151] They observed the dissolution of caryophyllene **96**, isocaryophyllene **116**, caryophyllene 4β,5α-epoxide **117**, and isocaryophyllene 4β,5α-epoxide **118** in a system of acetonitrile and sulfuric acid followed by treatment with aqueous sodium hydrogen carbonate to afford tricyclic amides with two different cyclic skeletons (Figure 3.3). However,

the synthesis of tricyclic amides using various of nitriles with caryophyllene and derivatives were not explored.
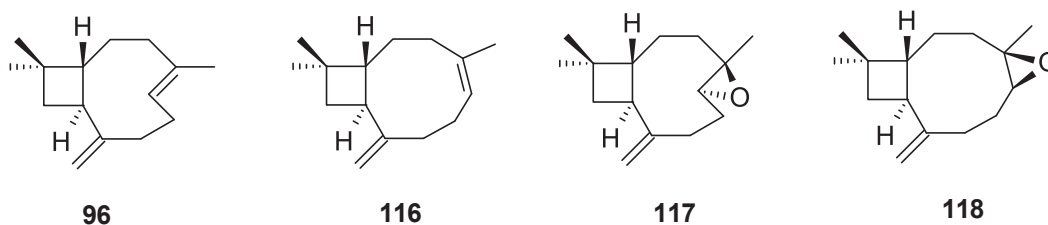
Figure 3.3: Structures of caryophyllene **96**, isocaryophyllene **116**, caryophyllene 4β,5α-epoxide **117**, isocaryophyllene and 4β,5α-epoxide **118**.

In this project, treating caryophyllene **96** with varies nitrile under strong acidic conditions afforded optically active tricyclic amides **119a-i** and **120a-d** (Table 3.1) of only two tricyclic skeletons, caryolane **119** and clovane **120** (Scheme 3.3).[151] The nitriles were chosen based on their reactivity and the ability to provide a variety of substituents at the C-18 position which can affect the biological activity of the respective compounds (Scheme 3.3). Furthermore, the reactivity of nitriles used and the observed yields of these compounds were a reflection on the composition of the two major conformers present in caryophyllene **96** under strong acidic conditions.
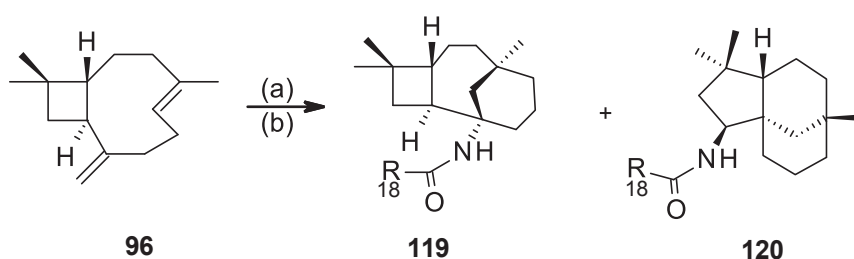
Scheme 3.3: General synthesis of **119** (caryolane), and **120** (clovane) from caryophyllene with various nitriles. Reaction conditions: (a) H_2SO_4, RCN. (b) H_2O.

It was observed that the dissolution of caryophyllene **96** with acetonitrile, propionitrile, chloroacetonitrile and benzonitrile under the Ritter reaction conditions furnished mainly optically active compounds of both caryolane **119** and clovane **120** skeletons in ratios of 1:1, 2:1, 3:1, and 4:1 respectively. It is expected that as the reactivity of the nitrile decreases with increase in the bulkiness, leading to the observed ratio of formation would favour the caryolane skeleton **119**. This selectivity toward the caryolane skeleton **119** was further confirmed when the least reactive and bulkier nitriles were used (Table 3.1).

Table 3.1: List of tricyclic amides synthesised from caryophyllene **96**.

Compound	R	Yield (%)	$[\alpha]_D^T$ (°)
119a	CH_3	36	49.6
119b	CH_3CH_2	55	42.9
119c	$ClCH_2$	63	30.6
119d	Ph	57	27.3
119e	$CH_3CH_2CH_2CH_2$	58	50.7
119f	$ClCH_2CH_2CH_2CH_2$	59	27.7
119g	$ClCH_2CH_2$	29	32.3
119h	H_2NCH_2	75	-21.0
119i	CH_3S	1	31.0
120a	CH_3	36	-24.4
120b	CH_3CH_2	28	-4.3
120c	$ClCH_2$	28	3.9
120d	Ph	19	18.0

The structures of the compounds shown in Table 3.1 were confirmed by 1D and 2D-NMR experiments, their assignments were based on the published data for *N*-[(*1R,2S,5R,8R*)-4,4,8-trimethyl-1-tricyclo[6.3.1.02,5]dodecanyl]acetamide **119a** and *N*-[(*1S,2S,5S,8S*)-4,4,8-trimethyl-2-tricyclo[6.3.1.01,5]dodecanyl]acetamide **120a**.[151] Similar chemical shifts and distinct splitting of H-2 and NH resonances proved the structural identities of synthesised compounds, while specific optical rotations suggest all synthesised compounds were optically active (Table 3.1). It is worth noting that the ^{1}H NMR spectra of all the caryolane **119a-i** skeleton compounds showed characteristic H-16 (δ 5.10 ppm), H-2 and H-11' (multiplet, δ

2.00 – 2.50 ppm) resonances (Figure 3.4). The coupling constants of H-2 and H-11' were not possible to be measured. The overlapping of H-2 and H-11' was confirmed by the HSQC NMR experiment (Figure 3.5).
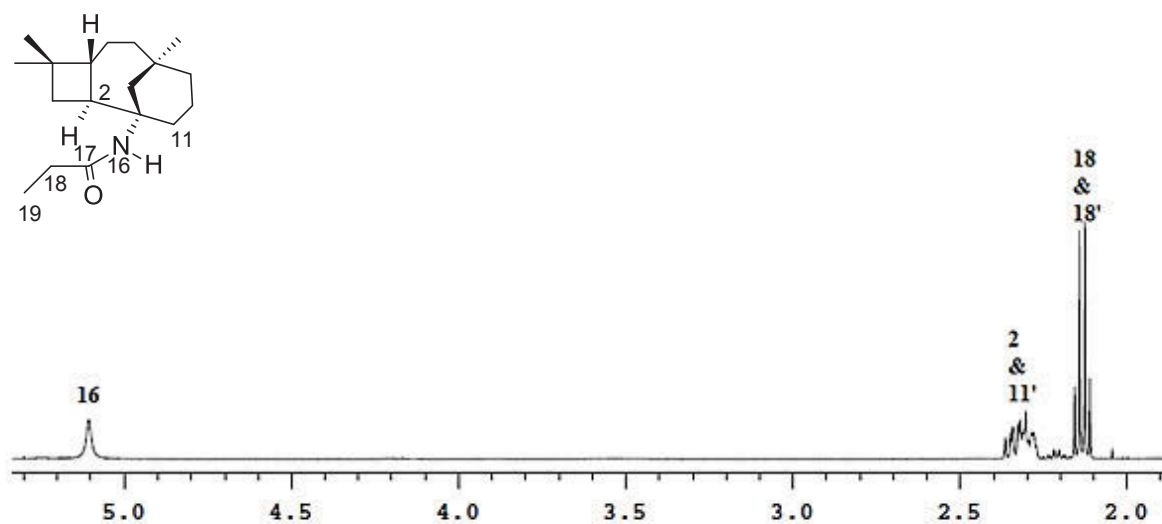
Figure 3.4: ^{1}H NMR spectrum of compound **119b**, showing region 2.00 – 5.80 ppm.
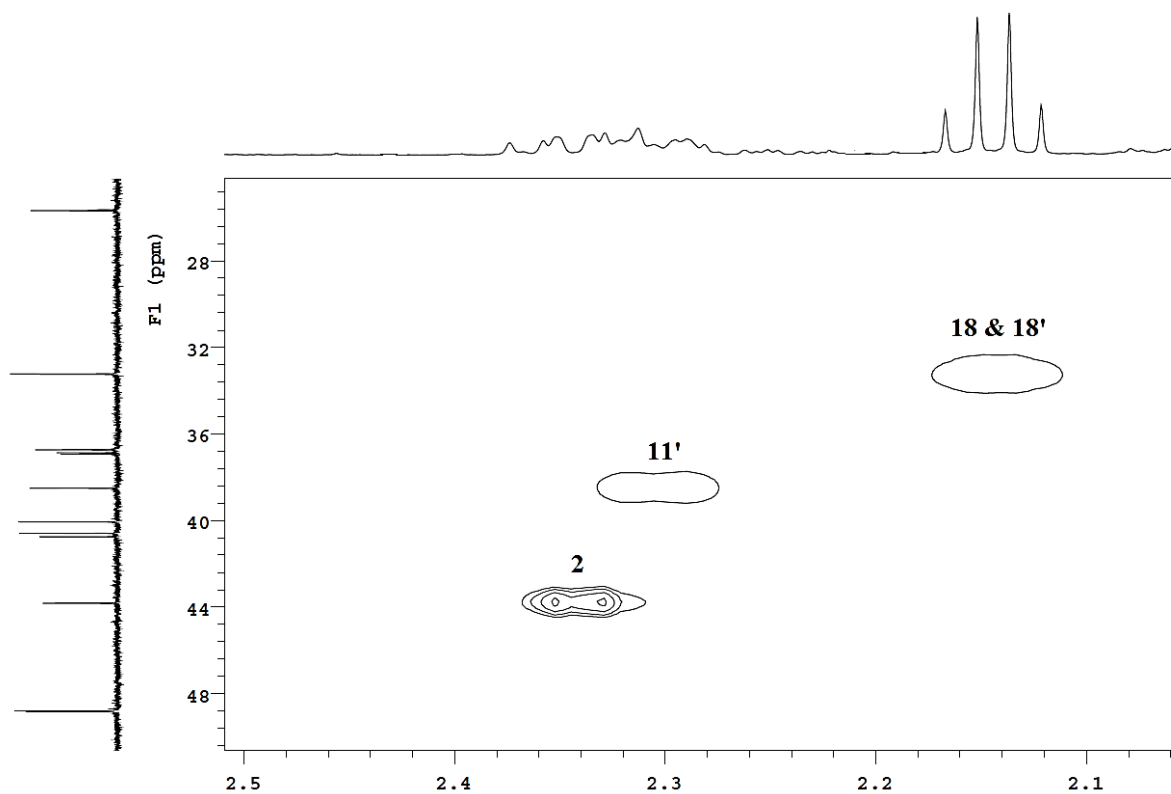
Figure 3.5: 2D HSQC spectrum of compound **119b**, showing region 2.10 – 2.50 ppm.

The ^{1}H NMR spectra of all the clovane **120a-d** skeleton compounds showed the characteristic H-16 (doublet, δ 5.25 ppm, J = 8.50 Hz) and H-2 (doublet of the doublet of doublets, δ 4.15 ppm, J = 6.00, 9.50, 12.50 Hz) resonances (Figure 3.6). Furthermore, the identities of the synthesised compounds were supported by HRMS analysis.
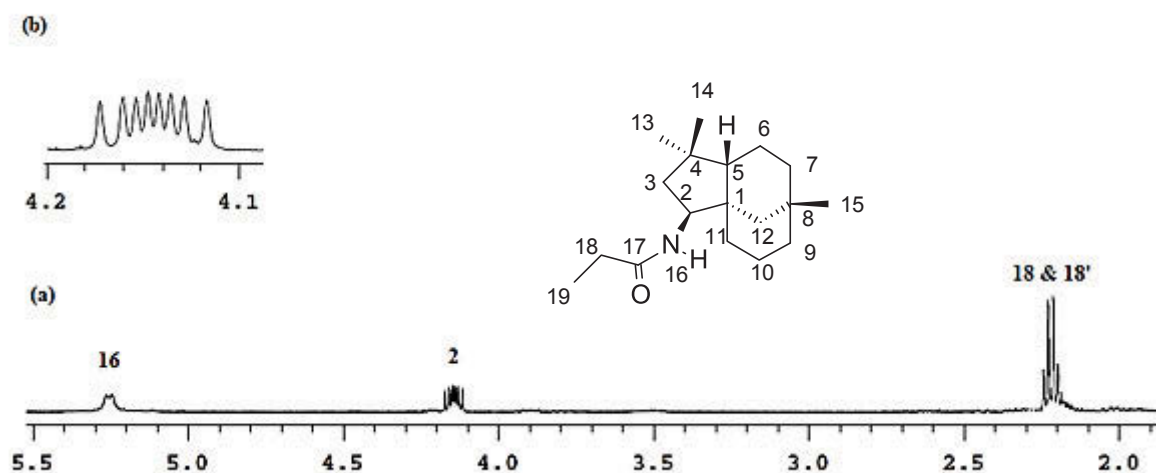
Figure 3.6: (a) ^{1}H NMR spectrum of compound **120b**, showing region 2.00 – 5.50 ppm, (b) Expansion of region 4.10 – 4.20 ppm.

3.1.3 Ritter reaction of caryophyllene monoepoxide with various nitriles

The formations of oxazolines from the reaction of epoxides with nitriles were reported in literature.[153-156] In 2003, Yarovaya *et al.* reported the synthesis of substituted 2-oxazolines **122** and **123** under acid catalysed conditions of citral 6,7-epoxides **121** with acetonitrile. The reaction proceeds *via* the epoxide ring opening followed by the formation of the 2-oxazoline ring shown in Scheme 3.4.[157] However, there are no reports for the synthesis of oxazoline compounds using caryophyllene epoxide as starting material.
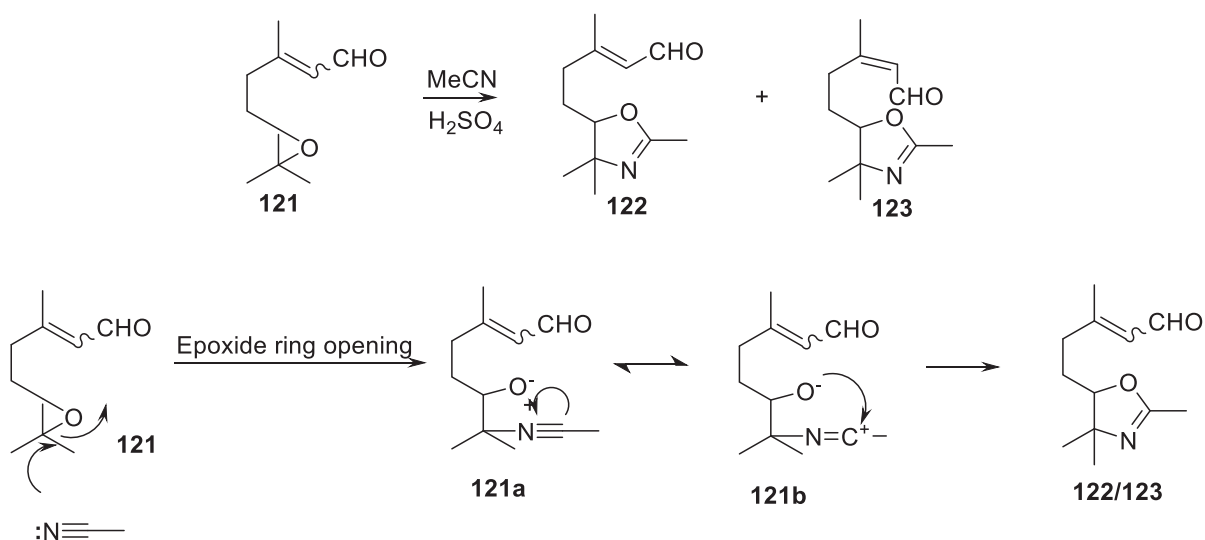
Scheme 3.4: Proposed mechanism of substituted 2-oxazolines **122/123** from 6,7-epoxide **121**.

Aebi, Barton and Lindsey demonstrated over a mild acid-catalysed hydration of caryophyllene oxide **117** and isocaryophyllene oxide to form glycol **124** stereoisomers at C-9 position (Scheme 3.5).[140]
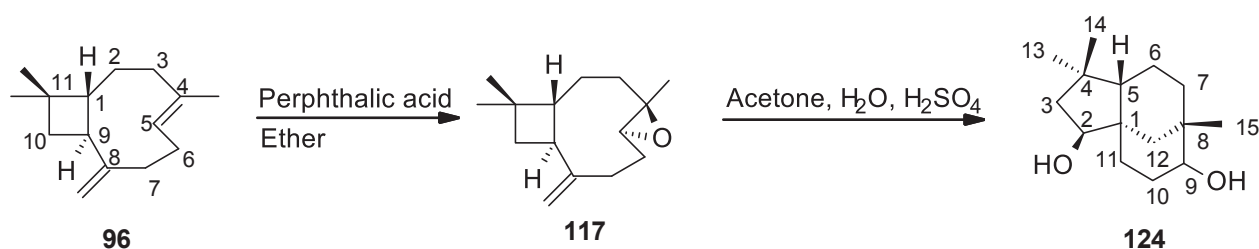
Scheme 3.5: General synthesis of glycol from caryophyllene.

With these synthetic outcome found in **117**, there is a great potential for **117** to be used as starting material. The approach would allow for the expansion of the library as well as diversifying the structures of the compounds.

The reaction between 4β,5α-epoxide **117** and various nitriles under Ritter reaction conditions yielded the alcohol-amide **125** and diamide structures **126** in four minutes (Scheme 3.6).
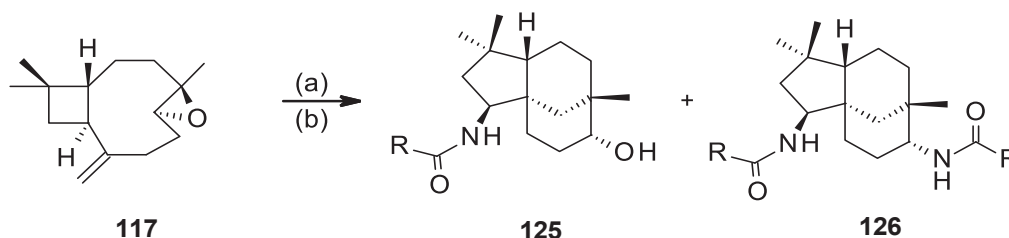
Scheme 3.6: General synthesis of compounds from caryophyllene monoepoxide **117** *via* the Ritter reaction. Reaction conditions: (a) H_2SO_4, RCN. (b) H_2O.

The reaction conditions were optimised by varying parameters such as reaction time (1 min – 4 h and 24 h) and temperature (0 °C for 30 min then at room temperature) with the attempt to favour the formation of alcohol-amide structure **125**. The ratio between the formation of compounds **125** and **126** was dependent on the duration of the reaction in an acidic medium as well as the size and nucleophilicity of the nitriles (Table 3.2). However, due to the catalytic nature of concentrated sulfuric acid that led to the formation of dication at C-2 and C-9 positions respectively. In which case, only the diamides **126a-e** were isolated (Table 3.3). It was observed that carbocations formed at the C-2 and C-9 positions, perhaps in less than 1 minute in the presence of concentrated sulfuric acid and acetonitrile at 0 °C. Reaction times were extended for the slightly weaker nucleophiles and/or bulkier nitriles to afford the diamide **126** as the only product.

Table 3.2: Ratio of formation of alcohol-amide and diamide based on the duration of the reaction.

Time (min)	Acetonitrile		Propionitrile	
	Compound **125a**	Compound **126e**	Alcohol-amide	Compound **126d**
1	4	1	-	-
5	-	1	-	-
30	-	1	-	-
60	-	1	-	-
120	-	1	-	-
180	-	1	-	1
240	-	1	-	1
Overnight	-	1	-	1

It is worth mentioning that the cation arising from the epoxide ring underwent rearrangement forming exclusively the clovane skeleton products **125** and **126** as shown in Scheme 3.7. Out of the two possible carbocations **117b** and **117d** that formed, **117b** underwent nucleophilic attack with another mole of nitrile to provide the clovane **125**. While **117d** reacted with 2 mole equivalent of nitrile to give **126** (Table 3.3).[158] The formation of the major diamide products **126a-e** resulted from the dehydration of **117c** to form carbocation intermediate **117d** that further reacted with another mole of nitrile to give **126**.
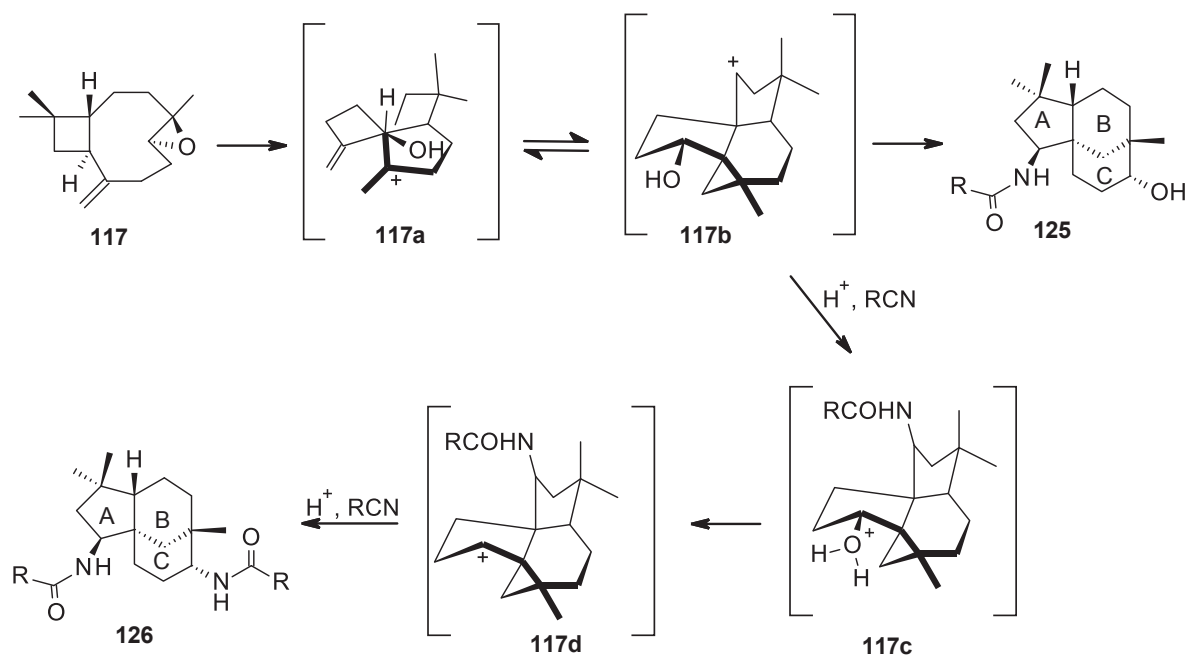
Scheme 3.7: Epoxide ring opening and rearrangement.

Table 3.3: List of tricyclic amide-alcohol, and diamides synthesised from caryophyllene monoepoxide **117**.

Compound	R	Yield (%)	$[\alpha]_D^T(°)$
125a	CH$_3$	20	-28.7
126a	ClCH$_2$	34	-15.4
126b	CH$_3$CH$_2$CH$_2$CH$_2$	9	-63.9
126c	Ph	17	0.36
126d	CH$_3$CH$_2$	56	-33.4
126e	CH$_3$	71	-54.4

The structures of the synthesised compounds **125a** and **126a-e** were confirmed using 1D and 2D-NMR experiments; their assignments were based on the spectral data from their corresponding mono-amides **120a-d**. The orientation of the amide substituents at the C-2 position in compounds **125a** and **126a-e** were assigned based on published data for clovane-2,9-diols **124**, similar chemical shifts and coupling constants confirmed the orientations of the amides.[137] The ^{1}H NMR spectra for compounds **125a** and **126d** are analogous to each other,

with the exception of H-9 resonances. The vicinal coupling constant for H-9 (doublet, δ 3.60 ppm, J = 9.00 Hz) for compound **126e** indicates that it is in the equatorial conformation as the C ring exists in the chair conformation. Similar coupling constants were observed for all diamide compounds **126a-e**. 2D NOESY experiment was carried out for compound **126e** to ascertain the relative stereochemistry at C-9. There were no cross-peaks observed between H-9 and H-15 protons which supported the *(R)*-configuration at C-9 (Figure 3.7).
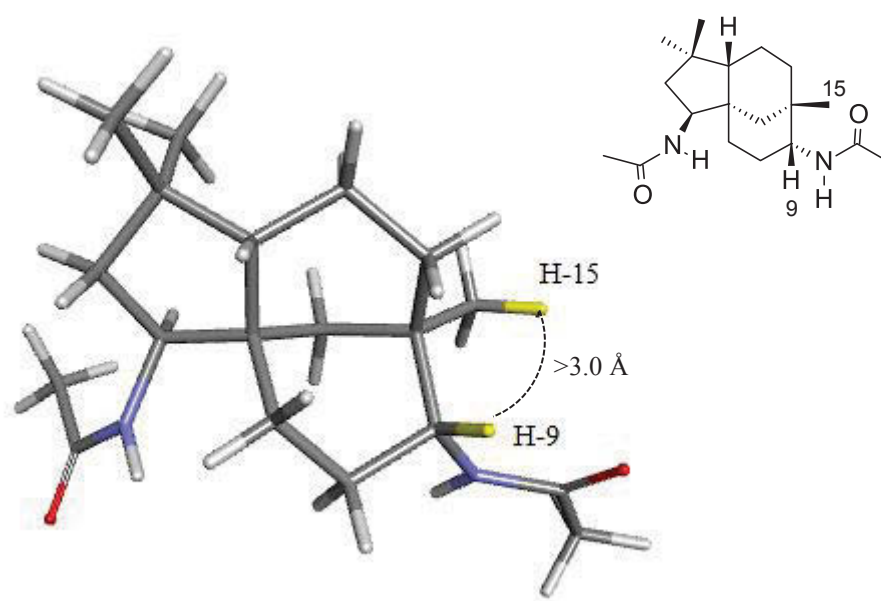
Figure 3.7: Molecular model of compound **126e** (Discovery Studio 4.5), showing no NOE correlations between H-9 and H-15 protons.

Consequently, H-9 (quartet, δ 3.30 ppm, J = 7.00 Hz) in compound **125a** is also in the equatorial position while the hydroxyl group is in the axial position as previously established in the literature.[137] 2D NOESY experiment was also carried out for compound **125a** to confirm the relative stereochemistry at C-9. There were no cross-peaks observed between H-9 and H-15 protons and supported the *(R)*-configuration at C-9 (Figure 3.8).
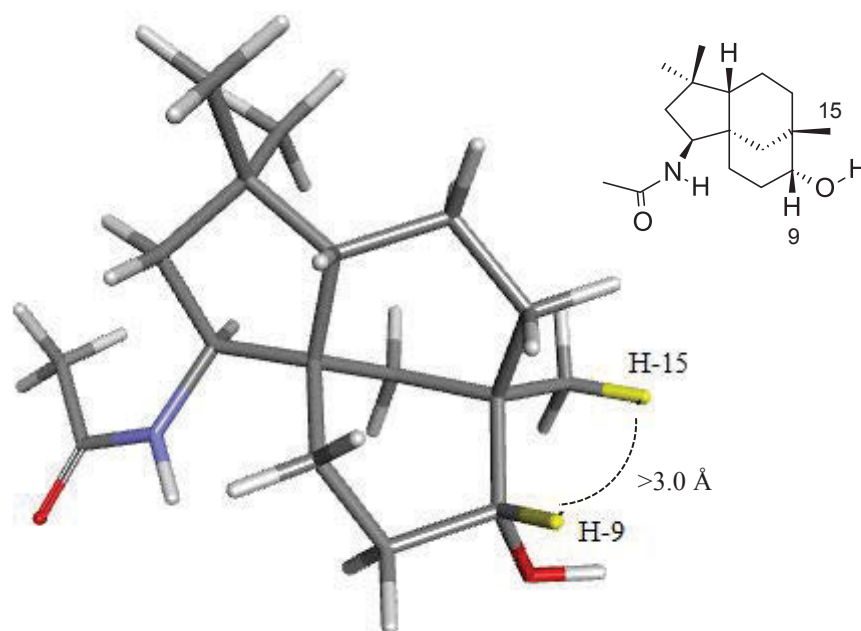
Figure 3.8: Molecular model of compound **125a** (Discovery Studio 4.5), showing no NOE correlations between H-9 and H-15 protons.

It is worth mentioning that the ^{1}H NMR spectra for the rest of the synthesised compounds showed characteristic H-2 (doublet of doublet of doublets, δ 4.15 ppm, J = 6.00, 9.50, 12.50 Hz) splitting for a clovane skeleton (Figure 3.9).
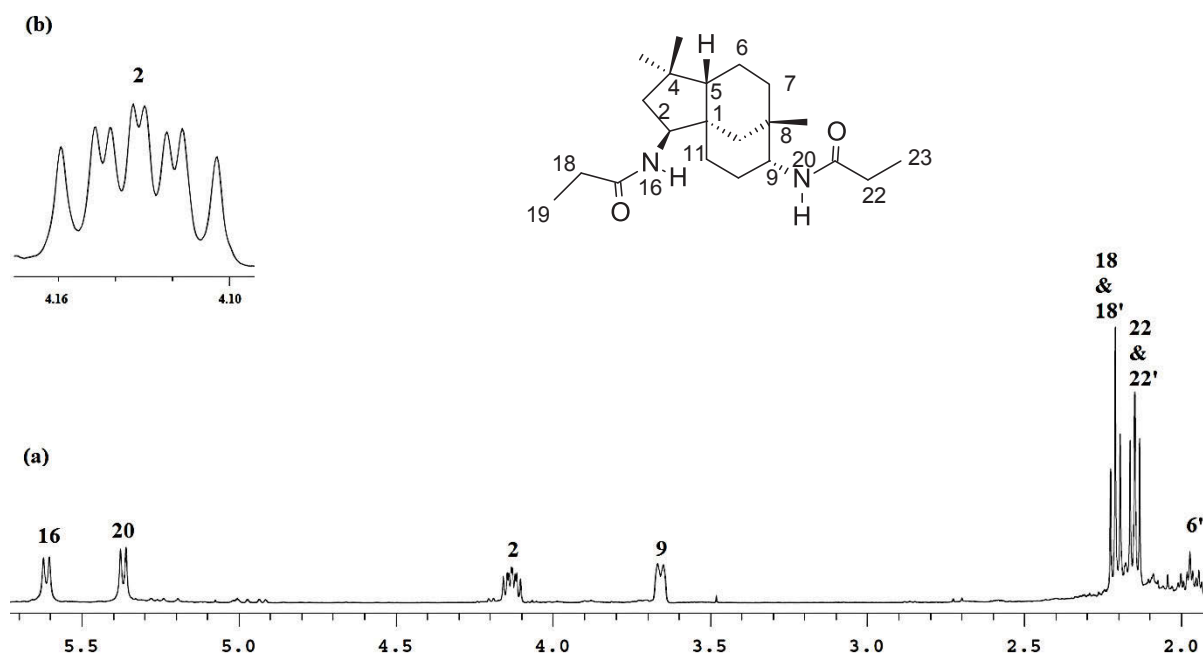
Figure 3.9: (a) ^{1}H NMR spectrum of **126d**, showing region 2.00 – 5.80 ppm, (b) Expansion of region 4.10 – 4.16 ppm.

3.2 Derivatisation of caryolane and clovane amines

The amide compounds described in Chapter 3.1.2 observed great potentiating anticancer effects against the triple-negative MDA-MB-231 breast cancer cell line (Figure 4.3). In light of this, the observed drug-like properties of these synthesised amides would make them ideal starting materials for further derivatisation. A small library of novel amines with similar structural integrity as their parent compounds **119c**, and **120c** has been developed using reductive alkylation, and their synthesis described in this chapter.

3.2.1 Amide cleavage under mild acidic conditions

As previously mentioned in Chapter 3, the Ritter reaction with caryophyllene resulted in the formation of two amide compounds **119c** and **120c**. The chloroacetyl (ClCH$_2$CO) group can

be readily cleaved under mild conditions with thiourea and acetic acid to afford primary amines **127a**, **128a** and **129** in reasonable yields, 58, 65, and 33% respectively (Scheme 3.8). Amines **127a** and **128a** were further derivatised *via* reductive alkylation with various aldehydes. The outcome of these reactions will be discussed in detailed in section 3.2.2.
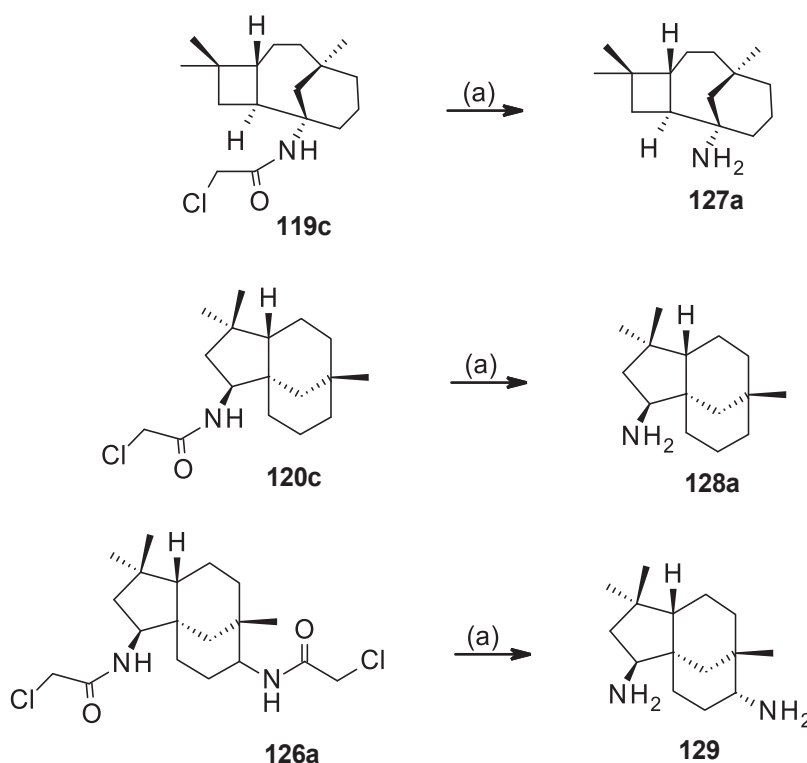
Scheme 3.8: Amide cleavage under mild acetic conditions, followed by reductive alkylation. Reaction conditions: (a) thiourea (2-mole equiv.), acetic acid in dry ethanol, reflux overnight.

The structures of the compounds **127a**, **128a** and **129** shown in Scheme 3.8 were confirmed by 1D and 2D-NMR experiments; their assignments were based on the spectral data from their respective amides **119c**, **120c**, and **126a**. Similar chemical shifts and coupling constants proved the structural identities of these compounds. The ^{1}H NMR spectral data of compounds **133a** and **134a** showed the absence of chloroamide (ClCH$_2$CONH) resonances at δ 5.30 ppm. This was further confirmed by the absence of carbonyl resonances in the typical region of δ 172 ppm in the ^{13}C NMR spectra of **133a** and **134a**.

Furthermore, the H-2 (doublet of triplets, δ 2.26 ppm, J = 2.50, 16.00 Hz) splitting pattern for **127a** remained the same for a caryolane skeleton (Figure 3.10c). Whereas, the ^{1}H NMR spectrum for **128a** showed changes in the H-2 (doublet of doublets, δ 2.86 ppm, J = 5.50, 12.00 Hz) splitting which have not been observed before for a clovane skeleton (Figure 3.10a). The observed upfield chemical shift of H-2, as well as the change of splitting patterns in comparison to that of its precursor **118c** (Figure 3.10b), was expected for compound **128a** due to the presence of the primary amine functional group. Despite these small spectral differences, the rest of the NMR spectrum of **128a** remained relatively similar to its respective amide **120c**.
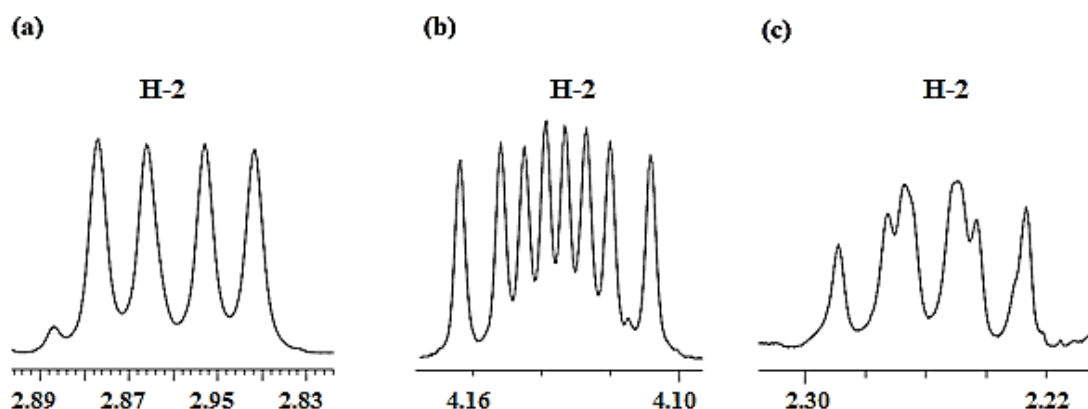
Figure 3.10: (a) ^{1}H NMR spectrum of **128a**, showing H-2 as a doublet of doublet at δ 2.86 ppm. (b) ^{1}H NMR spectrum of **120c**, showing a characteristic H-2 splitting pattern for clovane skeleton at 4.13 ppm. (c) ^{1}H NMR spectrum of **127a,** indicating a characteristic H-2 splitting pattern for caryolane skeleton at δ 2.26 ppm.

It is worth noting that due to the presence of the amine (NH$_2$) functional group, similar upfield chemical shift and changes in H-2 (doublet of doublets, δ 2.87 ppm, J = 6.00, 12.50 Hz). The

splitting pattern was also observed in the ^{1}H NMR spectrum of compound **129** (Figure 3.11) in comparison to its respective amide **126a**.
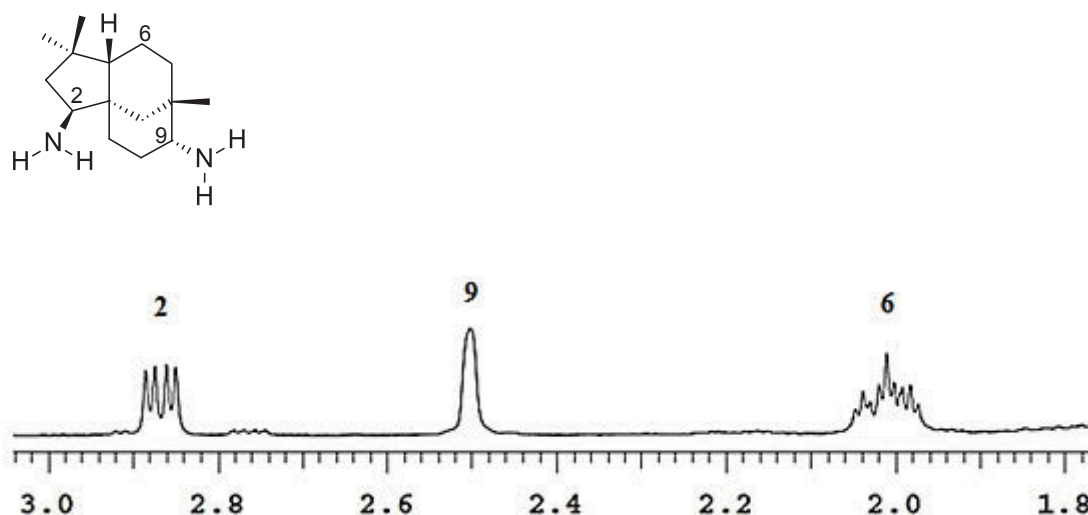
Figure 3.11: ^{1}H NMR spectrum of compound **129**, showing region 1.80 – 3.00 ppm.

3.2.2 Reductive alkylation of amides

The chemistry of nitrogen-containing compounds plays a central role in organic synthesis. The interaction between nitrogen-containing compounds and living organisms has led the pharmaceutical industry to the development of many drugs containing this atom. Amines are one of the most important functional groups amongst these nitrogen-containing compounds.[159] Methods such as reductive alkylation and amination of aryl halides have been used to synthesise amines of good yields.

To expand the library of alkaloid-like molecules for drug discovery, the existing library of tricyclic caryolane and clovane skeleton compounds was derivatised into a new library of tricyclic mono- and dialkylated-amines *via* a reductive *N*-alkylation method with various aldehydes (Scheme 3.9). Out of the newly synthesised derivatives **127a-e** and **128a-d**, a few

di-alkylated products **127b**, and **128b-c** were observed (Table 3.4). This was expected as the smaller aldehyde (formaldehyde) tend to alkylate faster due to less steric hindrance, whereas the bulkier aldehydes (butanal) required longer reaction time for the formation di-alkylated products. The mono-alkylated product was observed in the mixture of the di-alkylated product, however this could couldn't be controlled by either stoichiometry or reaction time. Furthermore, it was very difficult to isolate the mono-alkylated product from the di-alkylated product, hence it was decided to ultimately synthesis di-alkylated products.
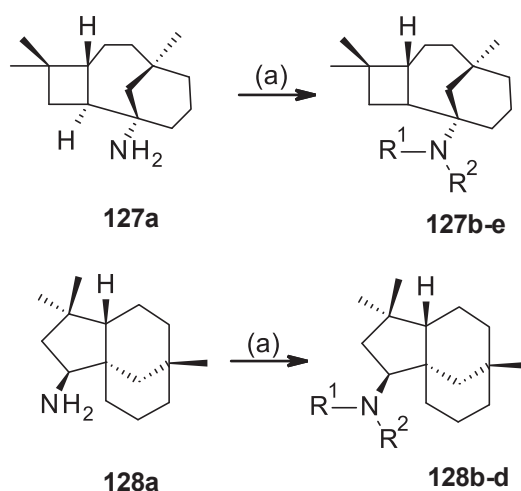
Scheme 3.9: Derivatisation of tricyclic caryolane and clovane skeleton.

Reaction conditions: (a) aldehyde (5-mole equiv.), NaB(OAc)₃H (10-mole equiv.) in

dichloromethane, acetic acid, overnight at room temperature.

Table 3.4: List of tricyclic caryolane and clovane skeleton derivatives.

Compound	R^1	R^2	Yield (%)	$[\alpha]_D^T (°)$
127a	H	H	58	-8.6
127b	CH$_3$	CH$_3$	71	-4.0
127c	CH$_3$CH$_2$CH$_2$	H	69	0.1
127d	CH$_3$(CH$_2$)$_3$	H	50	0.8
127e	CH$_3$(CH$_2$)$_4$	H	79	2.0
128a	H	H	65	9.2
128b	CH$_3$	CH$_3$	91	17.3
128c	CH$_3$(CH$_2$)$_3$	CH$_3$(CH$_2$)$_3$	57	13.9
128d	PhCH$_2$	H	66	32.4
129	H	H	33	-13.3

Following the amide cleavage, compounds **127a**, and **128a** were then subjected to reductive alkylation with 28% formaldehyde to yield tertiary amines **127b** and **128b** in 71 and 91% yield, respectively. The yields of **127b** and **128b** highlight the significance of steric hindrance of the substituents at the C-1 and C-2 positions of the caryolane and clovane skeletons, respectively, making amine **127a** less accessible by formaldehyde. It should be noted that just like the amides synthesised from caryophyllene, these novel amines are also optically active, except secondary amines **127c**, and **127d** which exists in a racemic mixture with observed specific optical rotations of 0.1 and 0.8 degrees, respectively (Table 3.4).

NMR analysis confirmed structures of compounds **127b** and **128b**; the ^{1}H NMR showed the newly formed $-N(CH_3)_2$ resonances at δ 2.21 and 2.31 ppm as broad singlets, respectively. Characteristic caryolane skeleton H-2 splitting (doublet of triplets, δ 2.16 ppm, $J = 8.00$, 14.50 Hz) was shown in the ^{1}H NMR spectrum of **127b**. While for compound **128b** only a multiplet (δ 2.20 – 2.30) for H-2 was observed, this was due to peak overlap with $-N(CH_3)_2$. 2D HSQC study of compound **128b** revealed the H-2 resonance overlapped with the $-N(CH_3)_2$ resonance at 2.20 – 2.30 ppm. Therefore, it was not possible to identify the splitting of H-2 (Figure 3.12). The extent of overlapping protons in the caryolane skeleton can be seen in the 2D HSQC spectral data of compound **127b**, as there are many multiplets in the region δ 0.9 – 1.9 ppm (Figure 3.13). The rest of the spectral features for **127b** and **128b** remained relatively similar to that of their starting amines, and their identities were further confirmed by HRMS analysis.
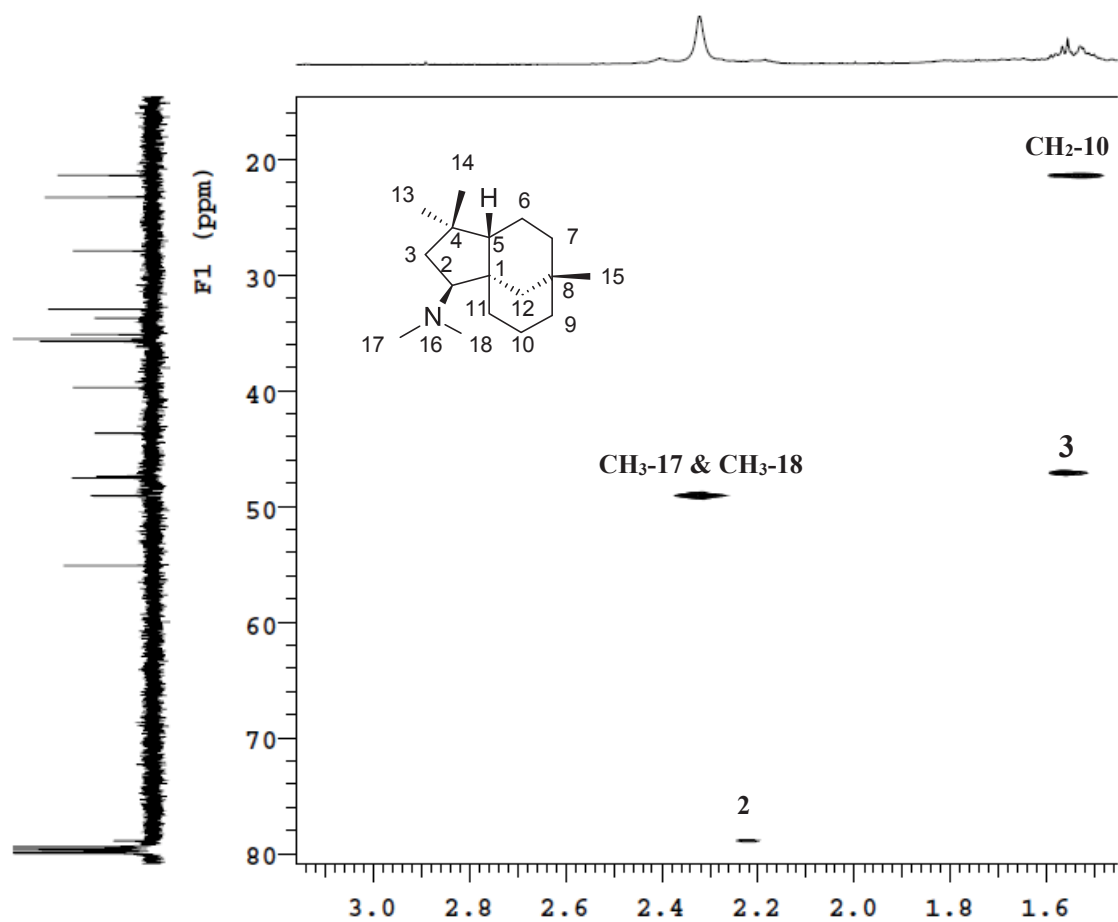
Figure 3.12: 2D HSQC NMR spectrum of compound **128b**, showing region 1.60 – 3.00 ppm.
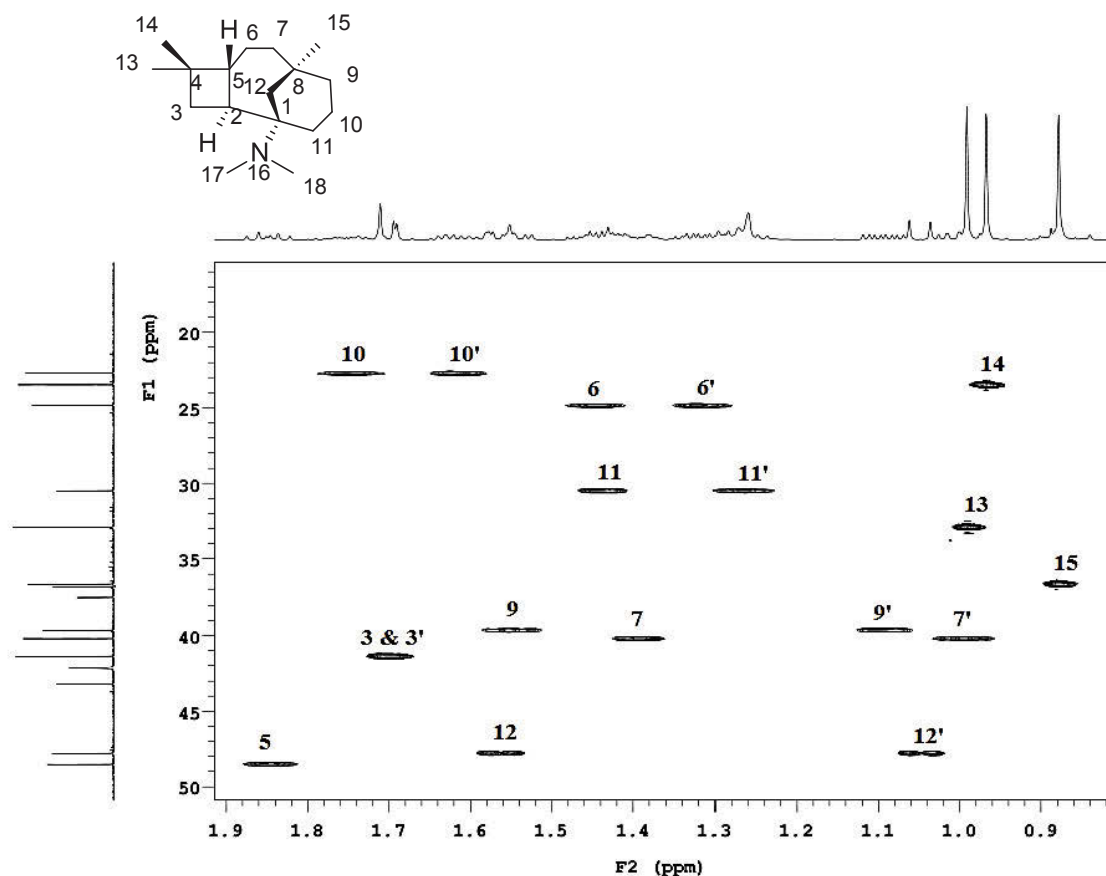
Figure 3.13: 2D HSQC NMR spectrum of compound **127b**, showing region 0.90 – 1.90 ppm.

As mentioned previously, di-alkylation product **128c** was observed when butanal was reacted with amine **128a**, however, no di-alkylation was observed for the reaction between butanal and the amine of the caryolane skeleton **127a**. The difference between the yields of the mono-alkylated **127d** (50%) and di-alkylated **128c** (59%) products suggests the steric hindrance at the C-1 position of caryolane is greater than that of the steric hindrance at the C-2 position of clovane.

Furthermore, structures of mono-substituted **127d** and di-substituted **128c** amines were also confirmed by NMR analysis; the ^{1}H NMR spectrum of the di-alkylated product **128c** which revealed CH$_2$-17/18 resonances as multiplets (δ 2.30 – 2.53 ppm), characteristic H-2 resonance (dd, δ 2.59 ppm, J = 13.00, 5.50 Hz) (Figure 3.14), and overlapping CH$_3$-23/24 resonances (t,

δ 0.90 ppm, $J = 7.50$ Hz). The overlapping resonances were resolved in the 2D HSQC experiment (Figure 3.15). The remainder of the synthesised amines in this chapter was characterised similarly.
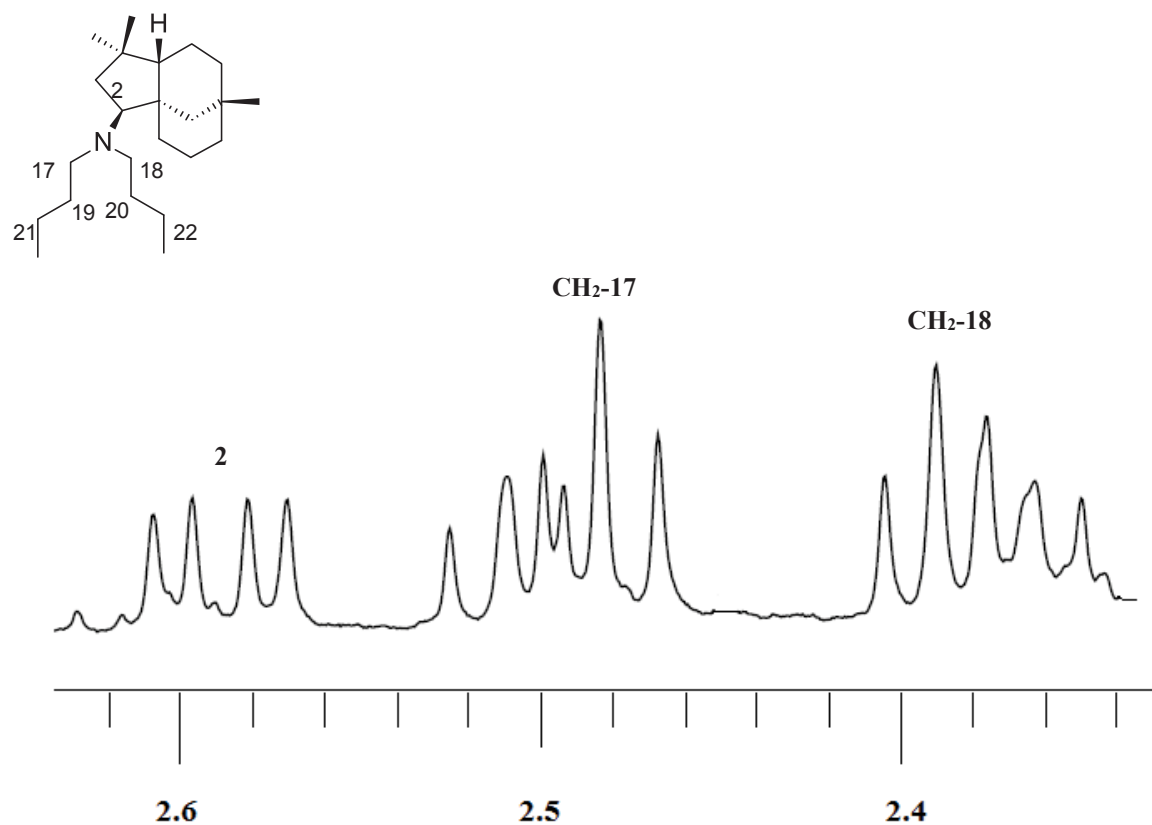
Figure 3.14: ^{1}H NMR spectrum of compound **128c** in CDCl$_3$ showing region 2.30 – 2.60 ppm.
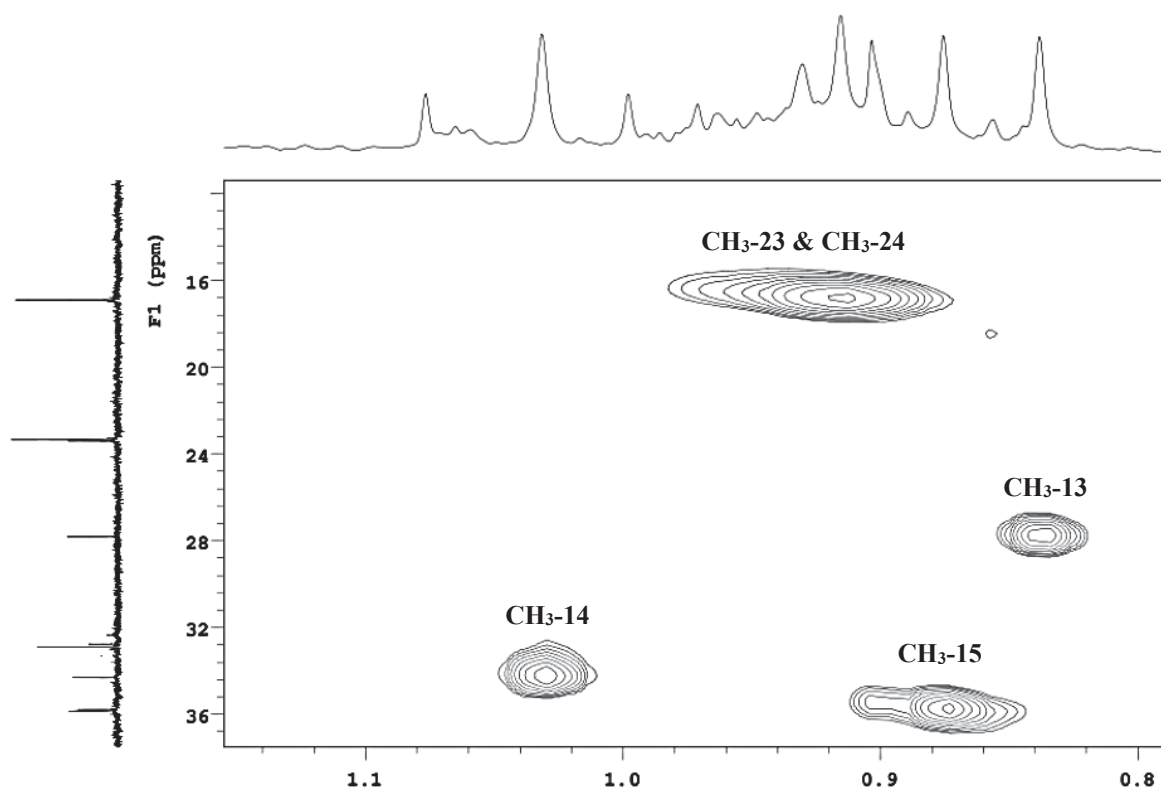
Figure 3.15: 2D HSQC NMR spectrum of compound **128c**, showing region 0.08 − 1.10 ppm.

3.3 Drug-like properties of synthesised compounds

As described earlier in Chapter 2, molecular modelling software Discovery Studio 4.5 (DS 4.5) was used to assess the drug-like properties and predict the ADMET properties of the synthesised compounds. A quantitative estimate of drug-likeness (QED) was used to evaluate the drug-likeness of synthesised compounds **119a-i**, **120a-d**, **125a**, **126a-e**, **127a-e**, **128a-d**, and **129**. QED values can range from zero (all properties unfavourable) to one (all properties favourable).[133] The molecular properties calculated by Discovery Studio are shown in Table 3.5. The data suggest that all synthesised compounds would make good drug candidates for further development. Based on the calculation, only four (**126c**, **127e**, and **128c-d**) of the synthesised compounds violated one of the Lipinski's rules of five, while all of the synthesised compounds scored highly (closest to 1, 0 − 1 scale) on the concept of drug-likeness (QED) (Table 3.5).

Table 3.5: Quantitative Drug-likeness (QED) and predicted molecular properties of synthesised compounds, as calculated in Discovery Studio.

Compound	MW[a]	LogP[b]	Solubility	HA[c]	HD[d]	Fractional PSA[e]	QED
119a	263.418	3.160	-5.241	1	1	0.094	0.773
119b	277.445	3.827	-5.557	1	1	0.089	0.816
119c	297.863	3.693	-5.802	1	1	0.089	0.774
119d	325.488	4.825	-6.900	1	1	0.080	0.829
119e	305.498	4.740	-6.457	1	1	0.080	0.798
119f	339.943	4.719	-7.030	1	1	0.076	0.721
119g	311.890	3.941	-6.132	1	1	0.084	0.786
119h	278.433	2.199	-4.833	2	2	0.170	0.813
119i	295.483	4.362	-5.576	2	1	0.162	0.822
120a	263.418	3.162	-5.389	1	1	0.093	0.773
120b	277.445	3.829	-5.704	1	1	0.088	0.816
120c	297.863	3.694	-5.959	1	1	0.088	0.774
120d	325.488	4.826	-7.057	1	1	0.080	0.829
125a	279.418	2.060	-4.275	2	2	0.153	0.772
126a	389.360	2.857	-6.198	2	2	0.143	0.727
126b	404.629	4.950	-7.376	2	2	0.122	0.601
126c	444.608	5.120	-8.347	2	2	0.122	0.688
126d	348.523	3.125	-5.646	2	2	0.143	0.820
126e	320.470	1.792	-5.059	2	2	0.156	0.815
127a	221.382	3.139	-4.855	1	1	0.097	0.668
127b	249.435	4.107	-4.986	1	0	0.010	0.676
127c	263.461	4.443	-6.392	1	1	0.037	0.793
127d	277.488	4.899	-6.931	1	1	0.035	0.770
127e	291.514	5.356	-7.479	1	1	0.033	0.719
128a	221.382	3.140	-4.990	1	1	0.096	0.668
128b	249.435	4.108	-5.069	1	0	0.010	0.676
128c	333.594	6.765	-8.017	1	0	0.007	0.500
128d	311.504	5.155	-7.762	1	1	0.033	0.813
129	236.396	1.749	-4.214	2	2	0.183	0.673

[a]MW: molecular weight
[b]LogP: logarithm of partition coefficient between *n*-octanol and water
[c]H-acceptors: hydrogen bond acceptors
[d]H-donors: hydrogen bond donors
[e]Fractional PSA: the ratio of polar surface area divided by the total surface area

3.4 ADMET studies

ADMET studies were conducted on the synthesised compounds to predict the pharmacokinetics of the drug from the point of administration to the point the drug is excreted from the organism. Based on the ADMET predictions calculated by DS 4.5 (Table 3.6), all of the synthesised compounds observed good human intestinal absorption scores, as well as very high to medium blood-brain barrier penetration abilities. Most of the compounds are unlikely to cause drug-drug interactions due to liver metabolism except secondary amines (**127c-e**, **128b-d**). This suggests good bioavailabilities of these synthesised compounds. Even though the predicted hepatotoxicity and plasma protein binding of the synthesised compounds were less than ideal (Table 3.6), it is worth noting that these two calculations do not take into account the IC_{50} of the compounds, and therefore the predicted hepatotoxicity is at an unknown concentration. Furthermore, the ADMET plot seen in Figure 3.16 showed all the calculated compounds fall within the 95 – 99% confidence eclipses, which indicates that the predictions are mathematically valid.

Table 3.6: ADMET properties of synthesised compounds, as calculated in Discovery Studio.

Compound	HIA level[a]	BBB[b]	CYP2D6[c]	Hepatotoxicity	Plasma protein binding	Aqueous solubility
119a	0	1	False	True	True	2
119b	0	1	False	True	True	2
119c	0	1	False	True	True	2
119d	0	0	False	True	True	1
119e	0	0	False	False	True	2
119f	0	0	False	True	True	2
119g	0	1	False	True	True	2
119h	0	2	False	True	True	3
119i	0	0	False	True	True	2
120a	0	1	False	True	True	2
120b	0	1	False	True	True	2
120c	0	1	False	True	True	2
120d	0	0	False	True	True	1
125a	0	2	False	False	False	3
126a	0	2	False	True	True	2
126b	0	1	False	False	True	2
126c	0	1	False	True	True	1
126d	0	2	False	True	True	2
126e	0	3	False	True	False	3
127a	0	1	False	False	True	2
127b	0	0	False	False	True	2
127c	0	0	True	False	True	2
127d	0	0	True	False	True	2
127e	0	0	True	True	True	1
128a	0	1	False	True	True	2
128b	0	0	True	False	True	2
128c	2	0	True	False	True	1
128d	0	0	True	False	True	1
129	0	2	False	True	False	3

[a]HIA level: human intestinal absorption level (inside 95% confidence level)
[b]BBB: blood brain barrier penetration levels
[c]CYP2D6: classification whether a compound is a CYP2D6 inhibitor using the cut-off Bayesian score of 0.161
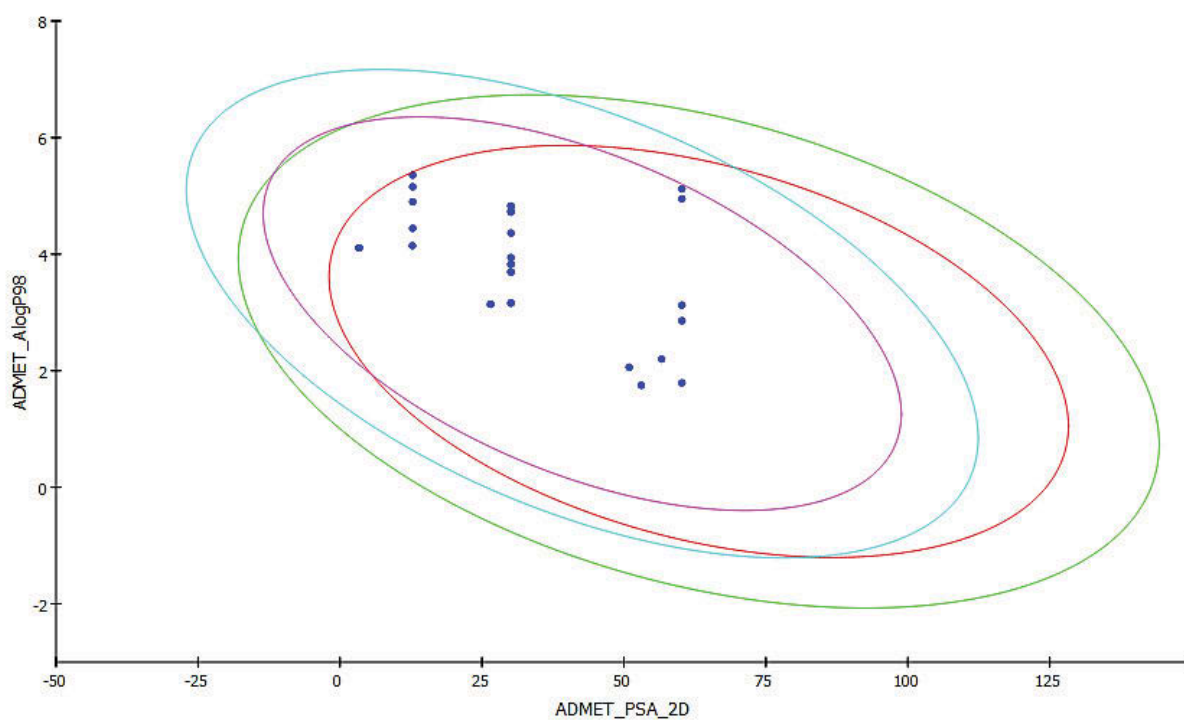
Figure 3.16: ADMET pot of synthesised compounds, as plotted in Discovery Studio.

The derivatisation reactions discussed in this chapter were able to provide diversity to the library of alkaloid-like compounds containing the caryolane **110** and clovane **111** core structures. In order to assess the anti-cancer activity of this class of compounds, several biological assays (anti-proliferative, cell cycle, and apoptosis) were carried out and described in Chapter 4.

Chapter 4   Biological Evaluation for Anticancer Activities

4.1 Introduction

As discussed in Chapter 1.1.1, the various subtypes of breast cancer overexpress receptors for oestrogen, progesterone and human epidermal growth factor receptor 2. Activation of these receptors drives cell proliferation, and modern chemotherapies have successfully targeted receptor activation to produce significant improvements in patient survival. Triple-negative lack all three receptors and are therefore unresponsive to current chemotherapy agents that target these receptors. Also, triple negative breast cancers are aggressive and highly metastatic and therefore represent an important target for anticancer drug development. Therefore, in this thesis, the anticancer activity of the synthesised alkaloid-like compounds was assessed against the triple negative MDA-MB-231 cell line. The active compounds to emerge from this testing were also assessed for activity against the lesser aggressive and more common ER+ breast cancer cell line MCF-7, and hence investigates the compounds' selectivity towards the triple negative breast cancer.

4.1.1 National Cancer Institute broad screening

The compound **63** was synthesised previously by our research group and selected by the US National Cancer Institute (NCI) as a candidate for their standard anticancer screening program.[160] Compound **63** was tested *in vitro* against nine classes of cancer types (leukaemia, non-small cell lung cancer, colon cancer, central nervous system cancer, melanoma, ovarian cancer, renal cancer, prostate cancer and breast cancer). Significant anticancer activity was determined in every case for the 48 different cell lines employed in the screening program; selective results are summarised in Appendix 7.1.1.

Compound **63** is more selective towards specific tumour types, observing strong IC_{50} values (Appendix 7.1.2) <10 μM towards leukaemia, colon, and melanoma cell lines (SK-MEL-28

IC$_{50}$ = 1.8 μM). Out of the six-cell lines screened for leukaemia CCRF-CEM, HL60, MOLT4, and RPMI-8226 showed activity with IC$_{50}$ of 4.4, 5.5, 2.4, and 4.1 μM respectively. This suggests that compound **63** is more active towards acute lymphoblastic leukemia both T-cell and B-cell, as well as acute promyelocytic leukemia, and less active towards chronic myelogenous leukaemia which observed a threefold increase in the IC$_{50}$ values comparing to that of lymphoblastic and promyelocytic leukaemia. The selectivity of compound **63** towards the lymphoblastic and promyelocytic leukemia cell lines could be due to the similarities present in the immunohistochemistry of the CCRF-CEM, HL60, MOLT4, and RPMI-8226 cell lines such as the CD antigen expression patterns, and the expression of both TCR-αβ and TdT genes.

Based on the NCI broad screening, compound **63** is an active anticancer agent with IC$_{50}$ < 10 μM on selective groups of tumour types such as leukaemia, colon, melanoma and breast cancer. One can only speculate the activity is related to the similarities in the immunohistochemistry patterns of these cell lines. Future investigation is needed to determine the connection between the observed activities across these cell lines from the broad screening. These results further indicated that the series of alkaloid-like compounds synthesised could be biologically active compounds, in particular against cancerous cells.

Amongst the breast cancer cell lines, some variation in activity was observed. The proliferation of most of these cell lines was potently inhibited by **63**. Even thought, aggressive and highly metastatic MDA-MB-231 cell line was the least active (IC$_{50}$ = 38.9 μM), this finding has provided a starting point of the discovery. In the current setting, the primary focus of this project is discovery agents that target breast cancer cell lines.

4.1.2 Antiproliferative activity in breast cancer cell lines

4.1.2.1 Antiproliferative activity of 3-azatricyclo[5.3.1.0^{4,9}]undec-2-ene system and derivatives in triple negative cell line

To evaluate the anticancer activity of the synthesised compounds, 3-(4,5-dimethylthiazol-2-yl)-5-(3-carboxymethoxyphenyl)-2-(4-sulfophenyl)-2H-tetrazolium (MTS) cell proliferation assay was performed using the aggressive triple negative breast cancer cell line, MDA-MB-231. Compounds **82a-c**, **84**, **90a-b**, **91a-b**, **92** and **93** were initially screened against MDA-MB-231 cells at 25 and 50 μM (Figure 4.1). From this screening, **82c** emerged as the only active compound and was selected for further MTS assays to determine an IC$_{50}$. Thus, MDA-MB-231 cells were treated with **82c** in varying concentrations, ranging from 1.00 μM to 28 μM and a dose-response curve was constructed (Figure 4.2A). Using a nonlinear regression analysis (Goodness of fit) from GraphPad Prism 7.02, an IC$_{50}$ of 7.9 ± 1.5 μM was determined. In contrast, the analogues synthesised from acetonitrile compounds **82a**, **90a**, **84**, and propionitrile compounds **82b** and **90b** were inactive at the maximum concentration tested of 50 μM (Figure 4.1). This suggests the antiproliferative activity of the compound increased dramatically when in the presence of chlorine at the C-2 and C-18 positions of the tricyclic scaffold. This was not surprising as the corresponding chloroacetyl derivatives can be easily alkylated with the amino acids in enzymes or receptors, and thus the cytotoxicity of compound **82c** could be due to the electrophilicity of the reagent used.
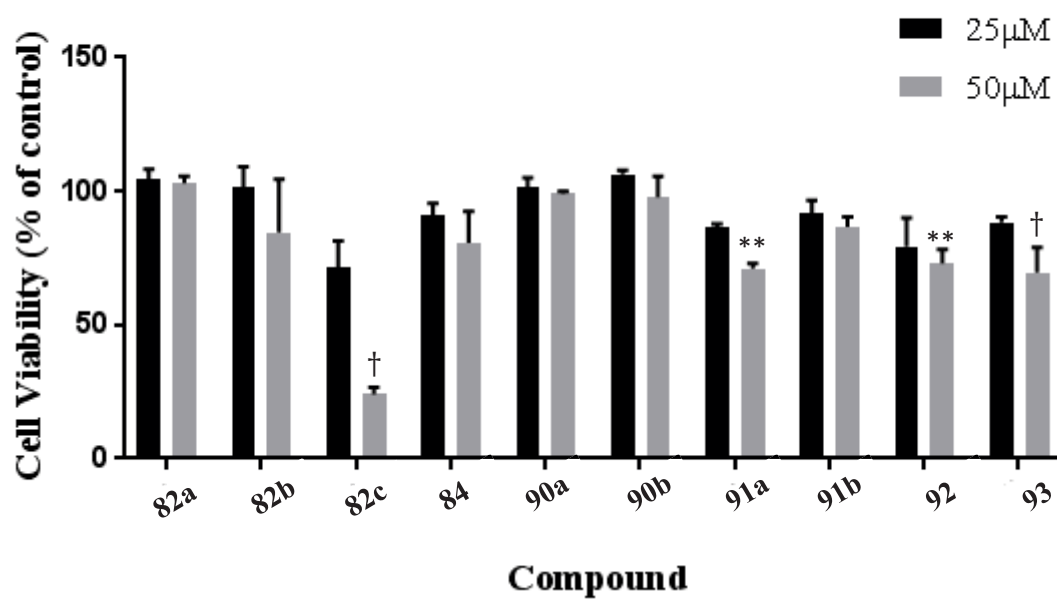
Figure 4.1: Effects of 3-azatricyclo[$5.3.1.0^{4,9}$]undec-2-ene system and derivatives on the proliferation of MDA-MB-231 breast cancer cells (48 hours, 25 and 50 μM). * indicates $p \leq$ 0.05, ** indicates $p \leq 0.01$, † indicates $p \leq 0.001$, ‡ indicates $p \leq 0.0001$.
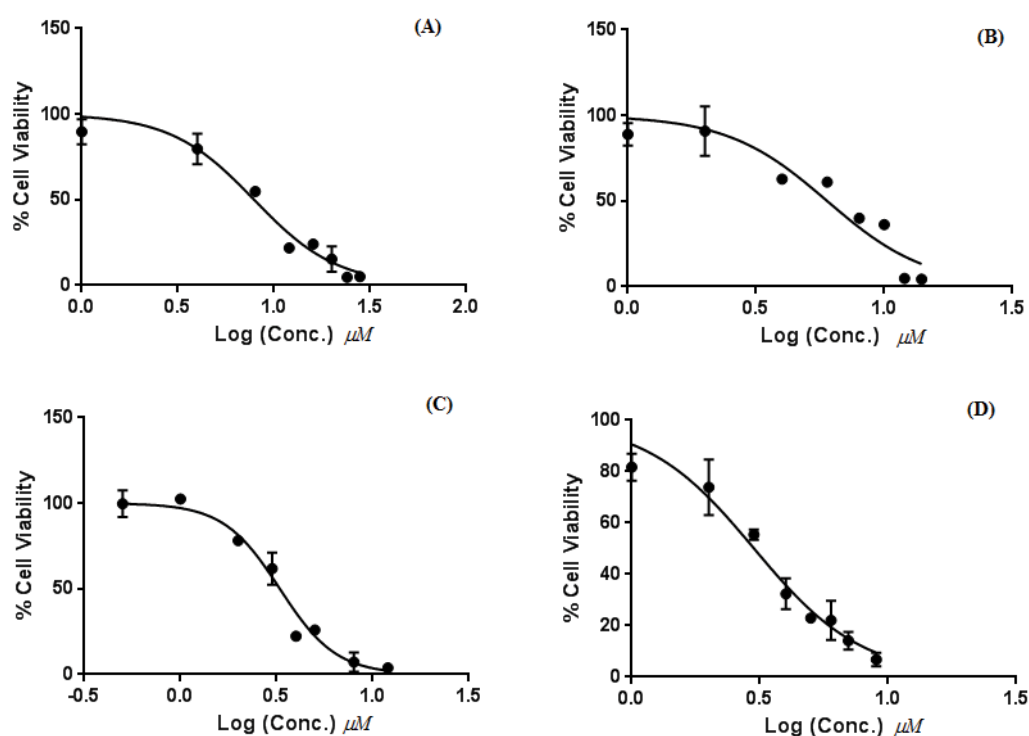
Figure 4.2: Dose-response curve of samples **82c** (A), **119c** (B), **120c** (C), and **126a** (D) on the proliferation of MDA-MB-231 breast cancer cells.

4.1.2.2 Antiproliferative activity of caryophyllene, monoepoxide and derivatives in triple negative cell line

The anticancer activity of the caryophyllene, monoepoxide and derivatives were also tested against MDA-MB-231 cells using the MTS assay under the same conditions described in section 4.1.2.1. Eight of the 28 compounds tested showed significant antiproliferative activity (Figure 4.3). Most notably, at 50 uM compounds **119c**, **120c** and **126a** decreased the proliferation to 17% (p = 0.0031), 2% (p = 0.0001), and 3% (p = 0.0001), respectively. Further studies were carried out on the active compounds **119c**, **119e**, **120c**, **126a**, **127a**, **127c**, **127d**, and **128d** in varying concentrations, ranging from 1.0 μM to 55 μM and the IC_{50} values were determined (Table 4.1). Compounds **119c**, **120c**, and **126a** exhibited high potencies, with IC_{50}

values of 5.9 ± 1.5, 3.2 ± 0.2, and 3.0 ± 0.2 µM, respectively. The extent of these decreases in cell viability was found to be much less pronounced in the analogues synthesised from other nitriles at the maximum concentration tested of 50 µM ($p > 0.05$). This suggests the antiproliferative activity of the compounds increased markedly when substituted with chlorine at the C-18 and C-21 positions of the tricyclic scaffold. It is worth noting, as mentioned earlier, this phenomenon was also observed with the 3-azatricyclo$[5.3.1.0^{4,9}]$undec-2-ene system and derivatives. Due to the observed correlation between the potency of the drug to the presence of the α-chloroamide functional group, it was suspected that the observed anticancer activity could be dependant on this particular functional group. Furthermore, it was suspected that this particular functional group could potentially be cytotoxic to healthy mammalian cells. Hence, compounds **119c**, **120c**, and **126a** were submitted for cytotoxic evaluation against noncancerous Vero cells to BIOTEC in Thailand (see section 4.1.3).
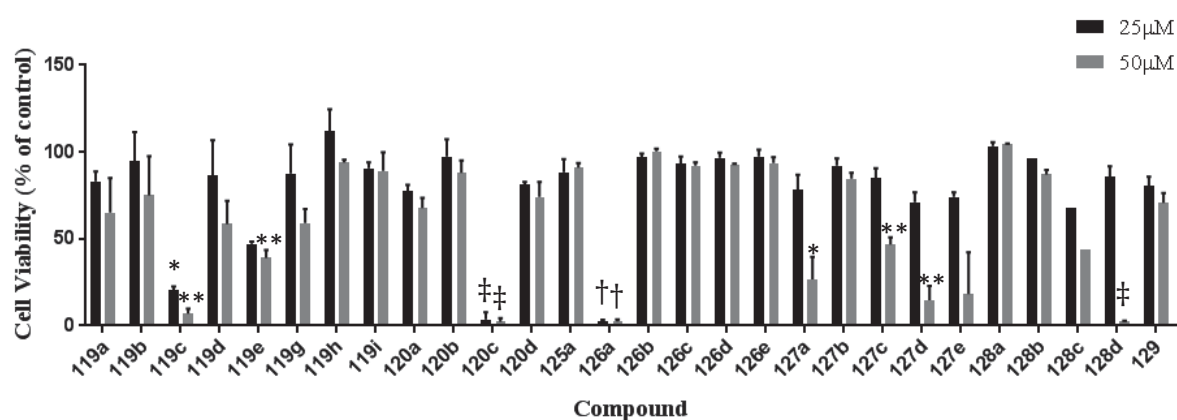
Figure 4.3: Effects of caryophyllene and monoepoxide derivatives on the proliferation of MDA-MB-231 breast cancer cells (48 hours, 25 and 50 µM). * indicates $p \leq 0.05$, ** indicates $p \leq 0.01$, † indicates $p \leq 0.001$, ‡ indicates $p \leq 0.0001$.

Table 4.1: Cytotoxicity (IC$_{50}$) of compounds active against MDA-MB-231 breast cancer cells.

Compound	IC$_{50}$ (μM)
119c	**5.9 ± 1.5**
120c	**3.2 ± 0.2**
119e	55.3 ± 12.5
127a	34.9 ± 2.2
127c	45.9 ± 5.0
127d	37.3 ± 1.1
128d	23.6 ± 0.5
126a	**3.0 ± 0.2**

4.1.2.3 Antiproliferative activity of selected compounds in ER+ cell line

To investigate the selectivity of the active compounds, cell proliferation assays at 25 and 50 μM on the ER+ (MCF-7) breast cancer cell line were performed on a selection of representative compounds (**82c**, **119c**, and **120c**). Compound **126a** was not chosen due to its structural similarity to that of **120c**. The effects of compounds **82c**, **119c**, and **120c** on the proliferation of MCF-7 cells after 48 h treatment are shown in Figure 4.4.

The anticancer activities of **82c**, **119c**, and **120c** are selective towards the more aggressive triple negative (MDA-MB-231) cell line while exhibiting no antiproliferative activities towards the MCF-7 cells at the highest concentration tested (50 μM). This suggests that compounds **82c**, **119c**, and **120c** could be triggering a specific pathway rather than in a randomised manner. Further investigation into the mechanism of action of these compounds is needed to confirm a specific pathway for the observed selectivity. Furthermore, the observed selectivity towards the more aggressive cancer cell line would make these compounds more attractive drug candidates for further development.
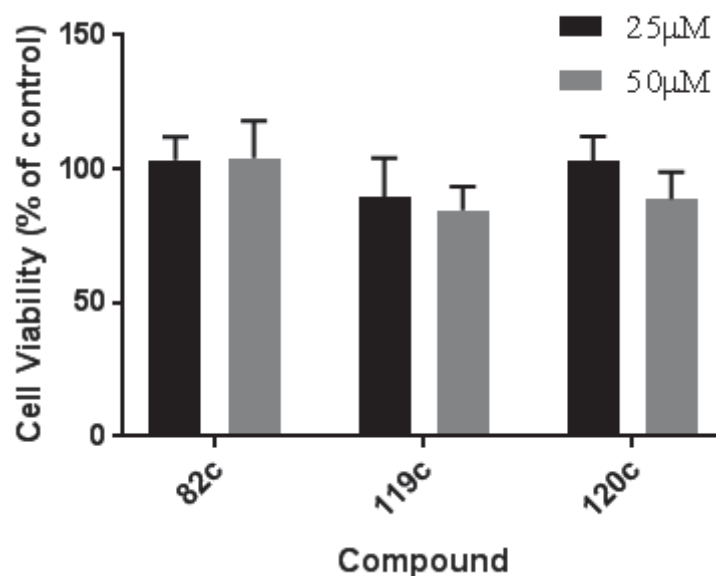
Figure 4.4: Effects of compounds **82c**, **119c**, and **120c** on the proliferation of MCF-7 breast cancer cells (48 h, 25 and 50 μM).

4.1.3 Cytotoxicity of active compounds on Vero cells

Compound **63** was assessed for its cytotoxicity on healthy mammalian Vero cell line (African green monkey kidney), as it was found to exhibit the highest cytotoxic activity in multiple cell lines across multiple tumour types. It was found that compound **63** reduced Vero cell viability by 77% of control at the maximum concentration tested (139 μM). In contrast **63** reduced MDA-MB-231 cell viability by 80% at 75 μM. This data clearly demonstrate the selectivity of **63** towards cancer cells over noncancerous cell lines. It is believed the observed cytotoxic effects towards Vero cells could be due to the α,β-unsaturated system (C-12, C-21, and C-22 position) on compound **63**, as such system is vulnerable to nucleophilic attack at the β-carbon.[161-162] Therefore, the α,β-unsaturated system in compound **63** was then selectively reduced to yield compound **84**. The cytotoxicity of **84** was assessed against Vero cells and as expected was found to be non-cytotoxic. However, the removal of the double bond at C-21 has

resulted in decreasing in anticancer activity of compound **84** ($IC_{50} > 50$ μM) against MDA-MB-231 cells.

Active compounds **82c**, **119c**, **120c**, and **126a**, were also assessed for its cytotoxicity on Vero cell line; they were found to exhibit cytotoxicity towards the Vero cells at 158 μM, 168 μM, 168 μM and 129 μM, respectively). In these assays, **82c**, **119c**, **120c**, and **126a** reduced Vero cell viability by 84, 93, 89 and 88% of control, respectively. In contrast **82c**, **119c**, **120c**, and **126a** reduced MDA-MB-231 cell viability by 90, 90, 96 and 86% of control at 20 μM, 10 μM, 6 μM and 7 μM. These data also demonstrate the selectivity of **82c**, **119c**, **120c**, and **126a** towards cancer cells over noncancerous cell lines. Although, the VERO cytotoxicity experiments have provided a better understanding of toxicity nature of the synthesised compound. The finding in VERO cells study could be further confirmed in the normal and non-transformed human breast epithelia cells.

4.1.4 Primary mechanism of action studies

4.1.4.1 Cell Cycle Study

To investigate the primary mechanism of action for the most potent compounds **82c**, **119c**, **120c**, and **126a**, their abilities to induce cell cycle arrest in MDA-MB-231 cells were assessed using flow cytometry. These studies revealed that each compound altered cell cycle progression, and the distribution of cells in each phase was not uniform across the series.

Treatment of MDA-MB-231 cells with **82c** (20 μM, 24 h) decreased the population of cells in G_0/G_1 by 20% ($p < 0.0001$), and increased the proportion of cells in the G_2/M phase by 15% ($p < 0.0001$) relative to control (Figure 4.5). These findings suggest that cell cycle arrest at the G_2/M phase contributes to the antiproliferative activity of **82c**. Similarly, compound **126a** (9 μM, 24 h) produced a decrease in the population of cells in the G_0/G_1 phase by 18% (p = 0.0001), and caused a significant increase in the number of cells in the G_2/M phase (91%, $p =$

0.0001) comparing to that of control (Figure 4.6). These findings suggest that cell cycle arrest at the G_2/M phase contributes to the antiproliferative activity of **126a**.
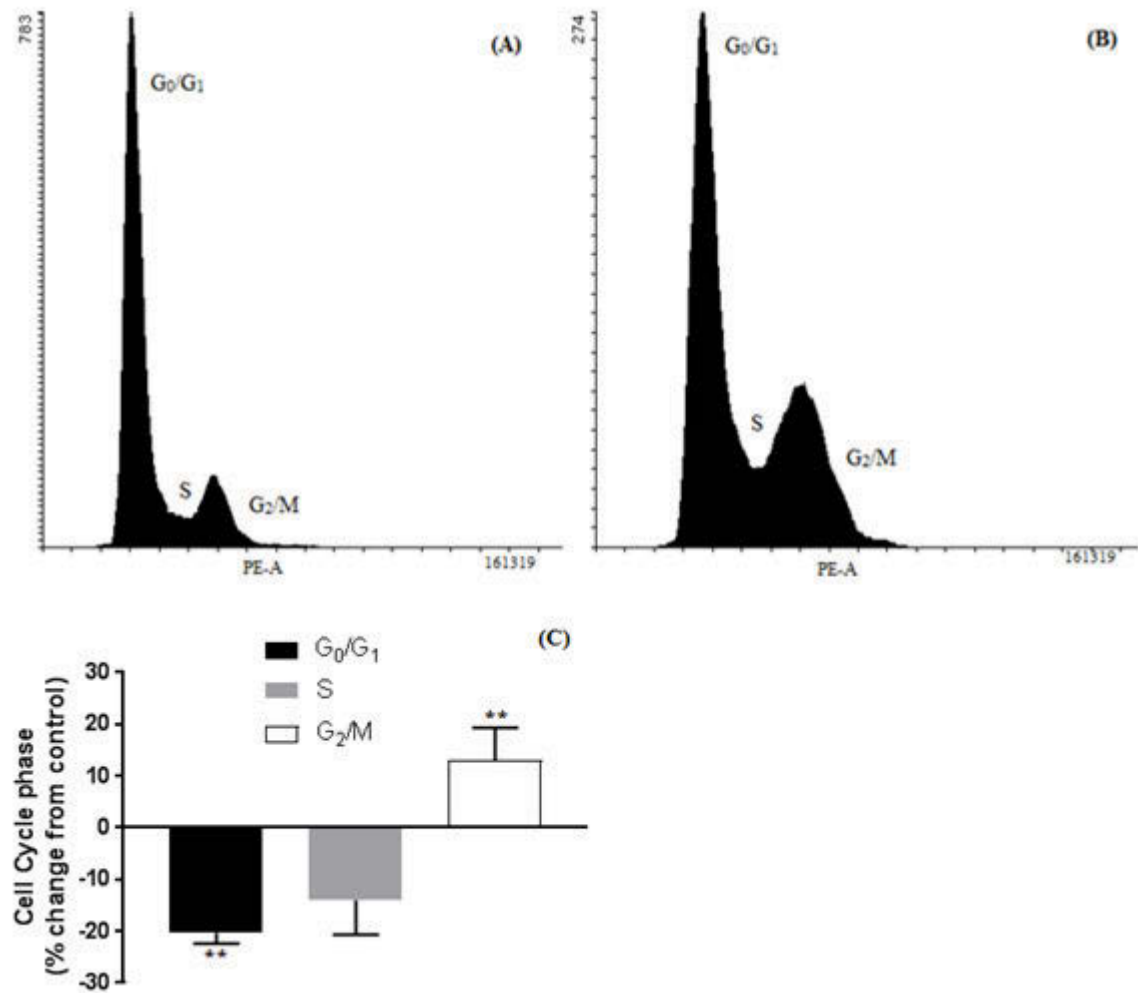
Figure 4.5: Effect of **82c** on the cell cycle progression of MDA-MB-231 cells. Cells were treated for 24 h with DMSO as control (A) and **82c** (20 µM, B). Panel (C) shows the percentage change from control. Data represent the mean ± SEM of at least 3 independent experiments. **indicates $p < 0.0001$.
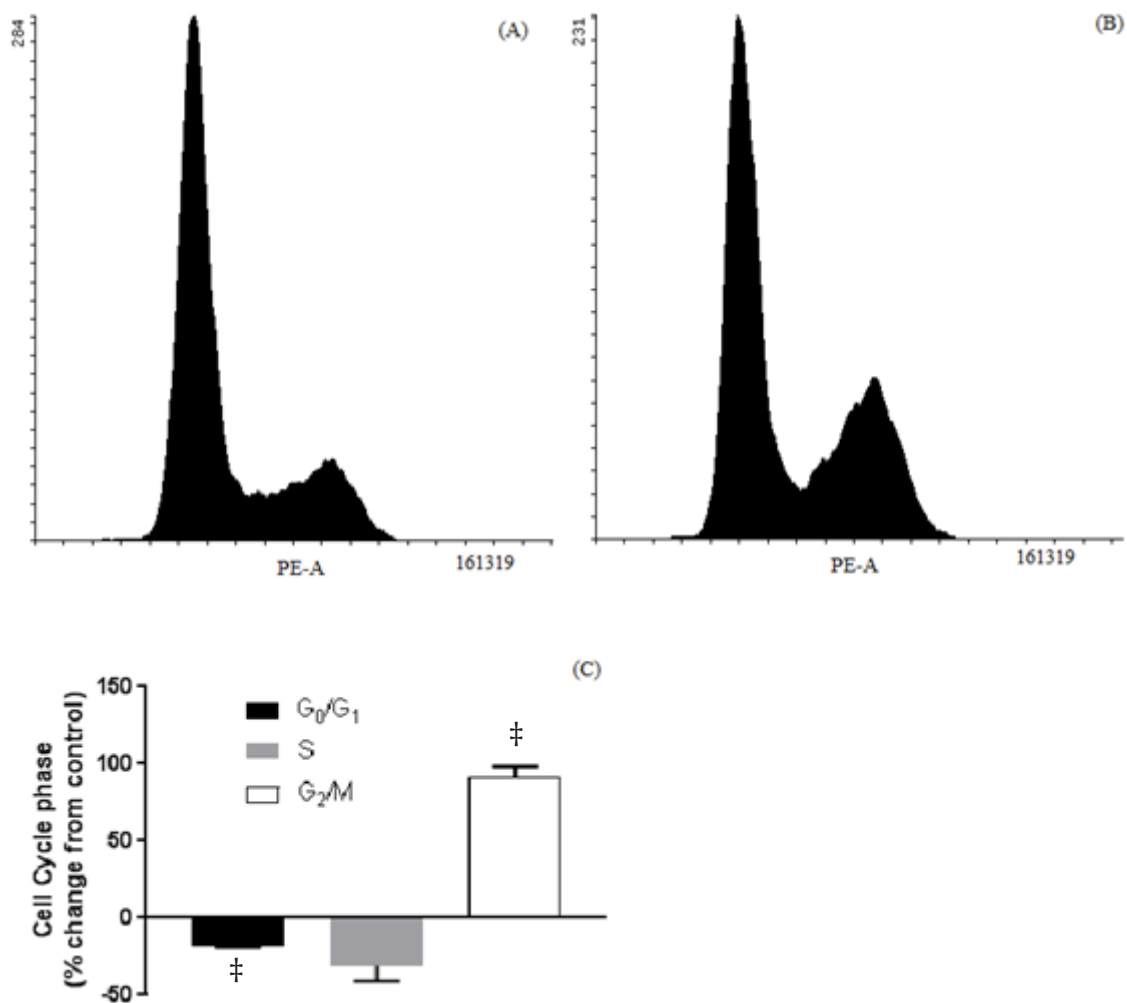
Figure 4.6: Effect of **126a** on the cell cycle progression of MDA-MB-231 cells. Cells were treated for 24 h with (A) DMSO (control), (B) **126a** (9 μM), (C) percentage change from control. Data represent the mean ± SEM of at least three independent experiments. ‡ indicates $p = 0.0001$.

Compounds **119c** and **120c** also caused cell cycle arrested in MDA-MB-231 cells, however in contrast to **82c** and **126c**, cells were seen to accumulate in the G_0/G_1 phase. As the result, increases in the population at the G_0/G_1 phase of 11% ($p = 0.0038$) were observed when treated with **119c**, and 5% ($p = 0.0014$), when treated with **120c**. Treatment with **119c** also decreased the populations of cells in both the S-phase and G_2/M phase by 28% ($p > 0.05$), and 33% ($p =$

0.0028) respectively (Figure 4.7). While **120c** altered the cell distribution in the S-phase by an increase of 24% ($p > 0.05$), and a decrease in the G_2/M phase of 34% ($p = 0.0008$) (Figure 4.8). Ultimately indicating that compounds **119c** and **120c** effects MDA-MB-231 cells' ability to complete the cell cycle.
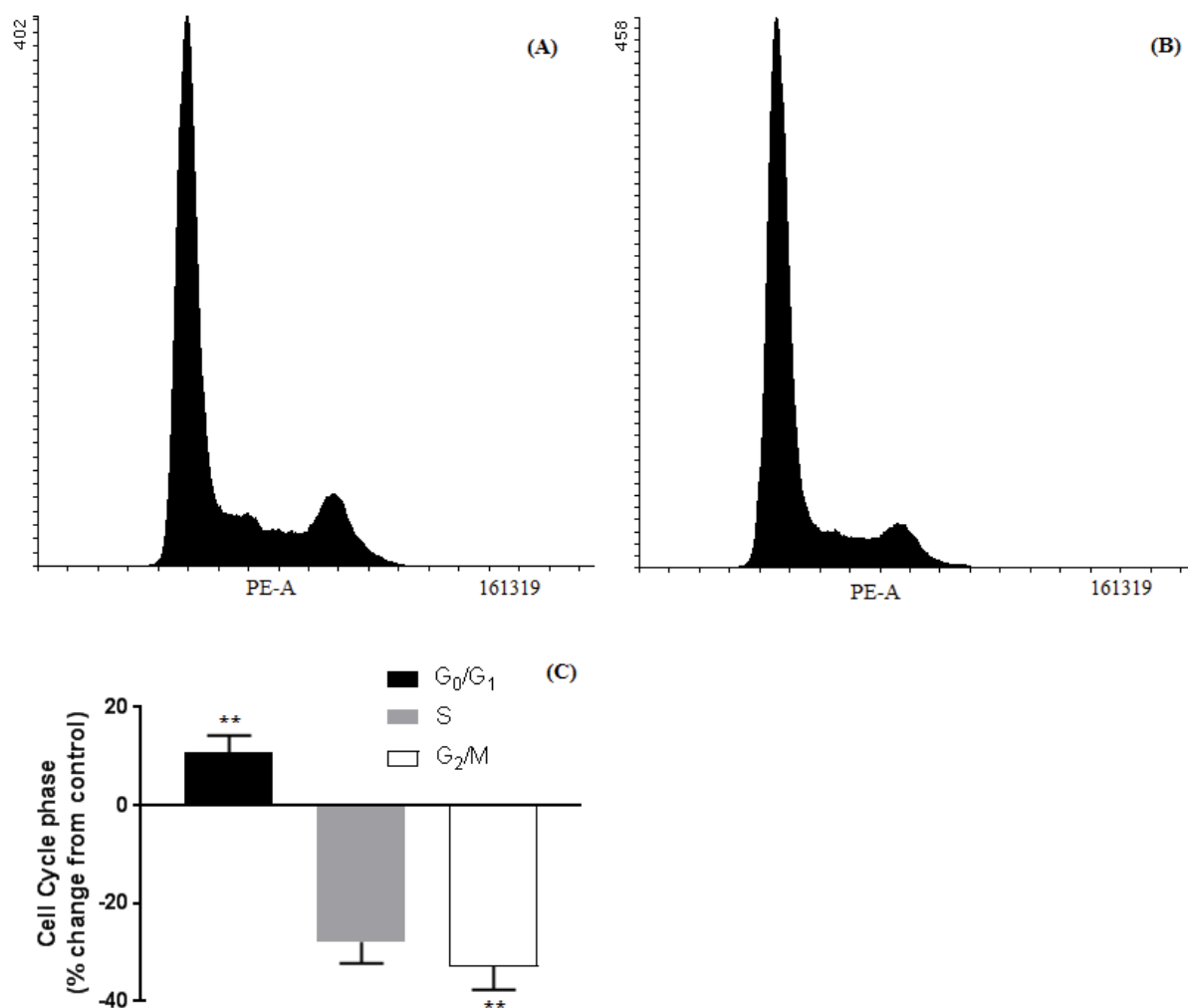
Figure 4.7: Effect of **119c** on the cell cycle progression of MDA-MB-231 cells. Cells were treated for 24 h with (A) DMSO (control), (B) **119c** (40 μM), (C) percentage change from control. Data represent the mean ± SEM of at least three independent experiments. **indicates $p < 0.05$.
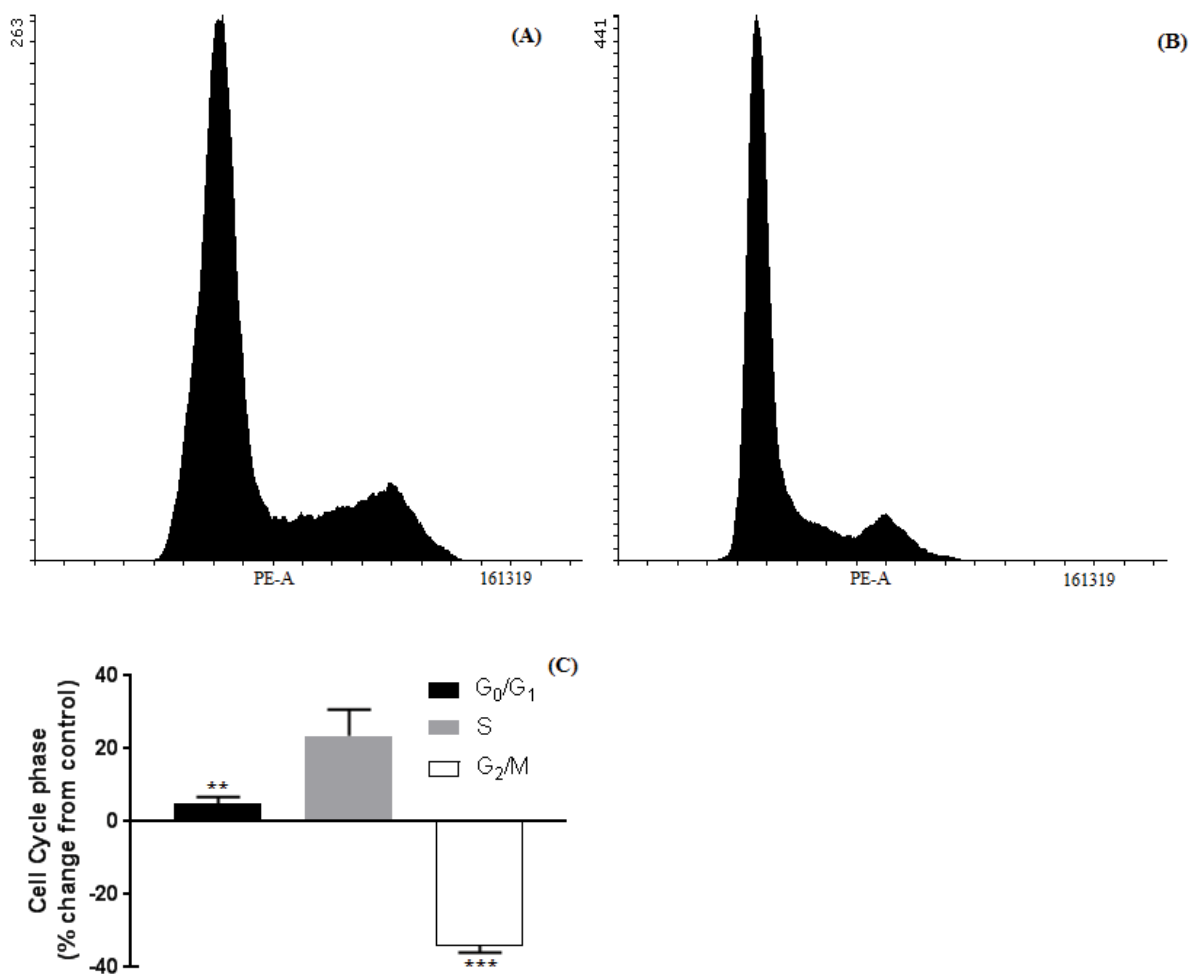
Figure 4.8: Effect of **120c** on the cell cycle progression of MDA-MB-231 cells. Cells were treated for 24 h with (A) DMSO (control), (B) **120c** (20 μM), (C) percentage change from control. Data represent the mean ± SEM of at least three independent experiments. **indicates $p < 0.05$. *** indicates $p = 0.0008$.

4.1.4.2 Activation of Apoptosis

The translocation of phospholipid phosphatidylserine (PS) to the outer leaflet of the cell plasma membrane is one of the hallmarks of apoptosis.[163] This is followed by a loss of membrane integrity and eventual cell death. The ability of compounds **82c**, **119c**, **120c**, and **126a** to induce apoptosis in MDA-MB-231 cells were assessed using flow cytometry.

MDA-MB-231 cells were treated with 20 and 40 μM of **82c** for 48 h and then stained with Annexin V-FTIC (which binds to exposed PS) and propidium iodide (PI). The cells are analysised by flow cytometry to determine the proportion of cells that is undergoing apoptosis, at either early apoptosis (Annexin-positive, PI-negative), late apoptosis (Annexin-positive, PI-positive) or total apoptosis (early + late apoptosis) (Figure 4.9).

MDA-MB-231 cells tested positive for Annexin V-FITC after treatment with **82c** (20 and 40 μM, *p* = 0.0223 and *p* = 0.0047) respectively, which indicates the majority of the treated cell population are in the early stage of apoptosis after treatment with the drug (Figure 4.9). The population of cells that underwent early apoptosis after treatment with **82c** (20 and 40 μM) was increased by 21 and 31% respectively, which suggests a dose-dependent increase in the apoptotic population.
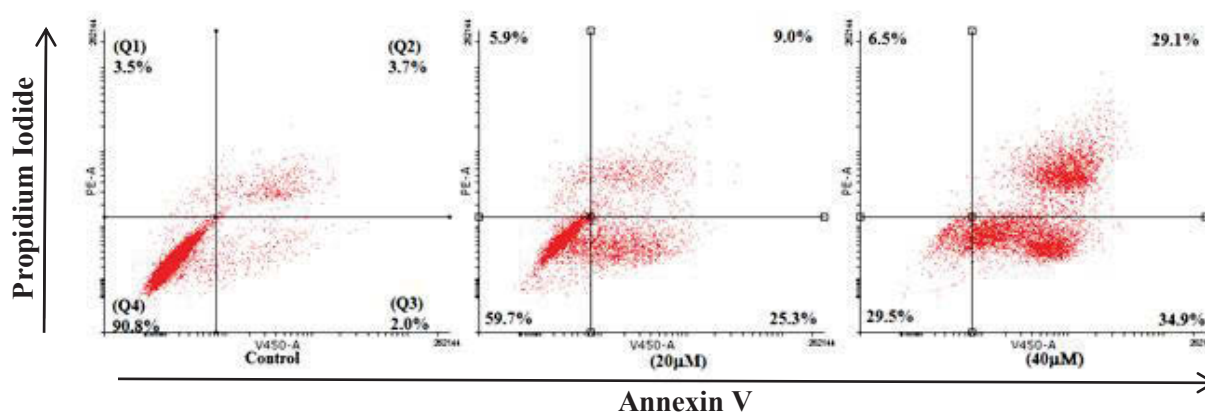
Figure 4.9: Effect of compound **82c** on the induction of apoptosis in MDA-MB-231 cells. Cells were treated with 20 and 40 μM concentrations of **82c** for 48 h, stained with Annexin V-FITC and PI, and the apoptotic effect was assessed by flow cytometry. Representative results are shown, with quadrants indicating the proportion of cells that are necrotic: Q1, late apoptotic: Q2, early apoptotic: Q3, and viable: Q4. Images are representative of 3 independent experiments.

Furthermore, after 48 h treatment with **119c**, **120c**, and **126a,** the MDA-MB-231 cells tested positive for both Annexin V-FITC and propidium iodide (PI), (20 and 40 μM, $p = 0.0016$ and $p = 0.0001$), (10 and 20 μM, $p = 0.0016$ and $p = 0.0080$) and (15 and 20 μM, $p = 0.0001$ and $p = 0.0001$), respectively. This indicates the majority of the cell population are in the late stages of apoptosis after treatment with the three compounds (Figure 4.10). Flow cytometer analysis indicates the population of cells that are in the late stages of apoptosis after treatment with **119c**, **120c**, and **126a** was increased by (10 and 20 μM, 7.3 and 5.3%), (20 and 40 μM, 8.1 and 39.2%), and (15 and 20 μM, 46.1 and 66.8%). These percentage increases suggest a dose-dependent increase in the apoptotic populations treated with compounds **120c** and **126a**.
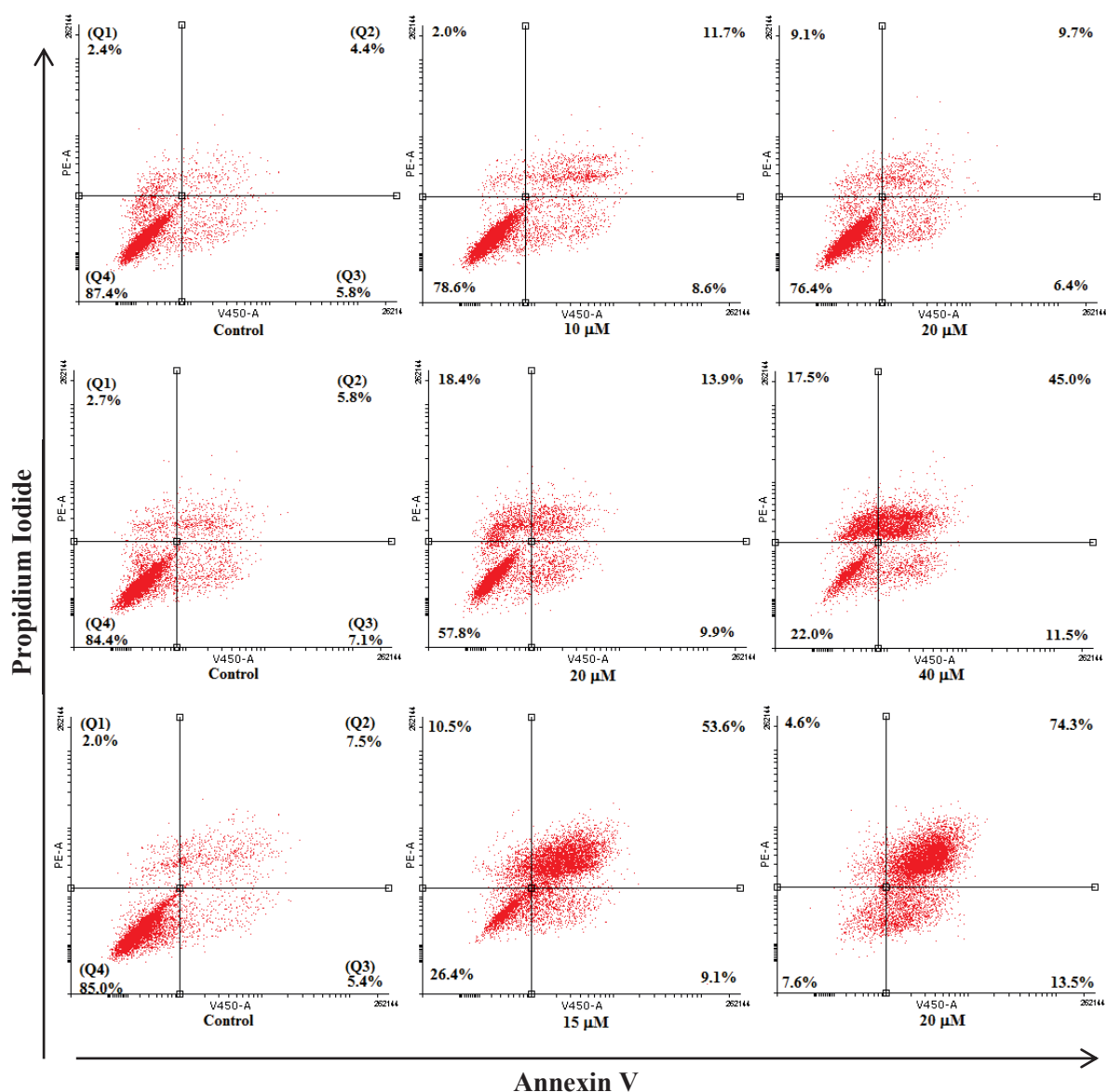
Figure 4.10: Effect of compounds **119c** (top), **120c** (middle) and **126a** (bottom) on the induction of apoptosis in MDA-MB-231 cells. Cells were treated with varying concentrations of **119c**, **120c** and **126a** for 48 h, stained with Annexin V-FITC and PI, and the apoptotic effect was assessed by flow cytometry. Representative results are shown, with quadrants indicating the proportion of cells that are necrotic: Q1, late apoptotic: Q2, early apoptotic: Q3, and healthy: Q4. Images are representative of three independent experiments.

Chapter 5   Conclusion and future directions

5.1 Conclusion from synthetic studies

A library of multi-cyclic alkaloid-like compounds possessing the 3-azatricyclo[5.3.1.0^{4,9}]undec-2-ene core structure was successfully synthesised in Chapter 2. This was achieved *via* multi-step synthesis starting from the Meerwein's ester which was transformed to the cyclic alkene precursor **72** *via* an aldol condensation, Michael addition, Dickman condensation, an acid hydrolysis, and Wittig reaction. From there the cyclic alkene **72** was then subjected to the Bridging Ritter reaction with various nitriles to afford a library of tricyclic imines **82a-c** with 3-azatricyclo[5.3.1.0^{4,9}]undec-2-ene core structure. Subsequent reactions were employed to derivatise the imine compounds while keeping their 3-azatricyclo[5.3.1.0^{4,9}]undec-2-ene core structure to afford compounds **63**, **84**, **90a-b**, **91a-b**, **92**, and **93**. Chapter 2 highlighted the influence of the variety of substituents at the C-2 and C-18 positions on the reactivity of the respective imines.

In Chapter 3 the acid catalysed cyclisations of caryophyllene **96** and its monoepoxide **117** were investigated *via* the Ritter reaction. This study revealed that when caryophyllene **96** was subjected to the Ritter reaction with various nitriles, the formation of optically active tricyclic amides of caryolane **119a-i** and clovane **120a-d** skeletons was observed. Interestingly, the dissolution of caryophyllene **96** with acetonitrile, propionitrile, chloroacetonitrile and benzonitrile in acidic medium yielded both caryolane **119** and clovane **120** skeletons in ratios of 1:1, 2:1, 3:1, and 4:1 respectively. This observation supports the acid catalysed Wagner-Meerwein rearrangement, as the reactivity of the nitriles decreases; the ratio of formation would favour the more kinetically stable of the two skeletons. In vitro testing revealed that compounds generated from the caryophyllene structure observed significant potentiating effect on the triple negative breast cancer (MDA-MB-231) cell line. In light of this, tricyclic amides

of both caryolane **119** and clovane **120** skeletons were further derivatised to expand our library of biologically active alkaloid-like molecules. The synthetic strategy employed for derivatisation involved amide cleavage under mild conditions, followed by reductive alkylation with various aldehydes to yield amines with similar structural integrity as their respective amides.

Furthermore, caryophyllene monoepoxide **117** was also used as a starting material for the expansion of the library, as well as allowing for structural diversity. The reaction between monoepoxide **117** and various nitriles under the Ritter reaction conditions yielded diamides **126a-e** as the major products. Reaction conditions such as time and temperature were investigated in order to favour the formation of alcohol-amide structure **125.** The outcome of this investigation highlighted that carbocations could be formed at the C-2 and C-9 positions in less than 1 minute in the presence of concentrated sulfuric acid and acetonitrile at 0 ºC. It was observed that the cation arising from the epoxide ring opening underwent rearrangement forming the clovane skeleton exclusively. The observed major diamide products resulted from the formation of a carbocation intermediate **117d** that further reacted with another mole nitrile to give the diamide structure **126**.

In summary, the Ritter reaction was successfully used as a viable method for generating chemically diverse libraries of biologically active alkaloid-like molecules.

5.2 Conclusion from biological studies

The anticancer activities of all of the synthesised compounds were assessed *via* several methods. The compounds' antiproliferative active in breast cancer cell lines (MDA-MB-231, MCF-7) were evaluated in-house *via in vitro* assays such as MTS, cell cycle analysis and induction of apoptosis studies using flow cytometry. Compounds **82c**, **119c/e**, **120c**, **126a**, **127a/c/d**, and **128d** effectively decreased the proliferation and viability of MDA-MB-231,

observed IC_{50} values were 7.9, 5.9, 69.3, 3.3, 3.0, 37.9, 40.4, 36.9, and 26.4 µM, respectively. In order to investigate the compounds' selectivity, active compounds were tested against an ER+ (MCF-7) breast cancer cell line. It was found that three of the active compounds were selective towards the more aggressive triple negative (MDA-MB-231) cell line, while exhibiting no antiproliferative activities towards the MCF-7 cells. Selectivity towards the harder to treat triple negative breast cancer cells make these compounds more ideal drug candidates for further development.

The NCI also established promising anticancer activities for compound **63** across multiple cancer types. However, compounds **63** observed general toxicity against healthy mammalian Vero cell line (African green monkey kidney). α,β-Unsaturated double bond was removed from compound **63** to afford compound **84** in order to rectify its observed toxicity. However, by removing the α,β-unsaturated system (C-12, C-21, and C-22 position) on compound **63** also decreased its anticancer activity.

Furthermore, cell cycle and apoptosis studies revealed compound **82c** promotes cell cycle arrest in the G2/M phase, as well as inducing apoptosis after 48 h of treatment. Moreover, compounds **119c**, **120c**, and **126a** also altered the distribution of cells throughout the cell cycle, as well as the ability to induce apoptosis in the MDA-MB-231 cells.

In addition to the in-house assays, the synthesised compounds were submitted to BIOTECH to assess the compounds' selectivity towards cancerous cells; active compounds were tested against noncancerous Vero cells. It was found that five of the active compounds were selective towards cancerous cells. Overall, our results indicate that the Bridging Ritter reaction can be

used to synthesise novel tricyclic alkaloid-like compounds with promising selective anticancer activities.

5.3 Future directions

Based on the promising biological results obtained, further investigation into other cancer types should be explored. The mechanism of action of these compounds should also be investigated to determine the reason for the observed selectivity towards the triple negative breast cancer cell line.

Chapter 6   Experimental

6.1   Chemistry

Reagents and analytical grade solvents were purchased from commercial sources. Compounds were purified by column chromatography using flash silica gel (60 − 80 μm). The purity of compounds was determined by NMR and High-resolution mass spectrometer. ^{1}H and ^{13}C NMR spectra were recorded on an Agilent 500 MHz spectrometer (500 MHz ^{1}H, 125 MHz ^{13}C) in deuterated chloroform (CDCl$_3$) unless otherwise specified. NMR assignments were based on COSY, HSQC, NOESY and DEPT experiments. ^{1}H and ^{13}C NMR assignments are based on the numbering system used in the systematic name. Infrared Spectroscopy was collected using an Agilent Cary 630 FTIR spectrometer. Optical rotation was measured using a Jasco P-200 polarimeter. High-resolution mass spectra (HRMS) were obtained on an Agilent 6510 Accurate-Mass Q-TOF Mass Spectrometer, equipped with an ESI source.

6.1.1   Synthesis of ketone-alkene

General conditions for Wittig reaction

The cyclic diene **72** was previously prepared by our research group as the precursor for generating the tricyclic imine scaffold.[86, 113-114, 118] The reaction proceeds *via* the Wittig reaction from the corresponding diketone and phosphonium ylide. Bicyclo[3.3.1]nonane-2,6-dione **77** (1.66 g, 10.9 mmol), potassium *tert*-butoxide (3.06 g, 27.1 mmol), triethyl benzyl ammonium chloride (0.014 g, 7.29 mmol), hydroquinone (0.014 g, 0.13 mmol), and methyl triphenyl phosphonium bromide (9.78 g, 27.3 mmol), were suspended in benzene (80 mL) in a round-bottom flask fitted with a condenser and drying tube. The mixture was stirred and heated to 80 ℃ for 5 min and stirred at room temperature overnight. Light petroleum ether was added (140 mL), and the mixture was stirred for a further 10 min. The mixture was put through a silica

plunge and solvents were removed *via* fractional distillation (first at 80 ºC, then at 110 ºC to remove benzene). The crude compound was purified by silica column chromatography using ethyl acetate: hexane (6:4) to yield compound **78** as pale yellow liquid (74%).

2-methylenebicyclo[3.3.1]nonan-6-one **78**
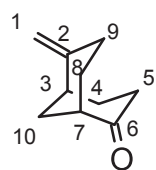
(1.20 g, 74%) pale yellow liquid; R_f (6:4 ethyl acetate /hexane) 0.64; ^{1}H NMR (500 MHz, CDCl$_3$) δ 4.75 (s, 1H, H-1a), 4.69 (s, 1H, H-1b), 2.74-2.78 (m, 1H, H-3), 2.54-2.59 (m, 1H, H-7), 2.50-2.56 (m, 1H, H-5a), 2.42 (q, J = 8.5 Hz, 1H, H-5b), 2.30-2.36 (m, 4H, 2H-4, 2H-8), 2.09-2.16 (m, 1H, H-10a), 2.02-2.08 (m, 1H, H-9a), 1.81-1.88 (m, 2H, H-10b, H-9b); ^{13}C NMR δ 218.5 (C-6), 153.7 (C-2), 111.2 (CH$_2$-1), 47.4 (CH-7), 41.23 (CH$_2$-5), 39.0 (CH-3), 36.0 (CH$_2$-9), 32.5 (CH$_2$-4), 32.4 (CH$_2$-8), 24.1 (CH$_2$-10); FT-IR ν_{max} (neat) 3360, 2963, 2968, 1696, 1659, 1460, 1429, 1400, 1389, 1345, 1302, 1250, 1223, 1198, 1079, 1066, 998, 826, 709 cm^{-1}; HRMS (ESI): found 151.1128, [M+H]$^+$, C$_{10}$H$_{15}$O required 151.1122, [M+H]$^+$.

General conditions for reduction of compound **78**

Ketone-alkene **78** (0.15 g, 1.00 mmol) was dissolved in dry methanol (10 mL) and placed in 50 mL round-bottomed flask fitted with a drying tube. NaBH$_4$ (0.380 g, 10-mole equiv.) was added slowly, and the mixture was stirred overnight at room temperature. The mixture was quenched with saturated NaHCO$_3$ (30 mL) and extracted with chloroform (20 mL x 2) and washed with saturated NaCl (30 mL). The solvent was removed under reduced pressure to yield compound **79** as a viscous liquid (0.12 g, 77%). No further purification was needed.

2-methylenebicyclo[3.3.1]nonan-6-ol **79**
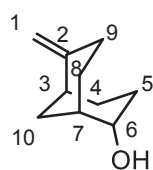
(0.12 g, 77%) pale yellow liquid; ^{1}H NMR (500 MHz, CDCl$_3$) δ 4.64 (t, J = 2.0 Hz, 2H, 2H-1), 3.84-3.90 (m, 1H, H-6), 2.38-2.48 (m, 2H, H-3, H-5a), 2.26-2.32 (m, 1H, H-5b), 1.96-2.06 (m, 2H, H-4a, H-7), 1.80-1.87 (m, 1H, H-8a), 1.64-1.78 (m, 4H, H-9a, H-8b, 2H-10), 1.52-1.64 (m, 2H, H-4b, H-9b); ^{13}C NMR δ 153.0 (C-2), 107.9 (CH$_2$-1), 73.4 (C-6), 37.0 (CH-3), 34.5 (CH-7), 34.0 (CH$_2$-9), 31.6 (CH$_2$-5), 31.4 (CH$_2$-8), 30.7 (CH$_2$-10), 24.1 (CH$_2$-4); FT-IR v$_{max}$ (neat) 3588, 3480, 2966, 2868, 2655, 1680, 1463, 1445, 1400, 1355, 1339, 1300, 1295, 1268, 1273, 1120, 1103, 1020, 977, 870, 821, 761 cm^{-1}; HRMS (ESI): found 153.1272, [M+H]$^+$, C$_{10}$H$_{17}$O required 153.1279, [M+H]$^+$.

6.1.2 Bridging Ritter Reaction with 2,6-dimethylenebicyclo-[3.3.1]-nonane and various nitriles

General conditions for Bridging Ritter reaction with 2,6-dimethylenebicyclo-[3.3.1]-nonane

A mixture of 98% H$_2$SO$_4$ (2 mL) and nitrile reagent (between 5 – 8 mole equiv.) in 100 mL round-bottomed flask fitted with a condenser and drying tube, was stirred in an ice bath. A solution of 2,6-dimethylenebicyclo[3.3.1]nonane **72** (0.77 g, 5.20 mmol) in benzene (5 mL) was added to the mixture drop-wise but rapidly. The reaction mixture was stirred at 0 ˚C for 30 min, then at room temperature overnight. Water (20 mL) was added to the mixture and stirring was continued for a further 30 min. The mixture was extracted with diethyl ether. The aqueous layer was quenched with 1M NaOH solution (18 mL) and extracted with chloroform (25 mL x 2). The organic layer was dried over Na$_2$SO$_4$ and solvent removed under reduced pressure. The crude product was purified by column chromatography ethyl acetate: hexane (4:6).

Exo-11-propanamido-4,endo-11-dimethyl-2-ethyl-3-azatricyclo[5.3.1.0^{4,9}]undec-2-ene **82b**
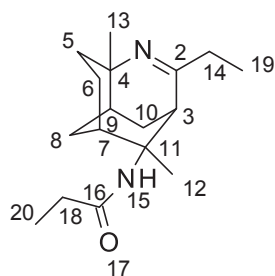
(1.22 g, 66%) yellow waxy solid; R_f (9:1 ethyl acetate/methanol) 0.75; ^{1}H NMR (500 MHz, CDCl$_3$) δ 5.22 (s, 1H, NH-15), 3.36 (s, 1H, H-3), 2.36 (q, *J* = 7.5 Hz, 2H, 2H-18), 2.15-2.21 (m, 2H, 2H-14), 1.82 (d, *J* = 10.5 Hz, 1H, H-9), 1.68-1.77 (m, 3H, H-7, H-10a, H-5a), 1.48-1.64 (m, 4H, H-8a, H-10b, H-5b, H-6a), 1.46 (s, 3H, C$\underline{H}_3$-13), 1.27 (s, 3H, C$\underline{H}_3$-12), 1.22-1.32 (m, 2H, H-6b, H-8b), 1.15 (t, *J* = 7.5 Hz, 3H, C$\underline{H}_3$-20), 1.13 (t, *J* = 7.5 Hz, 3H, C$\underline{H}_3$-19); ^{13}C NMR δ 174.8 (C=O), 173.1 (C-2), 62.1 (C-11/4), 61.0 (C-11/4), 40.7 (CH-1), 40.1 (CH-9), 37.7 (CH$_2$-18), 35.7 (CH$_2$-5), 34.9 (CH-7), 34.4 (CH$_3$-12), 33.6 (CH$_2$-14), 30.6 (CH$_2$-8), 30.3 (CH$_2$-10), 25.4 (CH$_3$-13), 22.1 (CH$_2$-6), 14.3 (CH$_3$-20), 12.6 (CH$_3$-19); FT-IR ν$_{max}$ (neat) 3440, 3249, 3190, 2925, 2110, 1650, 1554, 1449, 1371, 1354, 1112, 959, 941, 744 cm^{-1}; HRMS (ESI): found 277.2273, [M+H]$^+$, C$_{17}$H$_{29}$N$_2$O required 277.2280, [M+H]$^+$.

Exo-11-chloroacetamido-4,endo-11-dimethyl-2-chloromethyl-3-azatricyclo[5.3.1.0^{4,9}]undec-2-ene **82c**
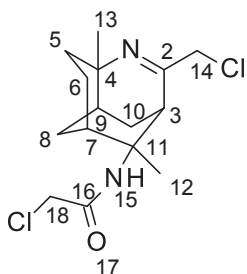
(1.10 g, 52%) yellow waxy solid; R_f (9:1 ethyl acetate/methanol) 0.76; ^{1}H NMR (500 MHz, CDCl$_3$) δ 6.14 (br s, 1H, NH-15), 4.19 (d, *J* = 11.5 Hz, 1H, H-18a), 4.12 (d, *J* = 11.5 Hz, 1H, H-18b), 4.00 (s, 2H, 2H-14), 3.48 (br s, 1H, H-3), 2.05 (d, *J* = 10.5 Hz, 1H, H-9), 1.85 (br s, 1H, H-7), 1.73-1.84 (m, 2H, H-10a, H-5a), 1.69 (d, *J* = 10.5 Hz, 1H, H-8a), 1.52-1.64 (m, 3H, H-6a, H-10b, H-5b), 1.50 (s, 3H, C$\underline{H}_3$-12), 1.36-1.38 (m, 1H, H-8b), 1.33 (s, 3H, C$\underline{H}_3$-13); ^{13}C NMR δ 169.1 (C=O), 165.0 (C=N), 60.4 (C-11/4), 60.1 (C-11/4), 49.7 (CH$_2$-18), 43.5 (CH$_2$-14), 37.0 (CH-1), 36.6 (CH-9), 33.2 (CH$_2$-10), 32.5 (CH-7), 31.6 (CH$_3$-13), 28.3 (CH$_2$-8), 27.8 (CH$_2$-

10), 22.7 (CH$_3$-12), 19.6 (CH$_2$-6); FT-IR v_{max} (neat) 3530, 3455, 3267, 3210, 2954, 2146, 1660, 1554, 1450, 1391, 1367, 1355, 1120, 944, 850, 722 cm^{-1}; HRMS (ESI): found 317.1195, [M+H]$^+$, C$_{15}$H$_{23}$Cl$_2$N$_2$O required 317.1187, [M+H]$^+$.

6.1.3 Derivatisation of 3-azatricyclo[5.3.1.0^{4,9}]undec-2-ene

General conditions for hydride reduction of tricyclic imines

Imine **82a/b** (0.450 g, 1.81 mmol) was dissolved in dry methanol (15 mL) and placed in a round-bottom flask fitted with a drying tube, NaBH(OAc)$_3$ (2.30 g, 10.86 mmol, 6-mole equiv.) was slowly added. The mixture was stirred overnight at room temperature. The reaction was quenched with saturated NaHCO$_3$ (20 mL), extracted with CHCl$_3$ (20 mL x 2), and washed with a saturated solution of NaCl (20 mL). The organic layer was dried with Na$_2$CO$_3$ and solvent was removed under reduced pressure to yield a viscous liquid which upon standing solidified to a waxy solid over a day. The product was purified by column chromatography ethyl acetate: methanol (8:2) to afford the reduced compounds as yellow waxy solids.

Exo-11-acetamido-2,4,endo-11-trimethyl-3-azatricyclo[5.3.1.0^{4,9}]undecane **90a**
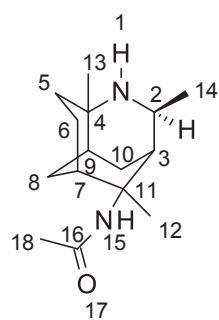
(0.36 g, 71%) yellow waxy solid; R$_f$ (8:2 ethyl acetate/methanol) 0.60; ^{1}H NMR (500 MHz, CDCl$_3$) δ 5.31 (s, 1H, NH-15), 3.50 (q, J = 7.5 Hz, 1H, H-2), 2.44 (br s, 1H, H-3), 2.06-2.09 (m, 1H, H-9), 1.95 (s, 3H, C$\underline{H}_3$-12), 1.59-1.83 (m, 7H, 2H-6, 2H-8, H-7, H-10a, H-5a), 1.58 (s, 3H, C$\underline{H}_3$-18), 1.50 (br d, J = 13.0 Hz, 1H, H-10b), 1.34 (d, J = 7.5 Hz, 3H, C$\underline{H}_3$-14), 1.12-1.17 (m, 1H, H-5b), 1.10 (s, 3H, C$\underline{H}_3$-13); ^{13}C NMR δ 171.7 (C=O), 63.9 (C-11/4), 56.8 (CH-2), 55.2 (C-11/4), 41.6 (CH-1), 38.8 (CH$_2$-5), 37.5 (CH$_3$-18), 37.1 (CH-9), 36.1 (CH-7), 34.3 (CH$_2$-8), 30.5 (CH$_2$-10), 28.1 (CH$_3$-12), 27.8 (CH$_3$-14), 26.3 (CH$_3$-13), 22.8 (CH$_2$-6); FT-IR v_{max} (neat)

3256, 3191, 2956, 2925, 2873, 1648, 1550, 1457, 1372, 1353, 1234, 1112, 1076, 940, 721 cm^{-1}; HRMS (ESI): found 251.2115, [M+H]$^+$, C$_{15}$H$_{27}$N$_2$O required 251.2123, [M+H]$^+$.

Exo-11-propanamido-4,endo-11-dimethyl-2-ethyl-3-azatricyclo[5.3.1.0^{4,9}]undecane **90b**
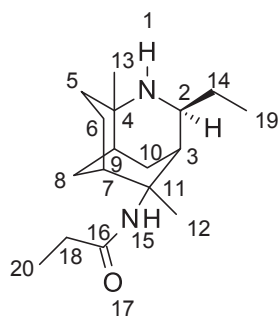
(0.49 g, 97%) yellow waxy solid; R$_f$ (8:2 ethyl acetate/methanol) 0.62; ^{1}H NMR (500 MHz, CDCl$_3$) δ 5.29 (s, 1H, NH-15), 3.12 (td, *J* = 7.5, 5.5 Hz, 1H, H-2), 2.57-2.59 (m, 1H, H-3), 2.16 (dq, *J* = 7.5, 1.0 Hz, 2H, 2H-14), 1.96 (dd, *J* = 11.0, 1.0 Hz, 1H, H-9), 1.82-1.98 (m, 1H, H-6a), 1.76-1.82 (m, 2H, H-5a, H-7), 1.65-1.72 (m, 2H, H-6b, H-10a), 1.58 (s, 3H, CH$_3$-12), 1.55-1.60 (m, 3H, H-5b, 2H-18), 1.46-1.49 (m, 2H, H-10b, 2H-8a), 1.25-1.27 (m, 1H, H-8b), 1.14 (t, *J* = 7.5 Hz, 3H, CH$_3$-20), 1.10 (s, 3H, CH$_3$-13), 0.97 (t, *J* = 7.5 Hz, 3H, CH$_3$-19); ^{13}C NMR δ 172.63 (C=O), 61.9 (CH-2), 61.0 (C-11/4), 60.0 (C-11/4), 37.3 (CH-1), 36.6 (CH$_2$-18), 35.5 (CH-9), 34.6 (CH$_3$-12), 34.3 (CH-7), 32.3 (CH$_2$-5), 31.8 (CH$_2$-14), 31.2 (CH$_2$-8), 28.2 (CH$_2$-10), 23.3 (CH$_3$-13), 20.4 (CH$_2$-6), 12.7 (CH$_3$-19), 10.1 (CH$_3$-20); FT-IR v$_{max}$ (neat) 3286, 3260, 2985, 2883, 2673, 1659, 1549, 1432, 1377, 1320, 1247, 1102, 1060, 989, 756 cm^{-1}; HRMS (ESI): found 279.2436, [M+H]$^+$, C$_{17}$H$_{31}$N$_2$O required 279.2436, [M+H]$^+$.

General conditions for Pd/C reduction of tricyclic imines

Imine **82c** (50 mg, 0.158 mmol) was dissolved in dry CH$_2$Cl$_2$ (10 mL) and placed in a round-bottom flask fitted with a hydrogen balloon, 5% Pd/C (25 mg, 0.012 mmol, 0.074-mole equiv.) was added to the mixture. The mixture was stirred overnight at room temperature. Pd/C was filtered and the solvent was removed under reduced pressure. The product was washed with hexane (20 mL) to yield imine **92** as a viscous liquid (0.035 g, 79%). No further purification was needed.

Exo-11-acetamido-4,*endo*-11-dimethyl-2-chloromethyl-3-azatricyclo[5.3.1.0^{4,9}]undec-2-ene

92
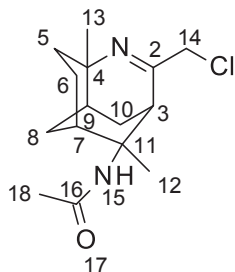
(0.04 g, 79%) viscous liquid; ^{1}H NMR (500 MHz, CDCl$_3$) δ 6.51 (br s, 1H, NH-15), 3.99 (s, 2H, 2H-14), 3.14 (s, 1H, H-3), 2.15 (s, 3H, C$\underline{H}_3$-18), 1.93 (d, J = 11.0 Hz, 1H, H-9), 1.77-1.84 (m, 1H, H-7), 1.53-1.84 (m, 6H, 2H-5, H-6a, 2H-8, H-10a), 1.51 (s, 3H, C$\underline{H}_3$-12), 1.32-1.38 (m, 2H, H-6b, H-10b), 1.29 (s, 3H, C$\underline{H}_3$-13); ^{13}C NMR δ 167.3 (C=O), 165.7 (C-2), 62.6 (C-11/4), 61.4 (C-11/4), 45.9 (CH$_2$-14), 42.8 (CH-1), 39.5 (CH-9), 35.6 (CH$_2$-5), 34.4 (CH-7), 34.3 (CH$_3$-13), 31.9 (CH$_3$-18), 30.2 (CH$_2$-8), 30.0 (CH$_2$-10), 25.2 (CH$_3$-12), 22.0 (CH$_2$-6); FT-IR ν$_{max}$ (neat) 3554, 3420, 3228, 3210, 2983, 2150, 1665, 1595, 1450, 1351, 1331, 1311, 1125, 957, 880, 778 cm^{-1}; HRMS (ESI): found 283.1585, [M+H]$^+$, C$_{15}$H$_{24}$ClN$_2$O required 283.1579, [M+H]$^+$.

General conditions for hydride reduction of tricyclic imines

Imine **92** (0.050 g, 0.158 mmol) was dissolved in dry ethanol (10 mL) and placed in a round-bottom flask fitted with a drying tube. NaBH$_4$ (0.067 g, 1.58 mmol, 10-mole equiv.) was added to the mixture. The mixture was stirred overnight at room temperature. The solvent was removed from under reduced pressure. The product was redissolved in CH$_2$Cl$_2$ (15 mL) and washed with saturated NaHCO$_3$ (30 mL). The organic layer was dried over Na$_2$CO$_3$ and solvent was removed under reduced pressure. The product was purified by column chromatography, ethyl acetate: methanol (9.5:0.5) to yield amine **93** as an off-white viscous liquid (0.035 g, 72%).

Exo-11-acetamido-4,endo-11-dimethyl-2-chloromethyl-3-azatricyclo[5.3.1.0^{4,9}]undecane **93**
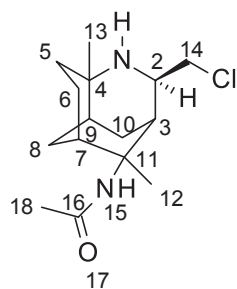
(0.04 g, 72%) off-white viscous liquid; R$_f$ (9.5:0.5 ethyl acetate/methanol) 0.64; ^{1}H NMR (500 MHz, CDCl$_3$) δ 6.58 (br s, 1H, NH-15), 3.98 (s, 3H, CH$_3$-18), 3.61 (td *J* = 13.5, 7.5 Hz, 1H, H-2), 2.45 (br s, 1H, H-7), 2.12-2.18 (m, 1H, H-3), 1.76-1.86 (m, 4H, H-8a, H-9, 2H-6), 1.65-1.74 (m, 2H, H-8b, H-10a), 1.62-1.64 (m, 1H, H-5a), 1.60 (s, 3H, CH$_3$-13), 1.50-1.56 (m, 1H, H-10b), 1.39 (d, *J* = 7.5 Hz, 2H, 2H-14), 1.27-1.34 (m, 1H, H-5b), 1.17 (s, 3H, CH$_3$-12); ^{13}C NMR δ 166.8 (C=O), 64.2 (C-11/4), 56.6 (CH-2), 56.0 (C-11/4), 46.0 (CH$_3$-18), 41.3 (CH-1), 37.9 (CH$_2$-5), 36.9 (CH-9), 36.9 (CH$_3$-13), 35.8 (CH-7), 33.7 (CH$_2$-8), 30.1 (CH$_2$-10), 27.5 (CH$_2$-14), 26.1 (CH$_3$-12), 22.7 (CH$_2$-6); FT-IR ν$_{max}$ (neat) 3279, 3265, 2952, 2800, 2651, 1660, 1589, 1450, 1395, 1388, 1200, 1120, 1080, 989, 877, 756 cm^{-1}; HRMS (ESI): found 285.1728, [M+H]$^+$, C$_{15}$H$_{26}$ClN$_2$O required 285.1734, [M+H]$^+$.

General conditions for reductive alkylation of 3-azatricyclo[5.3.1.0^{4,9}]undec-2-ene

Amine **90a/b** (0.23 g, 0.92 mmol) was dissolved in MeCN (20 mL), to which NaBH$_3$CN (1.15 g, 20-mole equiv.), 40% formaldehyde solution (2 mL) and a few drops of glacial acetic acid were added. The solution was stirred for 3 hours at room temperature. The solvent was removed under reduced pressure. The crude was dissolved in CHCl$_3$ (20 mL) and washed with saturated NaHCO$_3$ (30 mL), saturated NaCl (30 mL), and the organic layer was dried over Na$_2$SO$_4$ to yield a pale red viscous liquid. The crude was further purified by column chromatography ethyl acetate: methanol (9:1).

Exo-11-acetamido-2,3,4,endo-11-tetramethyl-3-azatricyclo[5.3.1.0^{4,9}]undecane **91a**
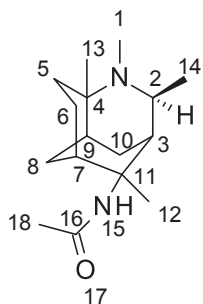
(0.12 g, 49%) red viscous liquid; R$_f$ (9:1 ethyl acetate/methanol) 0.26; ^{1}H NMR (500 MHz, CDCl$_3$) δ 5.17 (s, 1H, NH-15), 3.05 (q, *J* = 7.5 Hz, 1H, H-2), 2.47 (br s, 1H, H-3), 2.29 (s, 3H, CH$_3$-1), 2.01-1.98 (m, 1H, H-9), 1.93 (s, 3H, CH$_3$-12), 1.64-1.90 (m, 7H, H-5a, 2H-6, 2H-8, H-7, H-10a), 1.58 (s, 3H, CH$_3$-18), 1.49 (d, *J* = 4.0 Hz, 1H, H-10b), 1.30 (d, *J* = 7.5 Hz, 3H, CH$_3$-14),

1.14-1.22 (m, 1H, H-5b), 1.11 (s, 3H, CH$_3$-13) ; ^{13}C NMR δ 171.7 (C=O), 63.9 (C-11/4), 56.8 (CH-2), 55.2 (C-11/4), 41.6 (CH-1), 38.8 (CH$_2$-5), 37.5 (CH$_3$-18), 37.1 (CH-9), 36.1 (CH-7), 36.0 (NCH$_3$), 34.3 (CH$_2$-8), 30.5 (CH$_2$-10), 28.1 (CH$_3$-12), 27.8 (CH$_3$-14), 26.3 (CH$_3$-13), 22.8 (CH$_2$-6); FT-IR ν$_{max}$ (neat) 3360, 3225, 2976, 2803, 2670, 1660, 1548, 1432, 1377, 1320, 1247, 1102, 1020, 982, 750 cm^{-1}; HRMS (ESI): found 265.2271, [M+H]$^+$, C$_{16}$H$_{29}$N$_2$O required 265.2280, [M+H]$^+$.

Exo-11-propanamido-3,4,endo-11-trimethyl-2-ethyl-3-azatricyclo[5.3.1.0^{4,9}]undecane **91b**
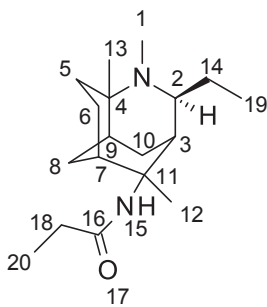
(0.06 g, 26%) red viscous liquid; R$_f$ (9:1 ethyl acetate/methanol) 0.30; ^{1}H NMR (500 MHz, CDCl$_3$) δ 5.27 (s, 1H, NH-15), 2.81 (td, *J* = 7.5, 5.5 Hz, 1H, H-2), 2.57 (br s, 1H, H-3), 2.38 (br s, 3H, CH$_3$-1), 2.15 (qd, *J* = 7.5, 3.0 Hz, 2H, 2H-14), 1.98-1.90 (m, 2H, H-6a, H-9), 1.76-1.84

(m, 3H, H-5a, H-7, H-8a), 1.68-1.74 (m, 2H, H-5b, H-10a), 1.60-1.66 (m, 4H, H-6b, H-8b, 2H-18), 1.59 (s, 3H, CH$_3$-12), 1.42-1.48 (m, 1H, H-10b), 1.15 (br s, 3H, CH$_3$-13), 1.13 (t, *J* = 7.5 Hz, 3H, CH$_3$-20), 1.07 (t, *J* = 7.5 Hz, 3H, CH$_3$-19); ^{13}C NMR δ 175.9 (C=O), 63.7 (C-11/4), 62.0 (C-11/4), 42.0 (CH-2), 40.0 (CH-1), 39.3 (NCH$_3$), 39.3 (CH-9), 39.2 (CH-7), 34.1 (CH$_2$-14), 33.8 (CH$_2$-8), 31.6 (CH$_2$-18), 30.3 (CH$_3$-13), 29.7 (CH$_2$-10), 25.1 (CH$_3$-12), 23.9 (CH$_2$-8),

16.7 (CH_2-6), 15.3 (CH_3-19), 12.7 (CH_3-20); FT-IR ν_{max} (neat) 3360, 3200, 2966, 2873, 2652, 1648, 1540, 1467, 1377, 1335, 1240, 1174, 1033, 960, 763 cm^{-1}; HRMS (ESI): found 293.2579, [M+H]$^+$, $C_{18}H_{33}N_2O$ required 293.2593, [M+H]$^+$.

General conditions for hydride reduction of lactam 63

Compound **63**[13] (0.05 g, 0.14 mmol) was dissolved in dry methanol (10 mL) and placed in a round-bottom flask fitted with a drying tube, NiCl$_2$.6H$_2$O (0.100 g, 0.43 mmol) was dissolved in dry methanol (5 mL) and added to the lactam solution. NaBH$_4$ (0.200 g, 40-mole equiv.) was added slowly to the mixture while stirring. The mixture was stirred overnight at room temperature. The reaction was quenched with saturated NaHCO$_3$ (20 mL), extracted with CHCl$_3$ (20 mL x 2), and the combined organic layers were washed with saturated NaCl (20 mL). The organic layer was dried over Na$_2$CO$_3$ and solvent was removed under reduced pressure to yield a yellow viscous liquid. The product was purified by column chromatography ethyl acetate: methanol (9:1) to afford the reduced compound **84** as a yellow viscous liquid (0.035 g, 70%).

Methyl*(E)*-[*exo*-11-acetylamino-9α,*endo*-11-dimethyl-2-*oxo*-1,2,4,5,5α,6,7,8,9,9α-decahydro-4,7-methanopyrrolo[1,2-a]-quinolin-1-ylidane]ethanoate **84**
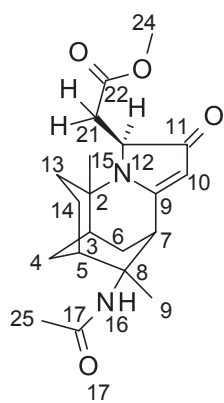
(0.03 g, 70%) yellow viscous liquid; R$_f$ (9:1 ethyl acetate/methanol) 0.53; ^{1}H NMR (500 MHz, CDCl$_3$) δ 5.48 (br s, 1H, NH-16), 5.09 (s, 1H, H-10), 3.95 (d, *J* = 2.0 Hz, H-7), 3.44 (s, 3H, C$\underline{H}_3$-24), 2.91 (dd, *J* = 15.5, 3.5 Hz, 1H, H-21a), 2.81 (dd, *J* = 15.5, 6.5 Hz, 1H, H-21b), 2.14 (dd, *J* = 6.5, 3.5 Hz, 1H, H-12), 2.07 (br s, 1H, H-3), 1.94-1.98 (m, 1H, H-5), 1.96 (s, 3H, C$\underline{H}_3$-25), 1.95-1.85 (m, 3H, H-4b, H-6b, H-13a), 1.60-1.70 (m, 3H, H-4a,

H-6a, H-14a), 1.30-1.54 (m, 2H, H-13b, H-14b), 1.50 (s, 3H, C$\underline{H}_3$-15), 1.34 (s, 3H, C$\underline{H}_3$-19); ^{13}C NMR δ 201.9 (C-11), 187.1 (C-9), 173.4 (C-17), 172.5 (C-22), 103.5 (CH-10), 62.9 (C-2/8), 62.6 (C-2/8), 61.6 (CH-12), 54.5 (CH$_3$-24), 40.9 (CH$_2$-21), 39.6 (CH-3), 39.0 (CH-7), 38.0 (CH-5), 33.9 (CH$_3$-15), 32.8 (CH$_2$-13), 32.3 (CH$_2$-4), 28.5 (CH$_2$-6), 27.4 (CH$_3$-25), 24.5 (CH$_3$-19), 21.8 (CH$_2$-14); FT-IR v_{max} (neat) 3366, 2927, 2083, 1730, 1648, 1517, 1433, 1371, 1238, 1179, 1157, 1124, 1101, 1032, 995, 864, 778 cm^{-1}; HRMS (ESI): found 361.2115, [M+H]$^+$, C$_{20}$H$_{29}$N$_2$O$_4$ required 361.2127, [M+H]$^+$.

6.1.4 Ritter Reaction of Caryophyllene with various nitriles

General conditions for the preparation of Ritter compounds using Caryophyllene as starting material

98% H$_2$SO$_4$ (2 mL), and nitrile reagent (5-mole equiv.) were stirred in an ice bath in 100 mL round-bottomed flask fitted with a condenser and drying tube. Caryophyllene **96** (1.00 g, 4.89 mmol) was dissolved in benzene (5 mL) and added to the mixture drop-wise but rapidly. The reaction mixture was stirred at 0 ˚C for 30 min, then at room temperature overnight. Water was added to the mixture and stirring was continued for a further 30 min. The mixture was extracted with diethyl ether. The aqueous layer was quenched with NaOH (18 mL, 1 M) and extracted with chloroform (20 mL x 2). The organic layer was dried over Na$_2$SO$_4$ and solvent removed under reduced pressure. The crude product mixture was purified by silica column chromatography using either ethyl acetate: hexane (7:3), diethyl ether: hexane (2:3), chloroform: ethyl acetate (7:3), or ethyl acetate: methanol (4:1) as the solvent system.

N-[(*1R,2S,5R,8R*)-4,4,8-trimethyl-1-tricyclo[6.3.1.0²,⁵]dodecanyl]acetamide **119a**
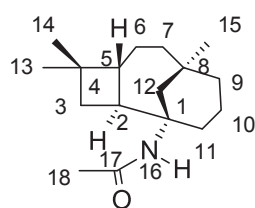
(0.46 g, 36%) white waxy solid; R_f (7:3 ethyl acetate/hexane) 0.46; $[\alpha]_{589}^{20}$ 49.6º (*c* 1.0, CHCl₃); ¹H NMR (500 MHz, CDCl₃) δ 5.40 (br s, 1H, NH), 2.26-2.36 (m, 2H, H-2, H-11a), 1.87 (s, 3H, C$\underline{\text{H}}_3$-18), 1.65-1.80 (m, 3H, H-5, H-3a, H-10a), 1.24-1.60 (m, 8H, 2H-6, 2H-7, 2H-9, H-10b, H-11b), 1.10 (s, 2H, 2H-12), 1.00-1.08 (m, 1H, H-3b), 0.93 (s, 3H, C$\underline{\text{H}}_3$-13), 0.92 (s, 3H, C$\underline{\text{H}}_3$-14), 0.82 (s, 3H, C$\underline{\text{H}}_3$-15); ¹³C NMR δ 171.7 (C=O), 58.1 (C-1), 48.9 (CH₂-12), 48.8 (CH-5), 43.8 (CH-2), 40.8 (CH₂-3), 40.7 (CH₂-7), 40.0 (CH₂-9), 38.4 (CH₂-11), 36.9 (C-8), 36.8 (C-4), 36.7 (CH₃-15), 33.2 (CH₃-14), 27.0 (CH₃-18), 25.6 (CH₂-6), 23.4 (CH₃-13), 22.6 (CH₂-10); FT-IR ν$_{max}$ (neat) 3254, 3067, 2945, 2926, 2915, 2861, 1637, 1558, 1457, 1364, 1303, 1221, 1181, 1092, 965, 749 cm⁻¹; HRMS (ESI): found 264.2340 [M+H]⁺, C₁₇H₃₀NO required 264.2327, [M+H]⁺.

N-[(*1S,2S,5S,8S*)-4,4,8-trimethyl-2-tricyclo[6.3.1.0¹,⁵]dodecanyl]acetamide **120a**
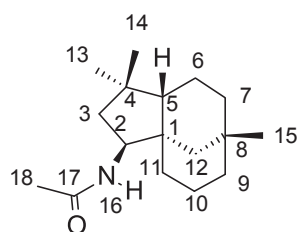
(0.46 g, 36%) white waxy solid; R_f (7:3 ethyl acetate/methanol) 0.34; $[\alpha]_{589}^{21}$ -24.4º (*c* 1.0, CHCl₃); ¹H NMR (500 MHz, CDCl₃) δ 5.27 (br d, *J* = 8.5, 1H, NH), 4.12 (ddd, *J* = 12.5, 8.5, 6.0 Hz, 1H, H-2), 1.99 (s, 3H, C$\underline{\text{H}}_3$-18), 1.61 (dd, *J* = 12.5, 6.0 Hz, 1H, H-3a), 1.40-1.58 (m, 2H, 2H-10), 1.05-1.41 (m, 10H, H-3b, H-5, 2H-6, 2H-7, H-9a, 2H-11, H-12a), 1.01-1.16 (m, 1H, H-12b), 1.02 (s, 3H, C$\underline{\text{H}}_3$-14), 0.94-1.00 (m, 1H, H-9b), 0.90 (s, 3H, C$\underline{\text{H}}_3$-13), 0.87 (s, 3H, C$\underline{\text{H}}_3$-15),.; ¹³C NMR δ 172.2 (C=O), 60.6 (CH-2), 53.9 (CH-5), 48.7 (CH₂-3), 46.6 (C-1), 45.9 (CH₂-12), 43.2 (CH₂-9), 40.4 (C-4), 36.1 (CH₂-11), 35.8 (CH₂-7), 35.4 (CH₃-15), 33.6 (CH₃-14), 32.8 (C-8), 27.3 (CH₃-13), 26.3 (CH₃-18), 23.2 (CH₂-6), 21.5 (CH₂-10); FT-IR ν$_{max}$ (neat)

3285, 3083, 2921, 2860, 1643, 1554, 1457, 1375, 1294, 1177, 1111, 1004, 968, 733 cm^{-1};

HRMS (ESI): found 264.2334, [M+H]$^+$, C$_{17}$H$_{30}$NO required 264.2327, [M+H]$^+$.

N-[(*1R,2S,5R,8R*)-4,4,8-trimethyl-1-tricyclo[6.3.1.02,5]dodecanyl]propanamide **119b**
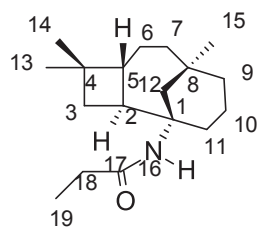
(0.75 g, 55%) pale yellow waxy solid; R$_f$ (4:6 diethyl ether/hexane) 0.40;[α]$_{589}^{21}$ 42.9º (*c* 1.0, CHCl$_3$); ^{1}H NMR (500 MHz, CDCl$_3$) δ 5.11 (br s, 1H, NH), 2.27-2.31 (m, 2H, H-2, H-11a), 2.13 (q, *J* = 7.5 Hz, 2H, 2H-18), 1.78-1.82 (m, 1H, H-5), 1.74-1.77 (m, 1H, H-10a), 1.71 (dd, *J* = 10.0, 8.0 Hz, 1H, H-7a), 1.11-1.62 (m, 9H, 2H-3, 2H-6, H-7b, 2H-9, H-10b, H-11b), 1.24 (s, 2H, 2H-12), 1.12 (t, *J* = 7.5 Hz, 3H, C$\underline{H}_3$-19), 0.98 (s, 3H, C$\underline{H}_3$-13), 0.97 (s, 3H, C$\underline{H}_3$-14), 0.88 (s, 3H, C$\underline{H}_3$-15); ^{13}C NMR δ 175.4 (C=O), 57.8 (C-1), 48.8 (CH-5), 48.8 (CH$_2$-18), 43.8 (CH-2), 40.7 (CH$_2$-12), 40.6 (CH$_2$-3), 40.1 (CH$_2$-7), 38.5 (CH$_3$-15), 36.9 (CH$_2$-9), 36.9 (C-8), 36.7 (C-4), 33.2 (CH$_3$-13), 33.2 (CH$_2$-11), 25.6 (CH$_2$-6), 23.4 (CH$_3$-14), 22.7 (CH$_2$-10), 12.9 (CH$_3$-19); FT-IR ν$_{max}$ (neat) 3282, 3070, 2946, 2922, 2863, 1642, 1547, 1457, 1360, 1285, 1237, 1180, 1071, 938, 691 cm^{-1}; HRMS (ESI): found 278.2475, [M+H]$^+$, C$_{18}$H$_{32}$NO required 278.2383, [M+H]$^+$.

N-[(*1S,2S,5S,8S*)-4,4,8-trimethyl-2-tricyclo[6.3.1.01,5]dodecanyl]propanamide **120b**
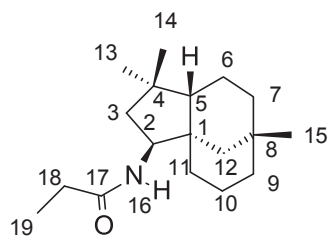
(0.38 g, 28%) pale yellow waxy solid; R$_f$ (4:6 diethyl ether/hexane) 0.34; [α]$_{589}^{22}$ -4.3º (*c* 1.0, CHCl$_3$); ^{1}H NMR (500 MHz, CDCl$_3$) δ 5.25 (br d, *J* = 8.5, 1H, NH), 4.14 (ddd, *J* = 12.5, 8.5, 6.0 Hz, 1H, H-2), 2.21 (q, *J* = 7.5 Hz, 2H, 2H-18), 1.61 (dd, *J* = 11.5, 6.0 Hz, 1H, H-3a), 1.46-1.59 (m, 2H, 2H-10), 1.65 (t, *J* = 7.5 Hz, 3H, C$\underline{H}_3$-19), 1.02 (s, 3H, C$\underline{H}_3$-15),

1.10-1.42 (m, 8H, H-3b, H-5, H-6a, 2H-7, H-9a, H-11a, H-12a), 0.94-1.08 (m, 4H, H-6b, H-9b, H-11b, H-12b), 0.90 (s, 3H, C$\underline{H}_3$-13), 0.87 (s, 3H, C$\underline{H}_3$-14); ^{13}C NMR δ 175.9 (C=O), 60.4 (CH-2), 54.0 (CH-5), 48.8 (CH$_2$-3), 46.6 (C-1), 46.0 (CH$_2$-12), 43.2 (CH$_2$-9), 40.4 (C-4), 36.1 (CH$_2$-11), 35.8 (CH$_2$-7), 35.4 (CH$_3$-14), 33.6 (CH$_3$-15), 32.8 (C-8), 32.7 (CH$_2$-18), 27.4 (CH$_3$-13), 23.2 (CH$_2$-6), 21.5 (CH$_2$-10), 12.7 (CH$_3$-19); FT-IR v_{max} (neat) 3258, 3082, 2944, 2920, 2860, 1639, 1559, 1460, 1379, 1332, 1277, 1198, 1070, 965, 774 cm^{-1}; HRMS (ESI): found 278.2371, [M+H]$^+$, C$_{18}$H$_{32}$NO required 278.2383, [M+H]$^+$.

2-chloro-*N*-[(*1R,2S,5R,8R*)-4,4,8-trimethyl-1-tricyclo[6.3.1.02,5]dodecanyl]acetamide **119c**
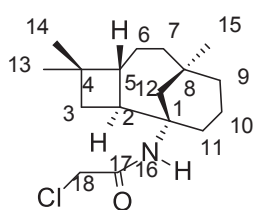
(0.92 g, 63%) yellow waxy solid; R$_f$ (7:3 chloroform/ethyl acetate) 0.50; $[\alpha]_{589}^{21}$ 30.6º (*c* 1.0, CHCl$_3$); ^{1}H NMR (500 MHz, CDCl$_3$) δ 6.31 (br s, 1H, NH), 3.95 (s, 2H, 2H-18), 2.38 (ddd, *J* = 19.0, 11.0, 8.0 Hz, 1H, H-2), 2.19-2.24 (m, 1H, H-11a), 1.75-1.85 (m, 2H, H-5, H-10a), 1.72 (dd, *J* = 9.5, 8.0 Hz, 1H, H-9a), 1.42-1.68 (m, 6H, H-3a, H-6a, 2H-7, H-10b, H-11b), 1.32-1.40 (m, 3H, H-6b, 2H-12,), 1.26 (dd, *J* = 11.0, 8.0 Hz, 1H, H-3b), 1.10-1.19 (m, 1H, H-9b), 1.00 (s, 3H, C$\underline{H}_3$-13), 0.99 (s, 3H, C$\underline{H}_3$-14), 0.90 (s, 3H, C$\underline{H}_3$-15); ^{13}C NMR δ 167.2 (C=O), 58.5 (C-1), 48.9 (CH-5), 48.0 (CH$_2$-12), 45.7 (CH$_2$-18), 43.7 (CH-2), 40.7 (CH$_2$-3), 40.3 (CH$_2$-7), 39.9 (CH$_2$-9), 37.8 (CH$_2$-11), 37.0 (C-8), 37.0 (C-4), 36.7 (CH$_3$-15), 33.2 (CH$_3$-14), 25.6 (CH$_2$-6), 23.3 (CH$_3$-13), 22.6 (CH$_2$-10); FT-IR v_{max} (neat) 3287, 3069, 2946, 2921, 2862, 1657, 1547, 1457, 1357, 1337, 127, 1058, 964, 809, 780, 679 cm^{-1}; HRMS (ESI): found 298.1929, [M+H]$^+$, C$_{17}$H$_{29}$ClNO required 298.1938, [M+H]$^+$.

2-chloro-*N*-[(*1S,2S,5S,8S*)-4,4,8-trimethyl-2-tricyclo[6.3.1.0^{1,5}]dodecanyl]acetamide **120c**
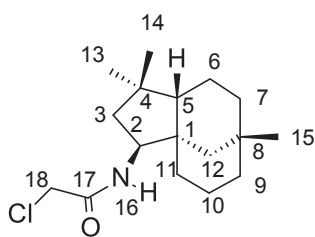
(0.41 g, 28%) yellow waxy solid; R_f (7:3 chloroform/ethyl acetate) 0.43;$[\alpha]_D^{22}$ 3.9º (*c* 1.0, CHCl_3); ^{1}H NMR (500 MHz, CDCl_3) δ 6.46 (br d, *J* = 8.5, 1H, NH), 4.00-4.15 (m, 1H, H-2), 4.07 (s, 2H, 2H-18), 1.65 (dd, *J* = 11.5, 6.0 Hz, 1H, H-3a), 1.50-1.60 (m, 2H, 2H-10), 1.43-1.48 (m, 1H, H-3b), 1.15-1.43 (m, 9H, H-5, 2H-6, 2H-7, H-9a, 2H-11, H-12a), 1.05 (s, 3H, C$\underline{H}$_3-15), 0.96-0.99 (m, 2H, H-9b, H-12b), 0.92 (s, 3H, C$\underline{H}$_3-13), 0.88 (s, 3H, C$\underline{H}$_3-14); ^{13}C NMR δ 167.9 (C=O), 61.0 (CH-2), 53.8 (CH-5), 48.4 (CH_2-3), 46.9 (C-1), 45.9 (CH_2-12), 45.6 (CH_2-18), 43.1 (CH_2-9), 40.6 (C-4), 35.9 (CH_2-11), 35.8 (CH_2-7), 35.4 (CH_3-14), 33.6 (CH_3-15), 32.8 (C-8), 27.4 (CH_3-13), 23.3 (CH_2-6), 21.5 (CH_2-10); FT-IR v_{max} (neat) 3283, 3084, 2945, 2921, 2862, 1652, 1541, 1457, 1364, 1334, 1237, 1153, 1095, 968, 856, 778, 711 cm^{-1}; HRMS (ESI): found 298.1943, [M+H]$^+$, C_{17}H_{29}ClNO required 298.1938, [M+H]$^+$.

N-[(*1R,2S,5R,8R*)-4,4,8-trimethyl-1-tricyclo[6.3.1.0^{2,5}]dodecanyl]benzamide **119d**
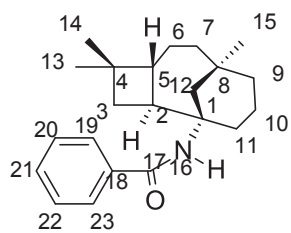
(0.91 g, 57%) white glassy solid; R_f (3:2 ethyl acetate/hexane) 0.70;$[\alpha]_D^{21}$ 27.3º (*c* 1.0, CHCl_3); ^{1}H NMR (500 MHz, CDCl_3) δ 7.70-7.773 (m, 1H, H-21), 7.44-7.48 (m, 2H, H-19), 7.38-7.43 (m, 2H, H-20), 5.86 (br s, 1H, NH), 2.40-2.50 (m, 2H, H-2, H-11a), 1.92 (dt, *J* = 13.0, 2.0 Hz, 1H, H-12a), 1.78-1.89 (m, 3H, H-5, H-3a, H-10a), 1.63-1.70 (m, 1H, H-10b), 1.12-1.62 (m, 9H, H-3b, 2H-6, 2H-7, 2H-9, H-11b, H-12b), 1.01 (s, 3H, C$\underline{H}$_3-13), 0.97 (s, 3H, C$\underline{H}$_3-14), 0.92 (s, 3H, C$\underline{H}$_3-15); ^{13}C NMR δ 169.3 (C=O), 137.8 (C-18), 133.6 (2CH-19), 131.1 (2CH-20), 129.5 (CH-21), 58.5 (C-1), 49.0 (CH_2-12), 48.8 (CH-5), 44.2 (CH-2), 40.8 (CH_2-3), 40.8 (CH_2-7), 40.0 (CH_2-9), 38.4 (CH_2-11), 37.0 (C-8), 37.0 (C-4), 36.7 (CH_3-15), 33.2 (CH_3-

14), 25.7 (CH$_2$-6), 23.4 (CH$_3$-13), 22.7 (CH$_2$-10); FT-IR ν_{max} (neat) 3306, 2945, 2917, 2861, 1638, 1601, 1527, 1486, 1457, 1358, 1304, 1190, 1148, 1072, 1000, 919, 859, 798, 710, 690 cm^{-1}; HRMS (ESI): found 326.2495, [M+H]$^+$, C$_{22}$H$_{32}$NO required 326.2484, [M+H]$^+$.

N-[(*1S,2S,5S,8S*)-4,4,8-trimethyl-2-tricyclo[6.3.1.0^{1,5}]dodecanyl]benzamide **120d**
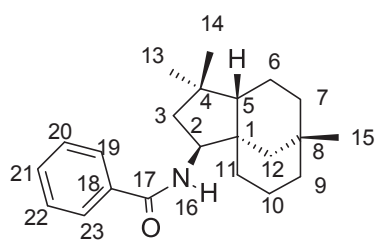
(0.30 g, 19%) white glassy solid; R$_f$ (3:2 ethyl acetate/hexane) 0.66; [α]$_D^{22}$ 18.0º (*c* 1.0, CHCl$_3$); ^{1}H NMR (500 MHz, CDCl$_3$) δ 7.70-7.79 (m, 1H, H-21), 7.47-7.52 (m, 2H, H-19), 7.39-7.46 (m, 2H, H-20), 6.00 (br d, *J* = 8.5, 1H, NH), 4.35 (ddd, *J* = 12.5, 8.5, 6.0 Hz, 1H, H-2), 1.72 (dd, *J* = 12.5, 6.0 Hz, 1H, H-3a), 1.52-1.57 (m, 2H, 2H-10), 1.48-1.51 (m, 1H, H-3b), 1.12-1.44 (m, 10H, H-5, 2H-6, 2H-7, H-9a, 2H-11, 2H-12), 1.06 (s, 3H, CH$_3$-14), 0.96-1.00 (m, 1H, H-9b), 0.96 (s, 3H, CH$_3$-13), 0.89 (s, 3H, CH$_3$-15); ^{13}C NMR δ 172.2 (C=O), 137.8 (C-18), 133.9 (2CH-19), 131.2 (2CH-20), 129.5 (CH-21), 60.6 (CH-2), 53.9 (CH-5), 48.7 (CH$_2$-3), 46.6 (C-1), 45.9 (CH$_2$-12), 43.2 (CH$_2$-9), 40.4 (C-4), 36.1 (CH$_2$-11), 35.8 (CH$_2$-7), 35.4 (CH$_3$-15), 33.6 (CH$_3$-14), 32.8 (C-8), 27.3 (CH$_3$-13), 23.2 (CH$_2$-6), 21.5 (CH$_2$-10); FT-IR ν_{max} (neat) 3309, 2942, 2921, 2861, 1631, 1534, 1488, 1457, 1371, 1309, 1290, 1216, 1155, 1071, 923, 800, 691 cm^{-1}; HRMS (ESI): found 326.2469, [M+H]$^+$, C$_{22}$H$_{31}$NO required 326.2484, [M+H]$^+$.

N-[(*1R,2S,5R,8R*)-4,4,8-trimethyl-1-tricyclo[6.3.1.02,5]dodecanyl]pentanamide **119e**

(0.87 g, 58%) pale yellow waxy solid; R_f (7:3 ethyl acetate/hexane) 0.51; $[\alpha]_{589}^{21}$ 50.7º (*c* 1.0, CHCl₃); ¹H NMR (500 MHz, CDCl₃) δ 5.15 (br s, 1H, NH), 2.26-2.36 (m, 2H, H-2, H-11a), 2.10 (t, *J* = 8.0 Hz, 2H, H-18), 1.74-1.83 (m, 2H, H-5, H-10a), 1.71 (dd, *J* = 9.5, 8.0 Hz, 1H, H-7a), 1.06-1.62 (m, 15H, 2H-3, 2H-6, H-7b, 2H-9, H-10b, H-11b, 2H-12, 2H-19, 2H-20), 0.98 (s, 3H, C$\underline{\text{H}}_3$-13), 0.97 (s, 3H, C$\underline{\text{H}}_3$-14), 0.92 (t, *J* = 7.5 Hz, 3H, C$\underline{\text{H}}_3$-21), 0.88 (s, 3H, C$\underline{\text{H}}_3$-15); ¹³C NMR δ 174.7 (C=O), 57.9 (C-1), 48.8 (CH₂-12), 48.8 (CH-5), 43.7 (CH-2), 40.7 (CH₂-18), 40.7 (CH₂-3), 40.1 (CH₂-7), 40.0 (CH₂-9), 38.5 (CH₂-11), 36.9 (C-8), 36.8 (C-4), 36.7 (CH₃-15), 33.2 (CH₃-14), 30.8 (CH₂-19), 25.6 (CH₂-20), 25.1 (CH₂-6), 23.4 (CH₃-21), 22.6 (CH₂-10), 16.5 (CH₃-13); FT-IR v_{max} (neat) 3276, 2946, 2924, 2860, 1637, 1544, 1457, 1362, 1341, 1269, 1204, 1105, 937, 809, 728, 691 cm⁻¹; HRMS (ESI): found 306.2786, [M+H]⁺, C₂₀H₃₆NO required 306.2797, [M+H]⁺.

3-chloro-*N*-[(*1R,2S,5R,8R*)-4,4,8-trimethyl-1-tricyclo[6.3.1.02,5]dodecanyl]propanamide **119f**

(0.98 g, 59%) pale yellow waxy solid; R_f (7:3 ethyl acetate/hexane) 0.49; $[\alpha]_{589}^{21}$ 27.7º (*c* 1.0, CHCl₃); ¹H NMR (500 MHz, CDCl₃) δ 5.13 (br s, 1H, NH), 3.59 (t, *J* = 6.0 Hz, 2H, 2H-21), 3.55 (t, *J* = 6.0 Hz, 2H, 2H-18), 2.27-2.36 (m, 2H, H-2, H-11a), 1.92-1.98 (m, 2H, 2H-20), 1.69-1.89 (m, 6H, 2H-19, 2H-12, H-7a, H-10a), 1.30-1.64 (m, 6H, H-10b, 2H-6, H-11b, H-9a, H-7b), 1.21-1.25 (m, 2H, H-3a, H-5), 1.08-1.17 (m, 2H, H-3b, H-9b), 0.98 (s, 3H, C$\underline{\text{H}}_3$-13), 0.97 (s, 3H, C$\underline{\text{H}}_3$-14), 0.88 (s, 3H, C$\underline{\text{H}}_3$-15); ¹³C NMR δ 173.9 (C=O), 58.1 (C-

1), 48.9 (CH-5), 48.8 (CH$_2$-12), 47.4 (CH$_2$-21), 46.3 (CH$_2$-20), 43.8 (CH-2), 40.8 (CH$_2$-3), 40.7 (CH$_2$-7), 40.0 (CH$_2$-9), 39.1 (CH$_2$-11), 36.9 (C-8), 36.8 (C-4), 36.7 (CH$_3$-15), 34.7 (CH$_2$-19), 33.7 (CH$_2$-18), 33.2 (CH$_3$-14), 25.4 (CH$_2$-6), 23.4 (CH$_3$-13), 22.6 (CH$_2$-10); FT-IR v_{max} (neat) 3295, 2946, 2926, 2864, 1643, 1541, 1457, 1362, 1341, 1281, 1134, 1101, 963, 727 cm^{-1}; HRMS (ESI): found 340.2420, [M+H]$^+$, C$_{20}$H$_{35}$ClNO required 340.2407, [M+H]$^+$.

3-chloro-*N*-[(*1R,2S,5R,8R*)-4,4,8-trimethyl-1-tricyclo[6.3.1.02,5]dodecanyl]propanamide
119g
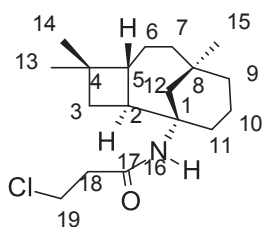
(0.44 g, 29%) yellow viscous liquid; R$_f$ (7:3 ethyl acetate/hexane) 0.44; [α]$_{589}^{21}$ 32.3º (*c* 1.0, CHCl$_3$); ^{1}H NMR (500 MHz, CDCl$_3$) δ 5.25 (br s, 1H, NH), 3.78 (t, *J* = 6.5 Hz, 2H, 2H-19), 2.55 (t, *J* = 6.5 Hz, 2H, 2H-18), 2.32 (m, 2H, H-2, H-11a), 1.80-1.85 (m, 1H, H-5), 1.73-1.80 (m, 1H, H-10a), 1.71 (dd, *J* = 10.0, 8.0 Hz, 1H, H-3a), 1.61-1.66 (m, 1H, H-10b), 1.26-1.60 (m, 6H, H-3b, 2H-6, H-7a, H-9a, H-11b), 1.24 (s, 2H, H-12), 1.08-1.18 (m, 2H, H-7b, H-9b), 0.99 (s, 3H, C$\underline{H}_3$-13), 0.97 (s, 3H, C$\underline{H}_3$-14), 0.88 (s, 3H, C$\underline{H}_3$-15); ^{13}C NMR δ 170.8 (C=O), 58.6 (C-1), 48.8 (CH$_2$-12), 48.7 (CH-5), 43.6 (CH-2), 43.2 (CH$_2$-19), 43.1 (CH$_2$-18), 40.7 (CH$_2$-3), 40.6 (CH$_2$-7), 40.0 (CH$_2$-9), 38.4 (CH$_2$-11), 36.9 (C-8), 36.9 (C-4), 36.6 (CH$_3$-15), 33.2 (CH$_3$-14), 25.5 (CH$_2$-6), 23.4 (CH$_3$-13), 22.6 (CH$_2$-10); FT-IR v_{max} (neat) 3293, 2945, 2923, 2863, 1644, 1551, 1457, 1376, 1333, 1286, 1219, 1154, 1101, 988, 944, 813, 778, 654 cm^{-1}; HRMS (ESI): found 312.2097, [M+H]$^+$, C$_{18}$H$_{31}$ClNO required 312.2094, [M+H]$^+$.

2-amino-*N*-[(*1R,2S,5R,8R*)-4,4,8-trimethyl-1-tricyclo[6.3.1.02,5]dodecanyl]acetamide **119h**
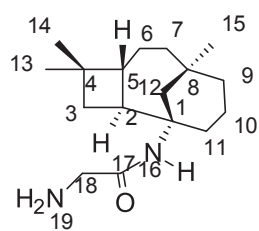
(1.09 g, 75%) brown viscous liquid; R_f (4:1 ethyl acetate/methanol) 0.33; $[\alpha]_{589}^{21}$ -21.0º (*c* 1.0, CHCl$_3$); ^{1}H NMR (500 MHz, CDCl$_3$) δ 7.54 (br s, 1H, NH), 3.29 (br s, 2H, 2H-18), 2.47-2.53 (m, 2H, H-2, H-11a), 1.80-1.90 (m, 1H, H-3a), 1.56-1.67 (m, 4H, H-7a, 2H-10, H-11b), 1.40-1.55 (m, 2H, 2H-9), 1.16-1.40 (m, 7H, H-3b, H-5, 2H-6, H-7b, 2H-12), 1.28 (s, 3H, C$\underline{H}_3$-13), 1.24 (s, 3H, C$\underline{H}_3$-14), 1.05 (s, 3H, C$\underline{H}_3$-15); ^{13}C NMR δ 173.5 (C=O), 59.6 (CH-5), 59.0 (C-1), 56.6 (C-8), 52.1 (CH$_2$-18), 47.2 (CH$_2$-12), 38.8 (C-4), 34.8 (CH$_3$-14), 34.5 (CH$_3$-15), 33.6 (CH$_2$-3), 33.4 (CH$_2$-7), 32.9 (CH$_2$-9), 32.1 (CH-2), 25.2 (CH$_3$-13), 24.9 (CH$_2$-11), 24.7 (CH$_2$-6), 21.0 (CH$_2$-10); FT-IR v_{max} (neat) 3391, 2921, 2867, 1654, 1521, 1449, 1370, 1241, 1223, 1189, 1020, 992, 919, 807, 729 cm^{-1}; HRMS (ESI): found 279.2446, [M+H]$^+$, C$_{17}$H$_{31}$N$_2$O required 279.2436, [M+H]$^+$.

S-methyl-*N*-[(*1R,2S,5R,8R*)-4,4,8-trimethyl-1-tricyclo[6.3.1.02,5]dodecanyl]carbamothioate **119i**
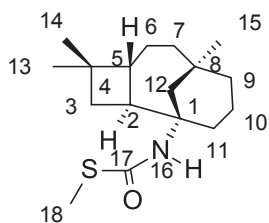
(0.015 g, 1%) orange viscous liquid; R_f (7:3 ethyl acetate/hexane) 0.42; $[\alpha]_{589}^{21}$ 31.0º (*c* 1.0, CHCl$_3$); ^{1}H NMR (500 MHz, CDCl$_3$) δ 2.30 (s, 3H, C$\underline{H}_3$-18), 2.16-2.22 (m, 2H, H-2, H-11a), 1.82-1.86 (m, 2H, H-3a, H-5), 1.50-1.80 (m, 6H, 2H-6, H-9a, H-11b, 2H-10), 1.44-1.50 (m, 1H, H-3b), 1.34-1.42 (m, 3H, 2H-7, H-9b), 1.12-1.20 (m, 2H, H-12), 1.02 (br s, 6H, C$\underline{H}_3$-15, C$\underline{H}_3$-14), 0.98 (s, 3H, C$\underline{H}_3$-13); ^{13}C NMR δ 211.9 (C=O), 61.3 (C-1), 49.4 (CH-5), 47.2 (CH-2), 45.4 (CH$_2$-12), 36.0 (CH$_2$-3), 35.4 (CH$_2$-7), 34.6 (CH$_2$-9), 33.8 (CH$_3$-15), 32.4 (C-8), 32.3 (C-4), 28.7 (CH$_2$-11), 27.1 (CH$_3$-13), 25.5 (CH$_3$-14), 19.9 (CH$_2$-6), 16.8 (CH$_2$-10), 14.6 (CH$_3$-18); FT-IR v_{max} (neat) 3196, 2924,

2861, 1647, 1558, 1449, 1396, 1363, 1190, 1165, 1070, 1037, 963, 789 cm^{-1}; HRMS (ESI): found 296.2057, [M+H]$^+$, C$_{17}$H$_{30}$NOS required 296.2048, [M+H]$^+$.

General conditions for the preparation of Ritter compounds using Caryophyllene monoepoxide **117** *as starting material*

98% H$_2$SO$_4$ (2 mL), and nitrile reagent (5-mole equiv.) were stirred in an ice bath in a round-bottomed flask fitted with a condenser and drying tube. Caryophyllene monoepoxide **117** (0.250 g, 1.14 mmol) was dissolved in benzene (5 mL) and added to the mixture drop-wise but rapidly. The reaction mixture was stirred at 0 ˚C for 30 min, then at room temperature overnight. Water was added to the mixture and stirring was continued for a further 30 min. The mixture was extracted with diethyl ether. The aqueous layer was quenched with saturated NaHCO$_3$ (20 mL) solution and extracted with chloroform (20 mL x 2). The organic layer was dried over Na$_2$SO$_4$ and solvent removed under reduced pressure. The crude product was purified by column chromatography using various solvent systems such as, ethyl acetate: hexane (1:1), chloroform: ethyl acetate (1:1), ethyl acetate: hexane (7:3), and ethyl acetate: hexane (3:2). Note: for the synthesis of compound **125a**, the reaction mixture was stirred for 4 min at 0º C before quenching with saturated NaHCO$_3$.

N-[(*1S,2S,5S,8S,9R*)-9-hydroxy-4,4,8-trimethyl-2-tricyclo[6.3.1.01,5]dodecanyl]acetamide **125a**
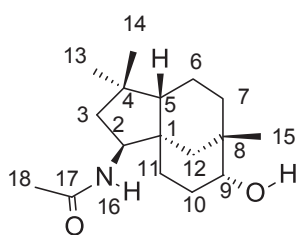
(0.06 g, 20%) as white glassy solid; R$_f$ (1:1 ethyl acetate/hexane) 0.28; [α]$_{589}^{22}$ -28.7º (*c* 1.0, CHCl$_3$); ^{1}H NMR (500 MHz, CDCl$_3$) δ 5.31 (br d, *J* = 9.5, 1H, NH), 4.14 (ddd, *J* = 12.5, 9.5, 6.0 Hz, 1H, H-2), 3.47 (q, *J* = 7.0 Hz, 1H, H-9), 1.98 (s, 3H, C$\underline{H}_3$-18), 1.80-2.00 (m,

1H, H-10a), 1.71 (br s, OH), 1.56 (d, J = 13.0 Hz, 1H, H-12a), 1.54-1.66 (m, 2H, H-3a, H-10b), 1.44-1.50 (m ,1H, H-11a), 1.35-1.45(m, 5H, H-3b, H-5, 2H-6, H-7a), 1.06-1.14 (m, 2H, H-7b, H-12b), 1.02 (s, 3H, C$\underline{H}_3$-14), 0.94 (s, 3H, C$\underline{H}_3$-15), 0.91 (s, 3H,C$\underline{H}_3$-13), 0.84-1.00 (m, 1H, H-11b); ^{13}C NMR δ 172.3 (C=O), 77.6 (CH-9), 60.3 (CH-2), 53.2 (CH-5), 48.6 (CH$_2$-3), 46.2 (C-1), 40.2 (C-4), 38.1 (CH$_2$-12), 37.5 (C-8), 35.7 (CH$_2$-7), 33.5 (CH$_3$-14), 30.8 (CH$_3$-15), 30.3 (CH$_2$-11), 28.1 (CH$_2$-10), 27.2 (CH$_3$-13), 26.4 (CH$_3$-18), 23.2 (CH$_2$-6); FT-IR v_{max} (neat) 3586, 3288, 2950, 2930, 2867, 1650, 1544, 1532, 1456, 1366, 1222, 1219, 1160, 1033, 966, 911, 775, 725 cm^{-1}; HRMS (ESI): found 280.2273, [M+H]$^+$, C$_{17}$H$_{30}$NO$_2$ required 280.2276, [M+H]$^+$.

2-chloro-N-[(1S,2S,5S,8S,9R)-2-[(2-chloroacetyl)amino]-4,4,8-trimethyl-9-tricyclo[6.3.1.01,5]dodecanyl]acetamide **126a**
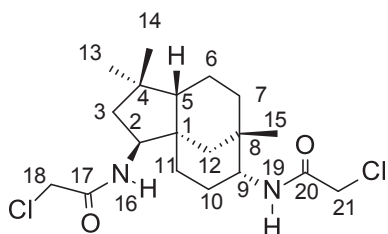
(0.15 g, 34%) yellow glassy solid; R$_f$ (7:3 ethyl acetate/hexane) 0.52; $[\alpha]_{589}^{22}$ -15.4º (C 1.0, CHCl$_3$); ^{1}H NMR (500 MHz, CDCl$_3$) δ 6.78 (d, J = 9.0 Hz, 1H, H-16), 6.44 (d, J = 9.5 Hz, 1H, H-19), 4.12 (ddd, J = 12.5, 9.0, 6.0 Hz, 1H, H-2), 4.07 (s, 2H, H-18), 4.05 (s, 2H, H-21), 3.52 (br d, J = 9.5 Hz, 1H, H-9), 2.01-2.08 (m, 1H, H-10a), 1.68 (dd, J = 11.5, 6.0 Hz, 1H, H-3a), 1.60-1.65 (m, 1H, H-10b), 1.52-1.58 (m, 1H, H-7a), 1.42-1.52 (m, 4H, H-3b, H-5, 2H-6), 1.30-1.35 (m, 1H, H-7b), 1.24-1.28 (m, 2H, 2H-12), 1.10-1.20 (m, 2H, 2H-11), 1.07 (s, 3H, C$\underline{H}_3$-15), 0.94 (s, C$\underline{H}_3$-13), 0.89 (s, C$\underline{H}_3$-14); ^{13}C NMR δ 168.3 (C-17/20), 167.9 (C-17/20), 60.8 (CH-2), 56.3 (CH-9), 53.4 (CH-5), 48.1 (CH$_2$-3), 46.5 (C-1), 45.7 (CH$_2$-18/21), 45.5 (CH$_2$-18/21), 40.6 (C-4), 40.1 (CH$_2$-12), 36.5 (CH$_2$-7), 36.2 (C-8), 33.3 (CH$_3$-15), 31.2 (CH$_2$-11), 31.0 (CH$_3$-14), 27.2 (CH$_3$-13), 26.0 (CH$_2$-10), 23.0 (CH$_2$-6); FT-IR v_{max} (neat) 3284, 2949, 2928, 2865, 1653, 1540, 1533, 1457, 1410,

1365, 1229, 1167, 1037, 968, 773, 730 cm^{-1}; HRMS (ESI): found 389.1746, [M+H]$^+$, $C_{19}H_{31}Cl_2N_2O_2$ required 389.1762, [M+H]$^+$.

N-[(*1S,2S,5S,8S,9R*)-4,4,8-trimethyl-2-(pentanoylamino)-9-tricyclo[6.3.1.01,5]dodecanyl]pentanamide **126b**
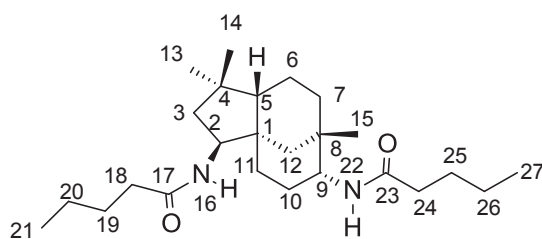
(0.04 g, 9%) white glassy solid; R$_f$ (7:3 ethyl acetate/hexane) 0.67; $[\alpha]_{589}^{22}$ -63.9º (*c* 1.0, CHCl$_3$); ^{1}H NMR (500 MHz, CDCl$_3$) δ 5.60 (d, *J* = 9.0 Hz, 1H, H-16/22), 5.35 (d, *J* = 9.0 Hz, 1H, H-16/22), 4.12 (ddd, *J* = 12.5, 9.0, 6.0 Hz, 1H, H-2), 3.64 (br d, *J* = 9.0 Hz, 1H, H-9), 2.20 (t, *J* = 7.5 Hz, 2H, H-18/24), 2.13 (t, *J* = 7.5 Hz, 2H, H-18/24), 1.92-2.00 (m, 1H, H-10a), 1.52-1.67 (m, 6H, H-3a, H-10b, 2H-19, 2H-25), 1.46-1.52 (m, 2H, 2H-7), 1.40-1.46 (m, 2H, 2H-6), 1.28-1.40 (m, 10H, H-3b, H-5, 2H-11, 2H-12, 2H-20, 2H-26), 1.02 (s, 3H, C<u>H</u>$_3$-15), 0.92 (t, *J* = 7.0 Hz, 3H, C<u>H</u>$_3$-21/27), 0.90 (t, *J* = 7.0 Hz, 3H, C<u>H</u>$_3$-21/27), 0.90 (s, 3H, C<u>H</u>$_3$-13), 0.85 (s, C<u>H</u>$_3$-14); ^{13}C NMR δ 175.7 (C-17/23), 175.3 (C-17/23), 60.6 (CH-2), 55.7 (CH-9), 53.6 (CH-5), 48.7 (CH$_2$-3), 46.4 (C-1), 40.5 (C-4), 40.4 (CH$_2$-12), 39.6 (CH$_2$-18/24), 39.32 (CH$_2$-18/24), 36.8 (CH$_2$-7), 35.9 (C-8), 33.3 (CH$_3$-15), 31.4 (CH$_2$-11), 31.3 (CH$_3$-14), 30.7 (CH$_2$-19/25), 30.6 (CH$_2$-19/25), 27.2 (CH$_3$-13), 26.2 (CH$_2$-10), 25.1 (CH$_2$-20/26), 25.1 (CH$_2$-20/26), 23.1 (CH$_2$-6), 16.5 (CH$_3$-21 and CH$_3$-27); FT-IR v$_{max}$ (neat) 3296, 2952, 2925, 2860, 1636, 1541, 1458, 1376, 1270, 1223, 1193, 1106, 993, 950, 853 cm^{-1}; HRMS (ESI): found 405.3478, [M+H]$^+$, $C_{25}H_{45}N_2O_2$ required 405.3481, [M+H]$^+$.

N-[(*1S,2S,5S,8S,9R*)-2-benzamido-4,4,8-trimethyl-9-

tricyclo[6.3.1.01,5]dodecanyl]benzamide **126c**
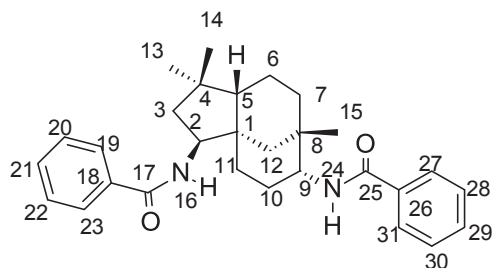
(0.09 g, 17%) yellow viscous liquid; R_f (3:2 ethyl acetate/hexane) 0.80; $[\alpha]_{589}^{22}$ 0.36º (*c* 1.0, CHCl$_3$); ^{1}H NMR (500 MHz, CDCl$_3$) δ 7.75 (d, *J* = 7.0 Hz, 2H, 2H-19/27), 7.66 (d, *J* = 7.0 Hz, 2H, 2H-19/27), 7.50 (t, *J* = 7.0 Hz, 1H, H-21/29), 7.46 (t, *J* = 7.0 Hz, 1H, H-21/29), 7.40 (t, *J* = 7.0 Hz, 2H, 2H-20/28), 7.33 (t, *J* = 7.0 Hz, 2H, 2H-20/28), 6.31 (d, *J* = 9.0 Hz, 1H, H-24), 5.32 (d, *J* = 8.5 Hz, 1H, H-16), 4.36 (ddd, *J* = 12.5, 8.5, 6.0 Hz, 1H, H-2), 3.86 (br d, *J* = 9.0 Hz, 1H, H-9), 2.10-2.03 (m, 1H, H-10a), 1.68-1.76 (m, 2H, H-3a, H-10b), 1.56-1.62 (m, 2H, H-7a, H-12a), 1.46-1.56 (m, 3H, H-6a, H-3b, H-5), 1.34-1.44 (m, 4H, H-6b, H-11a, H-7b, H-12b), 1.12-1.20 (m, 1H, H-11b), 1.07 (s, 3H, C$\underline{H}_3$-15), 0.97 (s, 3H, C$\underline{H}_3$-13), 0.96 (s, 3H, C$\underline{H}_3$-14); ^{13}C NMR δ 170.2 (C-17/25), 169.8 (C-17/25), 137.8 (C-18/26), 137.4 (C-18/26), 134.2 (CH-21/29), 133.9 (CH-21/29), 131.3 (2CH-20), 131.2 (2CH-28), 129.5 (2CH-19), 129.4 (2CH-27), 61.3 (CH-2), 56.4 (CH-9), 53.8 (CH-5), 48.6 (CH$_2$-3), 46.9 (C-1), 40.7 (C-4), 40.6 (CH$_2$-12), 36.7 (CH$_2$-7), 36.3 (C-8), 33.3 (CH$_3$-15), 31.5 (CH$_2$-11), 31.4 (CH$_3$-14), 27.3 (CH$_3$-13), 26.2 (CH$_2$-10), 23.1 (CH$_2$-6); FT-IR v$_{max}$ (neat) 3296, 2947, 2923, 2863, 1633, 1577, 1521, 1486, 1464, 1309, 1287, 1222, 1026, 995, 840, 798, 690 cm^{-1}; HRMS (ESI): found 445.2870, [M+H]$^+$, C$_{29}$H$_{37}$N$_2$O$_2$ required 445.2855, [M+H]$^+$.

N-[(*1S,2S,5S,8S,9R*)-4,4,8-trimethyl-2-(propanoylamino)-9-tricyclo[6.3.1.01,5]dodecanyl]propanamide **126d**
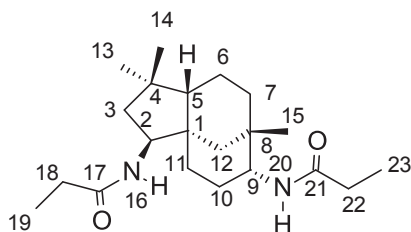
(0.22 g, 56%) white glassy solid; R_f (1:1 chloroform/ethyl acetate) 0.57; $[\alpha]_{589}^{22}$ -33.4º (*c* 1.0, CHCl$_3$); ^{1}H NMR (500 MHz, CDCl$_3$) δ 5.65 (d, *J* = 8.5 Hz, 1H, H-16), 5.32 (d, *J* = 9.0 Hz, 1H, H-20), 4.13 (ddd, *J* = 12.0, 8.5, 6.0 Hz, 1H, H-2), 3.67 (br d, *J* = 9.0 Hz, 1H, H-9), 2.24 (q, *J* = 7.5 Hz, 2H, 2H-18), 2.19 (q, *J* = 7.5 Hz, 2H, 2H-22), 1.94-2.02 (m, 1H, H-10a), 1.63 (dd, *J* = 12.0, 6.0 Hz, 1H, H-3a), 1.54-1.60 (m, 1H, H-10b), 1.51 (dt, *J* = 11.0, 2.5 Hz, 1H, H-7a), 1.43-1.48 (m, 1H, H-6a), 1.35-1.42 (m, 2H, H-3b, H-5), 1.22-1.34 (m, 3H, H-7b, 2H-12), 1.18 (t, *J* = 7.5 Hz, 3H, C*H*$_3$-19), 1.14 (t, *J* = 7.5 Hz, 3H, C*H*$_3$-23), 1.14-1.18 (m, 1H, H-11a), 1.03 (s, 3H, C*H*$_3$-15), 0.98-1.00 (m, 1H, H-11b), 0.94-0.98 (m, 1H, H-6b), 0.91 (s, C*H*$_3$-13), 0.87 (s, C*H*$_3$-14); ^{13}C NMR δ 176.5 (C-17), 176.0 (C-21), 60.7 (CH-2), 55.6 (CH-9), 53.6 (CH-5), 48.7 (CH$_2$-3), 46.4 (C-1), 40.5 (C-4), 40.4 (CH$_2$-12), 36.8 (CH$_2$-7), 36.0 (C-8), 33.3 (CH$_3$-15), 32.7 (CH$_2$-18/22), 32.6 (CH$_2$-18/22), 31.4 (CH$_2$-11), 31.2 (CH$_3$-14), 27.2 (CH$_3$-13), 26.2 (CH$_2$-10), 23.1 (CH$_2$-6), 12.8 (CH$_3$-19/23), 12.7 (CH$_3$-19/23); FT-IR v$_{max}$ (neat) 3297, 2937, 2864, 1637, 1541, 1459, 1375, 1223, 1173, 1102, 1020, 907, 804, 728 cm^{-1}; HRMS (ESI): found 349.2864, [M+H]$^+$, C$_{21}$H$_{37}$N$_2$O$_2$ required 349.2855, [M+H]$^+$.

N-[(*1S,2S,5S,8S,9R*)-2-acetamido-4,4,8-trimethyl-9-tricyclo[6.3.1.01,5]dodecanyl]acetamide

126e
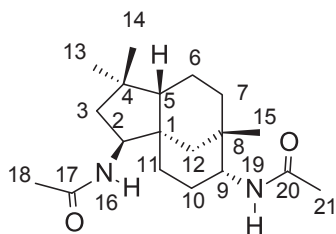
(0.26 g, 71%) white glassy solid; R_f (7:3 ethyl acetate/hexane) 0.51; $[\alpha]_{589}^{22}$ -54.4° (*c* 1.0, CHCl$_3$); ^{1}H NMR (500 MHz, CDCl$_3$) δ 5.73 (br d, *J* = 9.0 Hz, 1H, H-16/19), 5.36 (br d, *J* = 9.0, 1H, H-16/19), 4.12 (ddd, *J* = 12.5, 9.0, 5.5 Hz, 1H, H-2), 3.67 (br d, *J* = 9.0 Hz, 1H, H-9), 2.03 (s, CH$_3$-18/21), 1.99 (CH$_3$-18/21), 1.50-1.64 (m, 4H, H-3a, 2H-10, H-7a), 1.40-1.50 (m, 1H, H-6a), 1.24-1.45 (m, 4H, H-7b, H-3b, H-5, H-12a), 1.18-1.24 (m, 1H, H-11a), 1.03 (s, 3H, CH$_3$-15), 0.96-1.04 (m, 2H, H-6b, H-11b), 0.91 (s, 3H, CH$_3$-13), 0.87 (s, 3H, CH$_3$-14), 0.86-0.89 (m, 1H, H-12b); ^{13}C NMR δ 172.7 (C-17/20), 172.4 (C-17/20), 60.8 (CH-2), 55.9 (CH-9), 53.5 (CH-5), 48.7 (CH$_2$-3), 46.3 (C-1), 40.4 (C-4), 40.4 (CH$_2$-12), 36.8 (CH$_2$-7), 36.0 (C-8), 33.3 (CH$_3$-15), 31.5 (CH$_2$-11), 31.2 (CH$_3$-14), 27.2 (CH$_3$-13), 26.4 (CH$_3$-18/21), 26.3 (CH$_3$-18/21), 26.3 (CH$_2$-10), 23.1 (CH$_2$-6); FT-IR v_{max} (neat) 3289, 2935, 2859, 1635, 1540, 1455, 1372, 1222, 1102, 1030, 911, 859, 736 cm^{-1}; HRMS (ESI): found 321.2551, [M+H]$^+$, C$_{19}$H$_{33}$N$_2$O$_2$ required 321.2542, [M+H]$^+$.
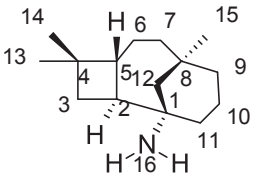
6.1.5 Amide cleavage under mild acidic conditions

General conditions for amide cleavage under mild conditions using thiourea
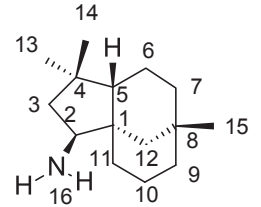
Amide **119c**, **120c** (0.10 g, 0.34 mmol) or **126a** (0.10 g, 0.26 mmol) was dissolved in dry ethanol (15 mL) and placed in a round-bottom flask fitted with a drying tube. A solution of thiourea (2-mole equiv.) dissolved in dry ethanol (5 mL) was added to the amide mixture. A few drops of acetic acid were added, and the mixture was stirred overnight at room temperature. The reaction was quenched with saturated NaHCO$_3$ (20 mL). The quenched reaction mixture was then extracted with CHCl$_3$ (20 mL x 2). The combined organic extracts were washed with

saturated NaCl (20 mL). The organic layer was dried with Na_2CO_3 and the solvent was removed under reduced pressure. The crude product washed with hexane (15 mL), and diethyl ether (15 mL). No further purification was needed.

(*1R,2S,5R,8R*)-4,4,8-trimethyltricyclo[6.3.1.0²,5]dodecan-1-amine **127a**

(0.04 g, 58%) brown viscous liquid; $[\alpha]_{589}^{22}$ -8.6º (*c* 1.0, CHCl₃); ¹H NMR (500 MHz, CD₃OD) δ 2.37 (ddd, *J* = 12.0, 11.0, 8.0 Hz, 1H, H-2), 1.84-1.96 (m, 2H, H-5, H-10a), 1.73-1.78 (m, 2H, 2H-12), 1.67-1.73 (m, 1H, H-10b), 1.1-1.66 (m, 10H, 2H-3, 2H-6, 2H-7, 2H-9, 2H-11), 1.05 (s, 3H, CH₃-13), 1.04 (s, 3H, CH₃-14), 0.92 (s, 3H, CH₃-15); ¹³C NMR δ 55.1 (C-1), 48.9 (CH₂-12), 47.5 (CH-5), 40.8 (CH-2), 39.5 (CH₂-3), 39.2 (CH₂-7), 38.8 (CH₂-9), 37.3 (CH₂-11), 37.1 (C-8), 36.6 (C-4), 35.2 (CH₃-15), 31.8 (CH₃-14), 24.4 (CH₂-6), 22.1 (CH₃-13), 22.0 (CH₂-10); FT-IR v_max (neat) 3296, 3190, 2945, 2921, 2862, 1638, 1542, 1457, 1376, 1363, 1286, 1223, 1199, 1100, 1064, 987, 922, 871, 733, 655 cm⁻¹; HRMS (ESI): found 222.2214, [M+H]⁺, $C_{15}H_{28}N$ required 222.2222, [M+H]⁺.

(*1S,2S,5S,8S*)-4,4,8-trimethyltricyclo[6.3.1.0¹,5]dodecan-2-amine **128a**

(0.05 g, 65%) brown viscous liquid; $[\alpha]_{589}^{22}$ 9.2º (*c* 1.0, CHCl₃); ¹H NMR (500 MHz, CDCl₃) δ 2.86 (dd, *J* = 12.0, 5.5 Hz, 1H, H-2), 1.57 (dd, *J* = 12.0, 5.5 Hz, 1H, H-3a), 1.50-1.60 (m, 2H, 2H-10), 1.04-1.26 (m, 9H, H-3b, H-5, 2H-6, 2H-7, H-9a, H-11a, H-12a), 1.01 (s, 3H, CH₃-14), 0.89 (s, 3H, CH₃-13), 0.84 (s, 3H, CH₃-15), 0.85-0.96 (m, 3H, H-9b, H-11b, H-12b); ¹³C NMR δ 64.2 (CH-2), 54.3 (CH-5), 52.0 (CH₂-3), 46.0 (C-1), 43.6 (CH₂-12), 40.0 (CH₂-9), 35.9 (C-4), 35.6 (CH₂-11), 34.8 (CH₂-7), 33.9 (CH₃-15), 32.8 (CH₃-14), 27.8 (C-8), 23.4 (CH₃-13), 21.4 (CH₂-10), 16.8 (CH₂-

6); FT-IR v_{max} (neat) 3294, 2942, 2928, 2860, 1641, 1552, 1467, 1388, 1366, 1276, 1202, 1100, 1064, 998, 852, 781, 667 cm^{-1}; HRMS (ESI): found 222.2213, [M+H]$^+$, $C_{15}H_{28}N$ required 222.2222, [M+H]$^+$.

(*1S,2S,5S,8S,9R*)-4,4,8-trimethyltricyclo[6.3.1.01,5]dodecan-2,9-diamine **129**
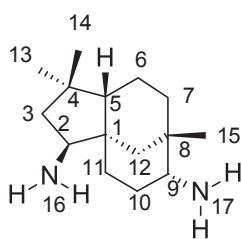
(0.02 g, 33 %) brown viscous liquid; $[\alpha]_{589}^{23}$ -13.3º (*c* 1.0, CHCl$_3$); ^{1}H NMR (500 MHz, CDCl$_3$) δ 2.87 (dd, *J* = 12.5, 6.0 Hz, 1H, H-2), 2.50 (br s, 1H, H-9), 1.97-2.05 (m, 1H, H-10a), 1.38-1.60 (m, 6H, H-3a, H-6a, H-7a, H-10b, H-11a, H-12a), 1.30-1.36 (m, 2H, H-3b, H-5), 1.16-1.21 (m, 1H, H-7b), 1.01 (s, 3H, C$\underline{H}_3$-15), 0.91 (s, 3H, C$\underline{H}_3$-14), 0.86-0.910 (m, 1H, H-11b), 0.84 (s, 3H, C$\underline{H}_3$-13), 0.75-0.85 (m, 2H, H-6b, H-12b); ^{13}C NMR δ 64.0 (CH-2), 58.9 (CH-9), 53.9 (CH-5), 51.9 (CH$_2$-3), 46.1 (C-1), 39.9 (C-4), 38.2 (CH$_2$-12), 37.3 (CH$_2$-7), 36.9 (C-8), 33.8 (CH$_3$-15), 31.6 (CH$_3$-14), 29.0 (CH$_2$-11), 28.7 (CH$_2$-10), 27.6 (CH$_3$-13), 23.4 (CH$_2$-6); FT-IR v_{max} (neat) 2923, 2861, 1560, 1458, 1377, 1364, 1284, 1228, 1021, 989, 816, 700 cm^{-1}; HRMS (ESI): found 237.2341, [M+H]$^+$, $C_{15}H_{29}N_2$ required 237.2331, [M+H]$^+$.

6.1.6 Reductive alkylation of amides

*General conditions for the reductive alkylation of amines **127a** and **128a***

Amine **127a** or **128a** (0.10 g, 0.45 mmol) was dissolved in dichloromethane (5 mL) and placed in a round-bottom flask fitted with a drying tube, aldehyde (5-mole equiv.), and $NaBH(OAc)_3$ (10-mole equiv.) was added slowly. The pH of the reaction mixture was adjusted to pH 4 *via* the addition of acetic acid. The mixture was stirred overnight at room temperature. The reaction was quenched with saturated $NaHCO_3$ (20 mL), extracted with $CHCl_3$ (20 mL x 2), and washed with saturated NaCl (20 mL). The combined organic layer was dried with Na_2CO_3 and solvent was removed under reduced pressure. The crude product was purified by column chromatography using diethyl ether: hexane in either (1:1) or (7:3) ratio.

(*1R,2S,5R,8R*)-*N,N*,4,4,8-pentamethyltricyclo[6.3.1.02,5]dodecan-1-amine **127b**
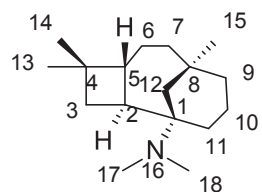
(0.08 g, 71 %) viscous liquid; R_f (1:1 diethyl ether/hexane) 0.62; $[\alpha]_{589}^{22}$ -8.6º (*c* 1.0, $CHCl_3$); ^{1}H NMR (500 MHz, $CDCl_3$) δ 2.21 (br s, 6H, C$\underline{H}_3$-17, C$\underline{H}_3$-18), 2.16 (ddd, *J* = 14.5, 12.0, 9.0 Hz, 1H, H-2), 1.85 (ddd, *J* = 14.5, 12.5, 7.0 Hz, 1H, H-5), 1.72-1.80 (m, 1H, H-10a), 1.68-1.72 (m, 2H, 2H-3), 1.59-1.65 (m, 1H, H-10b), 1.51-1.58 (m, 2H, H-9a, H-12a), 1.36-1.48 (m, 3H, H-6a, H-7a, H-11a), 1.22-1.35 (m, 2H, H-6b, H-11b), 1.16-1.12 (m, 1H, H-9b), 1.10-1.08 (m 2H, H-7b, H-12b), 0.99 (s, 3H, C$\underline{H}_3$-13), 0.96 (s, 3H, C$\underline{H}_3$-14), 0.87 (s, 3H, C$\underline{H}_3$-15); ^{13}C NMR δ 60.3 (C-1), 48.5 (CH-5), 47.8 (CH$_2$-12), 43.2 (CH-2), 42.1 (2CH$_3$-17 and 18), 41.4 (CH$_2$-3), 40.2 (CH$_2$-7), 39.6 (CH$_2$-9), 37.5 (C-8), 36.8 (C-4), 36.7 (CH$_3$-15), 32.9 (CH$_3$-13), 30.5 (CH$_2$-11), 24.8 (CH$_2$-10), 23.5 (CH$_3$-14), 22.7 (CH$_2$-6); FT-IR v$_{max}$ (neat) 2920, 2858, 2817, 2774, 1457, 1345, 1361, 1333, 1281, 1249, 1188, 1102, 1019, 968, 870, 797, 732 cm^{-1}; HRMS (ESI): found 250.2547, [M+H]$^+$, C$_{17}$H$_{32}$N required 250.2535, [M+H]$^+$.

(*1S,2S,5S,8S*)-*N,N*,4,4,8-pentamethyltricyclo[6.3.1.0¹,⁵]dodecan-2-amine **128b**
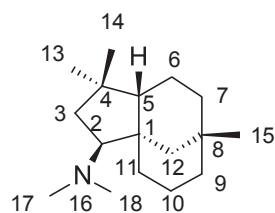
(0.10 g, 91 %) viscous liquid; R$_f$ (1:1 diethyl ether/hexane) 0.56; $[\alpha]_{589}^{23}$ 17.3° (*c* 1.0, CHCl$_3$); ^{1}H NMR (500 MHz, CDCl$_3$) δ 2.31 (br s, 6H, CH$_3$-17, CH$_3$-18), 2.20 (dd, *J* = 12.0, 6.0 Hz, 1H, H-2), 1.46-1.58 (m, 4H, 2H-3, 2H-10), 1.16-1.40 (m, 10H, H-5, 2H-6, 2H-7, H-9a, 2H-11, 2H-12), 1.02 (s, 3H, CH$_3$-15), 0.96-0.99 (m, 1H, H-9b), 0.88 (s, 3H, CH$_3$-13), 0.84 (s, 3H, CH$_3$-14); ^{13}C NMR δ 78.9 (CH-2), 55.1 (CH-5), 49.1 (2CH$_3$-17 and 18), 47.5 (C-1), 47.4 (CH$_2$-3), 47.1 (CH$_2$-12), 43.7 (CH$_2$-9), 39.7 (C-4), 35.7 (CH$_3$-13), 35.5 (CH$_2$-11), 35.1 (CH$_2$-7), 33.7 (CH$_3$-15), 32.9 (C-8), 27.9 (CH$_3$-14), 23.3 (CH$_2$-10), 21.4 (CH$_2$-6); FT-IR v$_{max}$ (neat) 2942, 2922, 2861, 2813, 2764, 1457, 1364, 1278, 1247, 1163, 1059, 1037, 966, 876, 778 cm^{-1}; HRMS (ESI): found 250.2543, [M+H]$^+$, C$_{17}$H$_{32}$N required 250.2535, [M+H]$^+$.

(*1R,2S,5R,8R*)-4,4,8-trimethyl-*N*-propyl-tricyclo[6.3.1.0²,⁵]dodecan-1-amine **127c**
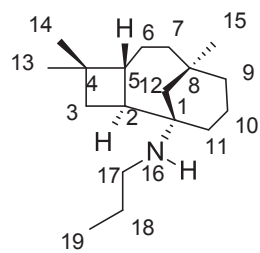
(0.08 g, 69 %) viscous liquid; R$_f$ (7:3 diethyl ether/hexane) 0.45; $[\alpha]_{589}^{22}$ 0.1° (*c* 1.0, CHCl$_3$); ^{1}H NMR (500 MHz, CDCl$_3$) δ 2.68 (ddd, *J* = 16.0, 11.0, 6.0 Hz, 1H, H-17a, splitting due to slow rotation), 2.43 (ddd, *J* = 16.0, 11.0, 6.0 Hz, 1H, H-17b, splitting due to slow rotation), 2.13-2.20 (m, 1H, H-2), 1.94-2.02 (m, 1H, H-5), 1.84-1.88 (m, 1H, H-12a), 1.62-1.74 (m, 6H, H-7a, H-9a, 2H-10, 2H-18), 1.38-1.54 (m, 4H, H-3a, H-6a, H-7b, H-9b), 1.26-1.34 (m, 1H, H-6b), 1.20-1.22 (m, 1H, H-12b), 1.07-1.16 (m, 2H, H-3b, H-11a), 1.03 (s, 3H, CH$_3$-13), 0.98-0.99 (m, 1H, H-11b), 0.97 (s, 3H, CH$_3$-14), 0.89 (t, *J* = 7.0 Hz, 3H, CH$_3$-19), 0.86 (s, 3H, CH$_3$-15); ^{13}C NMR δ 60.0 (C-1), 48.5 (CH$_2$-12), 48.2 (CH-5), 46.7 (CH$_2$-17), 42.3 (CH-2), 40.7 (CH$_2$-3), 40.0 (CH$_2$-7), 39.8 (C-8), 37.7 (C-4), 36.9 (CH$_2$-9), 36.8 (CH$_3$-15), 32.7 (CH$_2$-11), 32.7 (CH$_3$-13),

25.8 (CH$_2$-6), 24.7 (CH$_2$-18), 23.2 (CH$_3$-14), 22.7 (CH$_2$-10), 14.4 (CH$_3$-19); FT-IR v$_{max}$ (neat) 2921, 2863, 1559, 1457, 1397, 1378, 1288, 1222, 1121, 1020, 964, 752 cm^{-1}; HRMS (ESI): found 264.2688, [M+H]$^+$, C$_{18}$H$_{34}$N required 264.2691, [M+H]$^+$.

(*1S,2S,5S,8S*)-*N,N*-dibutyl-4,4,8-trimethyl-tricyclo[6.3.1.01,5]dodecan-2-amine **128c**
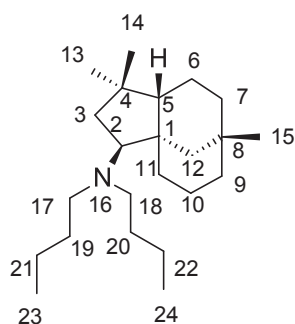
(0.09 g, 57 %) viscous liquid; R$_f$ (1:1 diethyl ether/hexane) 0.66; [α]$_{589}^{23}$ 13.9º (*c* 1.0, CHCl$_3$); ^{1}H NMR (500 MHz, CDCl$_3$) δ 2.59 (dd, *J* = 13.0, 5.5 Hz, 1H, H-2), 2.46-2.53 (m, 2H, 2H-17/18), 2.34-2.30 (m, 2H, 2H-17/18), 1.46-1.52 (m, 3H, 2H-10, H-12a), 1.12-1.42 (m, 17H, H-5, 2H-6, 2H-7, H-9a, 2H-11, H-12b, 2H-19, 2H-20, 2H-21, 2H-22), 1.14-1.17 (m, 2H, 2H-3), 1.02 (s, 3H, CH$_3$-14), 0.93-1.00 (m, 1H, H-9b), 0.90 (t, *J* = 7.5 Hz, 6H, CH$_3$-23, CH$_3$-24), 0.86 (s, 3H, CH$_3$-15), 0.83 (s, 3H, CH$_3$-13); ^{13}C NMR δ 73.7 (CH-2), 55.2 (2CH$_2$-17 and 18), 53.8 (CH-5), 47.7 (C-1), 47.1 (CH$_2$-3), 43.6 (CH$_2$-12), 43.5 (CH$_2$-9), 39.5 (C-4), 35.9 (CH$_2$-11), 35.8 (CH$_2$-7), 35.8 (CH$_3$-15), 34.3 (CH$_3$-14), 32.9 (2CH$_2$-19 and 20), 32.7 (C-8), 27.8 (CH$_3$-13), 23.4 (2CH$_2$-21 and 22), 23.3 (CH$_2$-10), 21.5 (CH$_2$-6), 16.9 (2CH$_3$-23 and 24); FT-IR v$_{max}$ (neat) 2925, 2863, 1653, 1541, 1457, 1364, 1232, 1182, 1076, 1005, 989, 813, 778, 734 cm^{-1}; HRMS (ESI): found 334.3486, [M+H]$^+$, C$_{23}$H$_{44}$N required 334.3474, [M+H]$^+$.

(*1R,2S,5R,8R*)-*N*-butyl-4,4,8-trimethyl-tricyclo[6.3.1.0²,⁵]dodecan-1-amine **127d**
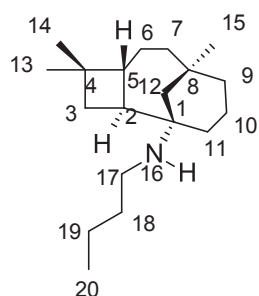
(0.06 g, 50 %) viscous liquid; R_f (7:3 diethyl ether/hexane) 0.50; $[\alpha]_{589}^{23}$ 0.8º (*c* 1.0, CHCl₃); ¹H NMR (500 MHz, CDCl₃) δ 2.88 (ddd, *J* = 16.5, 11.5, 6.5 Hz, 1H, H-17a, due to slow rotation), 2.59 (ddd, *J* = 16.5, 11.5, 6.5 Hz, 1H, H-17b, due to slow rotation), 2.24 (ddd, *J* = 12.5, 8.0, 5.0 Hz, 1H, H-2), 2.16-2.28 (m, 2H, H-5, H-12a), 1.90-2.00 (m, 2H, H-18), 1.82-1.90 (m, 4H, 2H-7, 2H-19), 1.70-1.76 (m, 2H, H-10a, H-11a), 1.57-1.66 (m, 1H, H-11b), 1.48-1.54 (m, 3H, H-3a, H-6a, H-12b), 1.40-1.46 (m, 1H, H-9a), 1.28-1.38 (m, 2H, H-6b, H-10b), 1.16-1.22 (m, 2H, H-3b, H-9b), 1.10 (s, 3H, C*H*₃-14), 0.99 (s, 3H, C*H*₃-13), 0.92 (s, 3H, C*H*₃-15), 0.92 (t, *J* = 8.0 Hz, 3H, C*H*₃-20); ¹³C NMR δ 63.3 (C-1), 48.5 (CH-5), 46.6 (CH₂-12), 44.8 (CH₂-17), 41.8 (CH-2), 40.9 (CH₂-3), 41.1 (CH₂-7), 39.3 (CH₂-9), 37.9 (C-8), 37.0 (C-4), 36.8 (CH₃-15), 35.4 (CH₂-11), 32.4 (CH₃-14), 31.0 (CH₂-18), 25.9 (CH₂-19), 23.0 (CH₂-6), 23.0 (CH₃-13), 22.3 (CH₂-10), 16.1 (CH₃-21); FT-IR ν_{max} (neat) 2949, 2925, 2865, 2728, 1583, 1458, 1379, 1363, 1264, 1121, 1093, 1001, 965, 897, 797, 735 cm⁻¹; HRMS (ESI): found 278.2835, [M+H]⁺, C₁₉H₃₆N required 278.2848, [M+H]⁺.

(*1S,2S,5S,8S*)-*N*-benzyl-4,4,8-trimethyl-tricyclo[6.3.1.0¹,⁵]dodecan-2-amine **128d**
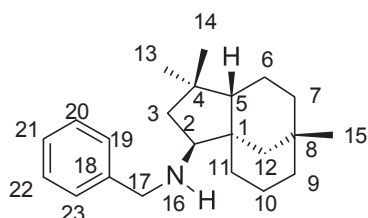
(0.09 g, 66 %) viscous liquid; R_f (1:1 diethyl ether/hexane) 0.58; $[\alpha]_{589}^{23}$ 32.4º (*c* 1.0, CHCl₃); ¹H NMR (500 MHz, CDCl₃) δ 7.40 (d, *J* = 7.5 Hz, 2H, 2H-19), 7.33 (t, *J* = 7.5 Hz, 2H, 2H-20), 7.28 (t, *J* = 7.5 Hz, 1H, H-21), 3.98 (d, *J* = 13.0 Hz, 1H, H-17a), 3.84 (d, *J* = 13.0 Hz, 1H, H-17b), 2.76 (dd, *J* = 12.0, 5.5 Hz, 1H, H-2), 1.70 (dd, *J* = 12.0, 5.5 Hz, 1H, H-3a), 1.43-1.60 (m, 3H, H-3b, 2H-10), 1.30-1.40 (m, 5H, H-5, H-6a, 2H-7, H-11a), 1.10-1.30 (m, 5H, H-6b,

H-9a, H-11b, 2H-12), 1.02 (s, 3H, C$\underline{\text{H}}_3$-15), 0.96-1.00 (m, 1H, H-9b), 0.87 (s, C$\underline{\text{H}}_3$-13), 0.77 (s, C$\underline{\text{H}}_3$-14); ^{13}C NMR δ 131.2 (2CH-19), 131.2 (2CH-20), 130.1 (CH-21), 129.0 (C-18), 69.3 (CH-2), 55.1 (CH$_2$-17), 54.3 (CH-5), 46.5 (C-1), 46.3 (CH$_2$-3), 45.7 (CH$_2$-12), 43.4 (CH$_2$-9), 40.3 (C-4), 35.8 (CH$_2$-11), 35.6 (CH$_3$-14), 35.2 (CH$_2$-7), 33.7 (CH$_3$-15), 32.9 (C-8), 27.6 (CH$_3$-13), 23.2 (CH$_2$-10), 21.4 (CH$_2$-6); FT-IR v_{max} (neat) 2921, 2861, 1494, 1452, 1381, 1331, 1131, 1064, 1026, 967, 746, 696 cm^{-1}; HRMS (ESI): found 312.2681, [M+H]$^+$, C$_{22}$H$_{34}$N required 312.2691, [M+H]$^+$.

(*1R,2S,5R,8R*)-4,4,8-trimethyl-N-pentyl-tricyclo[6.3.1.0^{2,5}]dodecan-1-amine **127e**
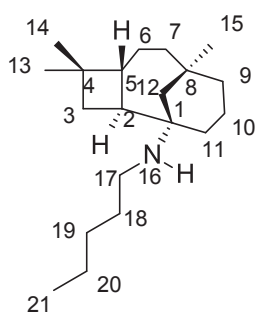
(0.10 g, 79 %) viscous liquid; R$_f$ (1:1 diethyl ether/hexane) 0.53; $[\alpha]_{589}^{23}$ 2.0º (*c* 1.0, CHCl$_3$); ^{1}H NMR (500 MHz, CDCl$_3$) δ 5.65 (br s, 1H, NH), 2.64 (ddd, *J* = 16.5, 11.0, 9.0 Hz, 1H, H-17a, splitting due to slow rotation), 2.41 (ddd, *J* = 16.5, 11.0, 9.0 Hz, 1H, H-17b, splitting due to slow rotation), 2.18 (ddd, *J* = 12.0, 8.0, 5.5 Hz, 1H, H-2), 1.86-1.96 (m, 1H, H-5), 1.67-1.80 (m, 6H, 2H-10, H-11a, H-12a, 2H-9),1.65 (dd, *J* = 12.0, 3.0 Hz, 1H, H-11b), 1.06-1.62 (m, 11H, H-3a, 2H-7, H-11b, H-12b, 2H-18, 2H-19, 2H-20), 1.06-1.13 (m, 1H, H-3b), 1.02 (s, 3H, C$\underline{\text{H}}_3$-14), 0.99 (s, 3H, C$\underline{\text{H}}_3$-13), 0.89 (t, *J* = 7.0 Hz, 3H, C$\underline{\text{H}}_3$-21), 0.87 (s, 3H, C$\underline{\text{H}}_3$-15); ^{13}C NMR δ 49.8 (C-1), 48.5 (CH-5), 48.5 (CH$_2$-12), 45.1 (CH$_2$-17), 42.4 (CH-2), 40.4 (CH$_2$-3), 40.4 (CH$_2$-7), 39.6 (CH$_2$-9), 37.6 (CH$_2$-11), 37.6 (C-8), 36.9 (C-4), 36.8 (CH$_3$-15), 32.9 (CH$_3$-14), 32.4 (CH$_2$-18), 25.5 (CH$_2$-19 and 20), 25.2 (CH$_2$-6), 23.3 (CH$_3$-13), 22.8 (CH$_2$-10), 16.7 (CH$_3$-21); FT-IR v_{max} (neat) 2947, 2921, 2857, 1668, 1457, 1376, 1364, 1217, 1122, 1021, 997, 892, 752, 698 cm^{-1}; HRMS (ESI): found 292.3008 [M+H]$^+$, C$_{20}$H$_{38}$N required 292.3004, [M+H]$^+$.

6.2 Cell Biology

6.2.1 National Cancer Institute Procedure

Compound 63 was screened under the standard conditions of the NCI anti-cancer screening program, against 48 cell lines covering nine cancer types.[164]

The human tumour cell lines of the cancer screening panel were grown in RPMI 1640 medium containing 5% fetal bovine serum and 2 mM of L-glutamine. Cells were inoculated into 96 well microtiter plates in 100 μL at plating densities ranging from 5,000 to 40,000 cells/well depending on the doubling time of individual cell lines. After cell inoculation, the plates were incubated at 37 °C, 5% CO_2, 95% air and 100% relative humidity for 24 h prior to addition of experimental drugs.

After 24 h, two plates of each cell line were fixed in situ with TCA, to represent a measurement of the cell population for each cell line at the time of drug addition (Tz). The cells were treated with the experimental drugs at 5 various concentrations (0.01 – 100 μM).

Following drug addition, the plates were incubated for an additional 48 h at 37 °C, 5% CO_2, 95% air, and 100% relative humidity. For adherent cells, the assay was terminated by the addition of cold TCA. Cells were fixed in situ by the gentle addition of 50 μL of cold 50% (w/v) TCA (final concentration, 10% TCA) and incubated for 60 min at 4 °C. The supernatant was discarded, and the plates were washed five times with tap water and air dried. Sulforhodamine B (SRB) solution (100 μl) at 0.4% (w/v) in 1% acetic acid was added to each well, and plates were incubated for 10 minutes at room temperature. After staining, the unbound dye was removed by washing five times with 1% acetic acid and the plates were air dried. The bound stain was subsequently solubilised with 10 mM trizma base, and the absorbance was read on an automated plate reader at a wavelength of 515 nm. For suspension cells, the methodology was the same except that the assay was terminated by fixing settled cells

at the bottom of the wells by gently adding 50 µl of 80% TCA (final concentration, 16% TCA).[164]

6.2.2 General reagents for cell culture

Penicillin and Streptomycin, Trypsin and foetal bovine serum were purchased from Thermo Fisher Scientific (Scoresby, Vic, Australia). Dulbecco's Modified Eagle's Medium (DMEM), phosphate-buffered saline (PBS) and DMSO were purchased from Sigma-Aldrich (Castle Hill, NSW, Australia). The CellTiter 96® AQueous One Solution Reagent was purchased from Promega (Alexandria, NSW, Australia).

6.2.3 Cell Culture and Viability Assays

Human MDA-MB-231 breast cancer cells were obtained as a gift from Prof. Michael Murray (University of Sydney) and grown at 37 ^{0}C in a humidified atmosphere of 5% CO_2 in DMEM supplemented with 10% fetal bovine serum and 1% Penicillin/Streptomycin. Confluent cells (80 – 90%) were harvested using trypsin/EDTA after washing with PBS.

For the MTS assay cells were seeded in 96-well flat-bottom plates at a density of 7 x 10^3 cells/well. Serum was removed after 24 h, after which cells were treated with various concentrations of the drugs (1 – 50 µM) in DMSO (maximum concentration 0.1%) for 48 h; control cells received solvent alone. In this assay the optimal point (48 hr) of this particular cell line has been established by Dr Tristan Rawling's research group and was therefore used as the normal protocol.[72] Cell viability was determined using the CellTiter 96® AQueous One Solution Cell Proliferation Assay (Promega, USA) as per the manufacturer's recommendation. MTS reagent was added to each well, and the absorbance of all wells was determined by measuring optical density at 550 nm (infinite M1000Pro, Tecan) after 4 h incubation at 37 ^{0}C. Blank-subtracted absorbance values were normalised to the DMSO control, which was

arbitrarily assigned as 100%. IC$_{50}$ values were defined as the drug concentration that prevented cell growth of more than 50% relative to the DMSO control. These were determined using nonlinear regression analysis with Prism 7.0 (GraphPad Software, CA, USA). Each compound was tested in triplicates. Note: the MTS assay was repeated with human MCF-7 breast cancer cells obtained as a gift from Asso. Prof. Mary Bebawy (University of Technology Sydney).

6.2.4 Cell cycle analysis

Cell cycle distribution was evaluated in MDA-MB-231 cells that were seeded in 6-well flat bottom plates at a density of 5 x 10^5 cells/well. Serum was removed after 24 hours, after which the cells were treated with various concentrations of drugs (20 – 40 µM) in DMSO (maximum concentration 0.1%) for 24 h, control wells only contained DMSO at 0.1%. Treated cells were then harvested and fixed overnight at 0 ^{0}C in 80% ethanol, centrifuged at 500 g for 10 minutes at 4 ˚C. Fixed cells were then washed twice with PBS and resuspended in 0.1 M PBS containing 0.1% (v/v) Triton X-100 and 0.1 mg/mL RNAse A. After staining with PI (50 µg/mL), cells were incubated for 30 min in the dark at 37 ˚C and subjected to flow cytometry (BD LSRFortessa X-20), with 1 x 10^4 events, per sample acquired. Cell cycle distribution was calculated using Flowing Software version 2.5.1.

6.2.5 Apoptosis/Necrosis

Annexin V-FITC/PI staining was used to evaluate the extent of apoptosis in MDA-MB-231 cells as per manufacturer's recommendation (BD Bioscience, Sydney, NSW, Australia). Cells were seeded in 6-well plates at a density of 1 x 10^5 cells/well, 24 hours after serum removal the cells were treated with synthesised compounds (20 - 40 µM) for 48 hours. Control wells were treated with DMSO only at 0.1% (v/v). Treated cells were trypsinised and washed twice with cold PBS. The cells were then resuspended in binding buffer (0.1 mL), 5 µL of Annexin

V-FITC reagent and PI (50 µg/mL). The cells were incubated for 20 min in the dark at 0 ˚C and subjected to flow cytometry as described above. The percentages of viable (Annexin V−/PI−), early apoptotic (Annexin V+/PI−), late apoptotic (Annexin V+/PI+), and necrotic (Annexin V−/PI+) cells were calculated using Flowing Software version 2.5.1.

6.2.6 Cytotoxicity against Vero cells

Cytotoxicity of compounds was assessed against Vero cells (African Green Monkey kidney cell lines) at 50 µg/mL concentration. The assays were determined externally by Bioassay Laboratory, BIOTEC, Thailand,[165] using the method described by O'Brien et al.[166] Cells at a logarithmic growth phase were harvested and diluted to 2.2 x 10^4 cells/ml, in fresh medium. Successively, 5 µL of the test sample diluted in 5% DMSO, and 45 µL of cell suspension were added to 384-well plates, incubated at 37 °C in a 5% CO2 incubator. After the incubation period of 3 days, 12.5 µL of 62.5 µg/ml resazurin solutions was added to each well and the plates were then incubated at 37 °C for 4 h. Fluorescence signal was measured using SpectraMax M5 multi-detection microplate reader (Molecular Devices, USA) at the excitation and emission wavelengths of 530 nm and 590 nm. Ellipticine was used as a positive control, and 0.5% DMSO and water were used as a negative control.

6.2.7 Statistical Analysis

All measurements were performed at least in triplicates unless otherwise stated. Data from multiple treatments were analysed by one-way ANOVA in combination with Fisher's Protected Least Significant Difference test.

Chapter 7   Appendices

7.1 National Cancer Institute broad screening

Appendix 7.1: Cytotoxicity $(IC_{50})^a$ of compound **63** against 48 Cancer cell lines.

Tumour Type	Cell line	IC$_{50}$ (µM)
Leukemia	CCRF-CEM	4.4
	HL-60 (TB)	5.5
	MOLT-4	2.4
	RPMI-8226	4.1
	K-562	15.3
	SR	18.3
Non-Small Cell Lung	NCI-H522	2.0
	EKVX	12.2
	HOP-92	18
	NCI-H322M	18.4
	HOP-62	19.8
	NCI-H226	22.2
	A549/ATCC	33.1
	NCI-H23	33.1
Colon Cancer	COLO-205	7.8
	HT29	7.5
	HCT-15	16.3
	SW-620	2.8
	KH12	17.1
	HCC-2998	40
CNS Cancer	SF-539	3.2
	SF-268	11.2
	SNB-75	16.1
Melanoma	SK-MEL-28	1.8
	SK-MEL-5	6.3
	MDA-MB-435	5.9
	M14	10.9
	UACC-257	16
	LOX IMVI	17
	SK-MEL-2	17.7
	UACC-62	18.1
Ovarian Cancer	OVCAR-3	11.8
	OVCAR-5	18.8
	IGROV1	20
	OVCAR-5	20.2
	OVCAR-4	21.1
Renal Cancer	CAKI-1	5.3
	RXF 393	6.7
	UO-31	2.7
	TK-10	16.4
	A498	18.7

	ACHN	20.2
Prostate Cancer	PC-3	15.7
	DU-145	16.9
Breast Cancer	MCF-7	7.1
	MDA-MB-231/ATCC	38.9
	HS 578T	10.9
	T-47D	22.7

[a]Concentration of compound **63** required to inhibit 50% growth of cancer cells.
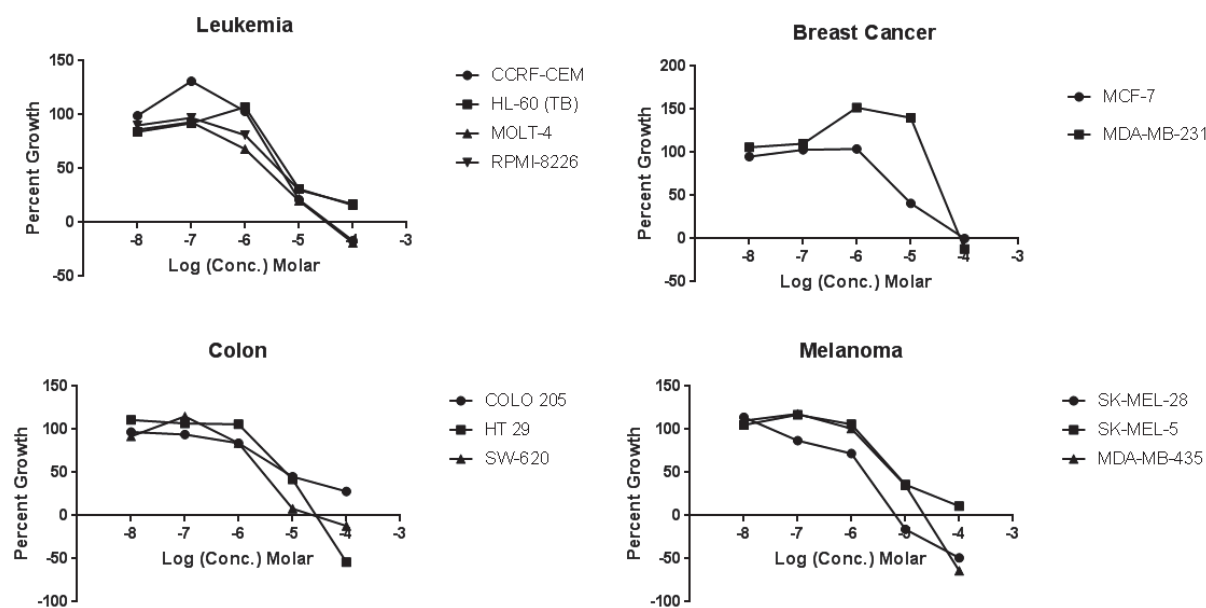
Appendix 7.2: Dose-response curves of compound **63** against leukaemia, breast cancer,

colon and melanoma cell lines.

Appendix 7.3: Cytotoxicity of active compounds against Vero cells.

Compound	Concentration Tested (µM)	Cytotoxicity (%)
63	139	77
82c	158	84
119c	168	92
120c	168	88
126a	129	88

Chapter 8   References

1.   Evans, W. C., *Trease and Evans' pharmacognosy*. Elsevier Health Sciences: 2009.

2.   Iannone, L. J.; Novas, M. V.; Young, C. A.; De Battista, J. P.; Schardl, C. L., Endophytes of native grasses from South America: biodiversity and ecology. *Fungal Ecology* **2012,** *5* (3), 357-363.

3.   Hesse, M., *Alkaloids: nature's curse or blessing?* Wiley-VCH: 2002.

4.   Dewick, P. M., *Medicinal natural products: a biosynthetic approach*. John Wiley & Sons: **2002**.

5.   Aniszewski, T., Alkaloids-secrets of Life: *Aklaloid Chemistry, Biological Significance, Applications and Ecological Role* **2007**.

6.   Wink, M., A Short History of Alkaloids. In *Alkaloids*, Roberts, M.; Wink, M., Eds. Springer US: **1998**; 11-44.

7.   Sneader, W. E., *Drug Discovery (The History)*. Wiley Online Library: 2005.

8.   Heinrich, M.; Barnes, J.; Gibbons, S.; Williamson, E. M., *Fundamentals of pharmacognosy and phytotherapy*. Elsevier Health Sciences: **2012**.

9.   Hocking, G. M., *A dictionary of natural products. Terms in the field of pharmacognosy relating to natural medicinal and pharmaceutical materials and the plants, animals and minerals from which they are derived*. Plexus Publishing, Inc.: **1997**.

10.   Buckingham, J., Dictionary of alkaloids. CRC Press. **2010**.

11.   Genilloud, O., Current challenges in the discovery of novel antibacterials from microbial natural products. *Recent patents on anti-infective drug discovery* **2012,** *7* (3), 189-204.

12.   Jordan, M. A.; Thrower, D.; Wilson, L., Mechanism of inhibition of cell proliferation by Vinca alkaloids. *Cancer research* **1991,** *51* (8), 2212-2222.

13. Kruczynski, A.; Barret, J.-M.; Etiévant, C.; Colpaert, F.; Fahy, J.; Hill, B. T., Antimitotic and tubulin-interacting properties of vinflunine, a novel fluorinated Vinca alkaloid. *Biochemical pharmacology* **1998,** *55* (5), 635-648.

14. Kruczynski, A.; Etievant, C.; Perrin, D.; Chansard, N.; Duflos, A.; Hill, B., Characterization of cell death induced by vinflunine, the most recent Vinca alkaloid in clinical development. *British journal of cancer* **2002,** *86* (1), 143-150.

15. Jordan, M. A.; Wilson, L., Microtubules as a target for anticancer drugs. *Nature Reviews Cancer* **2004,** *4* (4), 253-265.

16. Smith, G. A.; Pritchard, K.; Fennelly, D., Current status of vinorelbine for breast cancer. *Oncology-Huntington* **1995,** *9* (8), 767-779.

17. Bachner, M.; De Santis, M., Vinflunine in the treatment of bladder cancer. *Therapeutics and clinical risk management* **2008,** *4* (6), 1243.

18. Ng, J. S., Vinflunine: review of a new vinca alkaloid and its potential role in oncology. *Journal of Oncology Pharmacy Practice* **2010**, *17* (3), 209-224

19. Ramnath, N.; Schwartz, G. N.; Smith, P.; Bong, D.; Kanter, P.; Berdzik, J.; Creaven, P. J., Phase I and pharmacokinetic study of anhydrovinblastine every 3 weeks in patients with refractory solid tumors. *Cancer chemotherapy and pharmacology* **2003,** *51* (3), 227-230.

20. Ng, J. S., Vinflunine: review of a new vinca alkaloid and its potential role in oncology. *Journal of Oncology Pharmacy Practice* **2011,** *17* (3), 209-224.

21. Kinghorn, A. D.; EunKyoung, S.; Fuller, G.; McKeon, T.; Bills, D. In *Plants as sources of drugs*, Agricultural materials as renewable resources: nonfood and industrial applications., American Chemical Society: **1997**, *19* (50) 12423-12424.

22. Kemper, E. M.; van Zandbergen, A. E.; Cleypool, C.; Mos, H. A.; Boogerd, W.; Beijnen, J. H.; van Tellingen, O., Increased penetration of paclitaxel into the brain by inhibition of P-glycoprotein. *Clinical Cancer Research* **2003,** *9* (7), 2849-2855.

23. Fellner, S.; Bauer, B.; Miller, D. S.; Schaffrik, M.; Fankhänel, M.; Spruß, T.; Bernhardt, G.; Graeff, C.; Färber, L.; Gschaidmeier, H., Transport of paclitaxel (Taxol) across the blood-brain barrier in vitro and in vivo. *The Journal of clinical investigation* **2002,** *110* (9), 1309-1318.

24. Paller, C. J.; Antonarakis, E. S., Cabazitaxel: a novel second-line treatment for metastatic castration-resistant prostate cancer. *Drug design, development and therapy* **2011,** *5*, 117.

25. Rowinsky, E. K.; Calvo, E. In *Novel agents that target tublin and related elements*, Seminars in oncology, Elsevier: **2006**; 421-435.

26. Hsiang, Y.-H.; Hertzberg, R.; Hecht, S.; Liu, L., Camptothecin induces protein-linked DNA breaks via mammalian DNA topoisomerase I. *Journal of Biological Chemistry* **1985,** *260* (27), 14873-14878.

27. Kim, H. S.; Park, N. H.; Kang, S.; Seo, S. S.; Chung, H. H.; Kim, J. W.; Song, Y. S.; Kang, S. B., Comparison of the efficacy between topotecan- and belotecan-, a new camptothecin analog, based chemotherapies for recurrent epithelial ovarian cancer: a single institutional experience. *The journal of obstetrics and gynaecology research* **2010,** *36* (1), 86-93.

28. Ramsdell, H. S.; Kedzierski, B.; Buhler, D., Microsomal metabolism of pyrrolizidine alkaloids from Senecio jacobaea. Isolation and quantification of 6, 7-dihydro-7-hydroxy-1-hydroxymethyl-5H-pyrrolizine and N-oxides by high performance liquid chromatography. *Drug metabolism and disposition* **1987,** *15* (1), 32-36.

29. Segall, H.; Wilson, D.; Dallas, J.; Haddon, W. F., trans-4-Hydroxy-2-hexenal: a reactive metabolite from the macrocyclic pyrrolizidine alkaloid senecionine. *Science* **1985,** *229* (4712), 472-475.

30. Fu, P. P.; Xia, Q.; Lin, G.; Chou, M. W., Genotoxic pyrrolizidine alkaloids-mechanisms leading to DNA adduct formation and tumorigenicity. *International Journal of Molecular Sciences* **2002,** *3* (9), 948-964.

31. Li, N.; Xia, Q.; Ruan, J.; P Fu, P.; Lin, G., Hepatotoxicity and tumorigenicity induced by metabolic activation of pyrrolizidine alkaloids in herbs. *Current drug metabolism* **2011,** *12* (9), 823-834.

32. Woo, J.; Sigurdsson, S. T.; Hopkins, P. B., DNA interstrand cross-linking reactions of pyrrole-derived, bifunctional electrophiles: evidence for a common target site in DNA. *Journal of the American Chemical Society* **1993,** *115* (9), 3407-3415.

33. Hanna, M. M.; Abdelgawad, N. M.; Ibrahim, N. A.; Mohammed, A. B., Synthesis and antitumor evaluation of some novel pyrrolizine derivatives. *Medicinal Chemistry Research* **2012,** *21* (9), 2349-2362.

34. Perri, V.; Rochais, C.; Sopkova-de Oliveira Santos, J.; Legay, R.; Cresteil, T.; Dallemagne, P.; Rault, S., Hydrogenative desulphurization of thienopyrrolizinones: An easy and selective access to (Z)-phenethylidenepyrrolizinones with in vitro cytotoxic activity. *European journal of medicinal chemistry* **2010,** *45* (3), 1146-1150.

35. Liu, W.; Zhou, J.; Bensdorf, K.; Zhang, H.; Liu, H.; Wang, Y.; Qian, H.; Zhang, Y.; Wellner, A.; Rubner, G., Investigations on cytotoxicity and anti-inflammatory potency of licofelone derivatives. *European journal of medicinal chemistry* **2011,** *46* (3), 907-913.

36.   Guo, S.; Zhao, Y.; Zhao, X.; Zhang, S.; Xie, L.; Kong, W.; Gong, P., Synthesis and Anti-tumor Activities of Novel Methylthio-, Sulfinyl-, and Sulfonyl-8H-thieno [2, 3-b] pyrrolizin-8-oximino Derivatives. *Archiv der Pharmazie* **2007,** *340* (8), 416-423.

37.   Guo, S.-C.; Zhao, Y.-F.; Li, R.-D.; Xie, L.-J.; Yang, Y.-B.; Gong, P., Synthesis and biological evaluation of novel tricyclic oximino derivatives as antitumor agents. *Chemical Research in Chinese Universities* **2008,** *24* (1), 47-53.

38.   Rochais, C.; Cresteil, T.; Perri, V.; Jouanne, M.; Lesnard, A.; Rault, S.; Dallemagne, P., MR22388, a novel anti-cancer agent with a strong FLT-3 ITD kinase affinity. *Cancer letters* **2013,** *331* (1), 92-98.

39.   Lisowski, V.; Enguehard, C.; Lancelot, J.-C.; Caignard, D.-H.; Lambel, S.; Leonce, S.; Pierre, A.; Atassi, G.; Renard, P.; Rault, S., Design, synthesis and antiproliferative activity of tripentones: a new series of antitubulin agents. *Bioorganic & medicinal chemistry letters* **2001,** *11* (16), 2205-2208.

40.   Rochais, C.; Dallemagne, P.; Rault, S., Tripentones: a promising series of potent anti-cancer agents. *Anti-Cancer Agents in Medicinal Chemistry (Formerly Current Medicinal Chemistry-Anti-Cancer Agents)* **2009,** *9* (4), 369-380.

41.   Lisowski, V.; Léonce, S.; Kraus-Berthier, L.; Sopková-de Oliveira Santos, J.; Pierré, A.; Atassi, G.; Caignard, D.-H.; Renard, P.; Rault, S., Design, synthesis, and evaluation of novel thienopyrrolizinones as antitubulin agents. *Journal of medicinal chemistry* **2004,** *47* (6), 1448-1464.

42.   Romero, M. R.; Efferth, T.; Serrano, M. A.; Castaño, B.; Macias, R. I.; Briz, O.; Marin, J. J., Effect of artemisinin/artesunate as inhibitors of hepatitis B virus production in an "in vitro" replicative system. *Antiviral research* **2005,** *68* (2), 75-83.

43.   Li, H. L.; Han, T.; Liu, R. H.; Zhang, C.; Chen, H. S.; Zhang, W. D., Alkaloids from Corydalis saxicola and Their Anti-Hepatitis B Virus Activity. *Chemistry & biodiversity* **2008,** *5* (5), 777-783.

44.   Liang, K.-W.; Yin, S.-C.; Ting, C.-T.; Lin, S.-J.; Hsueh, C.-M.; Chen, C.-Y.; Hsu, S.-L., Berberine inhibits platelet-derived growth factor-induced growth and migration partly through an AMPK-dependent pathway in vascular smooth muscle cells. *European journal of pharmacology* **2008,** *590* (1), 343-354.

45.   Sarkar, F. H.; Adsule, S.; Li, Y.; Padhye, S., Back to the future: COX-2 inhibitors for chemoprevention and cancer therapy. *Mini reviews in medicinal chemistry* **2007,** *7* (6), 599-608.

46.   Singh-Ranger, G.; Salhab, M.; Mokbel, K., The role of cyclooxygenase-2 in breast cancer: review. *Breast cancer research and treatment* **2008,** *109* (2), 189-198.

47.   Fukuda, K.; Hibiya, Y.; Mutoh, M.; Koshiji, M.; Akao, S.; Fujiwara, H., Inhibition by berberine of cyclooxygenase-2 transcriptional activity in human colon cancer cells. *Journal of ethnopharmacology* **1999,** *66* (2), 227-233.

48.   Wu, H. L.; Hsu, C. Y.; Liu, W. H.; Yung, B. Y., Berberine-induced apoptosis of human leukemia HL-60 cells is associated with down-regulation of nucleophosmin/B23 and telomerase activity. *International journal of cancer* **1999,** *81* (6), 923-929.

49.   Kuo, C. L.; Chou, C. C.; Yung, B. Y.-M., Berberine complexes with DNA in the berberine-induced apoptosis in human leukemic HL-60 cells. *Cancer letters* **1995,** *93* (2), 193-200.

50.   Hsu, W.-H.; Hsieh, Y.-S.; Kuo, H.-C.; Teng, C.-Y.; Huang, H.-I.; Wang, C.-J.; Yang, S.-F.; Liou, Y.-S.; Kuo, W.-H., Berberine induces apoptosis in SW620 human colonic carcinoma cells through generation of reactive oxygen species and activation of JNK/p38 MAPK and FasL. *Archives of toxicology* **2007,** *81* (10), 719-728.

51.   Hwang, J.-M.; Kuo, H.-C.; Tseng, T.-H.; Liu, J.-Y.; Chu, C.-Y., Berberine induces apoptosis through a mitochondria/caspases pathway in human hepatoma cells. *Archives of toxicology* **2006,** *80* (2), 62-73.

52.   Sakai, K.; Shitan, N.; Sato, F.; Ueda, K.; Yazaki, K., Characterization of berberine transport into Coptis japonica cells and the involvement of ABC protein. *Journal of experimental botany* **2002,** *53* (376), 1879-1886.

53.   Lin, H.; Liu, T.; Wu, C.; Chi, C., Berberine modulates expression of mdr1 gene product and the responses of digestive track cancer cells to Paclitaxel. *British journal of cancer* **1999,** *81* (3), 416.

54.   Lin, H. L.; Liu, T. Y.; Lui, W. Y.; Chi, C. W., Up-regulation of multidrug resistance transporter expression by berberine in human and murine hepatoma cells. *Cancer* **1999,** *85* (9), 1937-1942.

55.   Society, A. C. Early history of cancer. (accessed 26/09/2016).

56.   Li, Z.; Kang, Y., Emerging therapeutic targets in metastatic progression: A focus on breast cancer. *Pharmacology & Therapeutics* **2016,** *161*, 79-96.

57.   Rakha, E. A.; Reis-Filho, J. S.; Ellis, I. O., Basal-Like Breast Cancer: A Critical Review. *Journal of Clinical Oncology* **2008,** *26* (15), 2568-2581.

58.   Heiser, L. M.; Sadanandam, A.; Kuo, W.-L.; Benz, S. C.; Goldstein, T. C.; Ng, S.; Gibb, W. J.; Wang, N. J.; Ziyad, S.; Tong, F.; Bayani, N.; Hu, Z.; Billig, J. I.; Dueregger, A.; Lewis, S.; Jakkula, L.; Korkola, J. E.; Durinck, S.; Pepin, F.; Guan, Y.; Purdom, E.; Neuvial, P.; Bengtsson, H.; Wood, K. W.; Smith, P. G.; Vassilev, L. T.; Hennessy, B. T.; Greshock, J.; Bachman, K. E.; Hardwicke, M. A.; Park, J. W.; Marton, L. J.; Wolf, D. M.; Collisson, E. A.; Neve, R. M.; Mills, G. B.; Speed, T. P.; Feiler, H. S.; Wooster, R. F.; Haussler, D.; Stuart, J. M.; Gray, J. W.; Spellman, P. T., Subtype and pathway specific responses to anticancer compounds in breast cancer. *Proceedings of the*

National Academy of Sciences of the United States of America **2012,** *109* (8), 2724-2729.

59.   Perou, C. M.; Sorlie, T.; Eisen, M. B.; van de Rijn, M.; Jeffrey, S. S.; Rees, C. A.; Pollack, J. R.; Ross, D. T.; Johnsen, H.; Akslen, L. A.; Fluge, O.; Pergamenschikov, A.; Williams, C.; Zhu, S. X.; Lonning, P. E.; Borresen-Dale, A.-L.; Brown, P. O.; Botstein, D., Molecular portraits of human breast tumours. *Nature* **2000,** *406* (6797), 747-752.

60.   Sotiriou, C.; Neo, S.-Y.; McShane, L. M.; Korn, E. L.; Long, P. M.; Jazaeri, A.; Martiat, P.; Fox, S. B.; Harris, A. L.; Liu, E. T., Breast cancer classification and prognosis based on gene expression profiles from a population-based study. *Proceedings of the National Academy of Sciences of the United States of America* **2003,** *100* (18), 10393-10398.

61.   Sørlie, T.; Tibshirani, R.; Parker, J.; Hastie, T.; Marron, J. S.; Nobel, A.; Deng, S.; Johnsen, H.; Pesich, R.; Geisler, S.; Demeter, J.; Perou, C. M.; Lønning, P. E.; Brown, P. O.; Børresen-Dale, A.-L.; Botstein, D., Repeated observation of breast tumor subtypes in independent gene expression data sets. *Proceedings of the National Academy of Sciences of the United States of America* **2003,** *100* (14), 8418-8423.

62.   Subik, K.; Lee, J.-F.; Baxter, L.; Strzepek, T.; Costello, D.; Crowley, P.; Xing, L.; Hung, M.-C.; Bonfiglio, T.; Hicks, D. G.; Tang, P., The Expression Patterns of ER, PR, HER2, CK5/6, EGFR, Ki-67 and AR by Immunohistochemical Analysis in Breast Cancer Cell Lines. *Breast Cancer : Basic and Clinical Research* **2010,** *4*, 35-41.

63.   Lee-Hoeflich, S. T.; Crocker, L.; Yao, E.; Pham, T.; Munroe, X.; Hoeflich, K. P.; Sliwkowski, M. X.; Stern, H. M., A Central Role for HER3 in HER2-Amplified Breast Cancer: Implications for Targeted Therapy. *Cancer research* **2008,** *68* (14), 5878-5887.

64.   Gusterson, B., Do 'basal-like' breast cancers really exist? *Nat Rev Cancer* **2009,** *9* (2), 128-34.

65. Onitilo, A. A.; Engel, J. M.; Greenlee, R. T.; Mukesh, B. N., Breast Cancer Subtypes Based on ER/PR and Her2 Expression: Comparison of Clinicopathologic Features and Survival. *Clinical Medicine & Research* **2009,** *7* (1/2), 4-13.

66. Livasy, C. A.; Karaca, G.; Nanda, R.; Tretiakova, M. S.; Olopade, O. I.; Moore, D. T.; Perou, C. M., Phenotypic evaluation of the basal-like subtype of invasive breast carcinoma. *Mod Pathol* **2006,** *19* (2), 264-71.

67. Fulford, L. G.; Easton, D. F.; Reis-Filho, J. S.; Sofronis, A.; Gillett, C. E.; Lakhani, S. R.; Hanby, A., Specific morphological features predictive for the basal phenotype in grade 3 invasive ductal carcinoma of breast. *Histopathology* **2006,** *49* (1), 22-34.

68. Choo, J. R.; Nielsen, T. O., Biomarkers for Basal-like Breast Cancer. *Cancers* **2010,** *2* (2), 1040-1065.

69. Badve, S.; Dabbs, D. J.; Schnitt, S. J.; Baehner, F. L.; Decker, T.; Eusebi, V.; Fox, S. B.; Ichihara, S.; Jacquemier, J.; Lakhani, S. R.; Palacios, J.; Rakha, E. A.; Richardson, A. L.; Schmitt, F. C.; Tan, P.-H.; Tse, G. M.; Weigelt, B.; Ellis, I. O.; Reis-Filho, J. S., Basal-like and triple-negative breast cancers: a critical review with an emphasis on the implications for pathologists and oncologists. *Mod Pathol* **2011,** *24* (2), 157-167.

70. Albrand, G.; Terret, C., Early breast cancer in the elderly: assessment and management considerations. *Drugs & aging* **2008,** *25* (1), 35-45.

71. Baumann, C. K.; Castiglione-Gertsch, M., Estrogen Receptor Modulators and Down Regulators: Optimal Use in Postmenopausal Women With Breast Cancer. *Drugs* **2007,** *67* (16), 2335-2353.

72. Murray, M.; Hraiki, A.; Bebawy, M.; Pazderka, C.; Rawling, T., Anti-tumor activities of lipids and lipid analogues and their development as potential anticancer drugs. *Pharmacol Ther* **2015,** *150*, 109-28.

73. Cleator, S.; Heller, W.; Coombes, R. C., Triple-negative breast cancer: therapeutic options. *The Lancet Oncology* **2007,** *8* (3), 235-244.

74. Criscitiello, C.; Azim, J. H. A.; Schouten, P. C.; Linn, S. C.; Sotiriou, C., Understanding the biology of triple-negative breast cancer. *Annals of Oncology* **2012,** *23* (suppl_6), vi13-vi18.

75. Szakacs, G.; Paterson, J. K.; Ludwig, J. A.; Booth-Genthe, C.; Gottesman, M. M., Targeting multidrug resistance in cancer. *Nat Rev Drug Discov* **2006,** *5* (3), 219-234.

76. Society, A. C. Cancer in the twenty-first century. (accessed 14/07/2016).

77. Ritter, J. J.; Minieri, P. P., A New Reaction of Nitriles. I. Amides from Alkenes and Mononitriles1. *Journal of the American Chemical Society* **1948,** *70* (12), 4045-4048.

78. Ritter, J. J.; Kalish, J., A New Reaction of Nitriles. II. Synthesis of t-Carbinamines. *Journal of the American Chemical Society* **1948,** *70* (12), 4048-4050.

79. Plaut, H.; Ritter, J. J., A New Reaction of Nitriles. VI. Unsaturated Amides1. *Journal of the American Chemical Society* **1951,** *73* (9), 4076-4077.

80. Johnson, F.; Madronero, R., In *Advances in Heterocyclic Chemistry*, A.R. Katritzky and A.J. Boulton, Academic Press: New York, 1966; Vol. 6, p 95.

81. Krimen, L. I.; Cota, D. J., Ritter reaction. *Org. React.* **1969,** *17*, 213-325.

82. Beckwith, A. L. J., In *The Chemistry of Amides*, J. Zabicky, Interscience: London, **1970**; 73.

83. Bonnett, R., Imidoyl halides. *Carbon-Nitrogen Double Bonds (1970)* **1970**, 597-662.

84. Bishop, R., Ritter-type Reactions. In *Comprehensive Organic Synthesis - Selectivity, Strategy and Efficiency in Modern Organic Chemistry, Volumes 1 - 9*, Trost, B. M.; Fleming, I., Eds. E. Winterfeldt, pergamon: Oxford, **1991**; Vol. 6, 261.

85. Meyers, A. I.; Sircar, J. C., In *The Chemistry of the Cyano Group*, Z. Rappoport: Interscience, New York, **1970**; 341.

86.   Ung, A. T.; Bishop, R.; Craig, D. C.; Scudder, M. L.; Yunus, J., Ritter reactions. VII. Diverse reactivity of the 3-azatricyclo[5.3.1.0^{4,9}]undec-2-ene system with dimethyl acetylenedicarboxylate. *Aust. J. Chem.* **1992,** *45* (3), 553-65.

87.   Pich, K. C.; Bishop, R.; Craig, D. C.; Scudder, M. L., Ritter reactions. IX. Transannular addition of nitriles to the 5H-dibenzo[a,d]cycloheptene ring system. *Aust. J. Chem.* **1994,** *47* (5), 837-51.

88.   Djaidi, D.; Bishop, R.; Craig, D. C.; Scudder, M. L., Ritter reactions. X. Structure of a new multicyclic amide-benzene inclusion compound. *J. Inclusion Phenom. Mol. Recognit. Chem.* **1995,** *20* (4), 363-72.

89.   Djaidi, D.; Bishop, R.; Craig, D. C.; Scudder, M. L., Ritter reactions. Part 11. The diverse reactivity of 5,10-(azenometheno)-5H-dibenzo[a,d]cyclohepten-11-yl amides with dimethyl acetylenedicarboxylate. *J. Chem. Soc., Perkin Trans. 1* **1996,** (15), 1859-1866.

90.   Lin, Q.; Ball, G. E.; Bishop, R., Ritter reactions. XII. Reappraisal of the reactivity of methyl Schiff bases with dimethyl acetylenedicarboxylate. *Tetrahedron* **1997,** *53* (31), 10899-10910.

91.   Greaves, P. M.; Landor, P. D.; Landor, S. R.; Odyek, O., Allenic amides by hydration of allenic nitriles with alkaline hydrogen peroxide and by a hitter reaction. *Tetrahedron Letters* **1973,** *14* (3), 209-210.

92.   Sasaki, T.; Eguchi, S.; Shoji, K., The chemistry of cyanoacetylenes. Part I. Reactions of nitrilium ions conjugated with acetylene. *Journal of the Chemical Society C: Organic* **1969,** (3), 406-408.

93.   Al Djaidi, D. S. Studies in Multicyclic Chemistry. The University of New South Wales, **2006**.

94.   Holmes, R. L.; Moreau, J. P.; Sumrell, G., Application of the ritter reaction to petroselinic acid. *J Am Oil Chem Soc* **1965,** *42* (11), 922-923.

95.   Roe, E. T.; Swern, D., Fatty Acid Amides. VI.2 Preparation of Substituted Amidostearic Acids by Addition of Nitriles to Oleic Acid3. *Journal of the American Chemical Society* **1953,** *75* (22), 5479-5481.

96.   Norell, J. R., Organic reactions in liquid hydrogen fluoride. I. Synthetic aspects of the Ritter reaction in hydrogen fluoride. *The Journal of Organic Chemistry* **1970,** *35* (5), 1611-1618.

97.   Magat, E. E.; Faris, B. F.; Reith, J. E.; Salisbury, L. F., Acid-catalyzed Reactions of Nitriles. I. The Reaction of Nitriles with Formaldehyde1. *Journal of the American Chemical Society* **1951,** *73* (3), 1028-1031.

98.   Christol, H.; Solladie, G., *Bull. Soc. Chim. Fr* **1995**, (10), 1299.

99.   Glikmans, G.; Torck, B.; Hellin, M.; Coussement, F., *Bull. Soc. Chim. Fr* **1966**, 1376.

100.   The Communications To The Editor. *The Journal of Organic Chemistry* **1963,** *28* (1), 278-280.

101.   Bacon, R. G. R.; Kochling, J., 1074. Preparation and decomposition of triphenylmethyl formate. *Journal of the Chemical Society (Resumed)* **1964**, 5609-5613.

102.   Magat, E. E.; Salisbury, L. F., Acid-catalyzed Reactions of Nitriles. III. The Reaction of Nitriles with N-Methylolamides. *Journal of the American Chemical Society* **1951,** *73* (3), 1035-1037.

103.   Ritter, J. J.; Murphy, F. X., N-Acyl-phenethylamines, and a new isoquinoline synthesis. *J. Am. Chem. Soc.* **1952,** *74*, 763-5.

104.   Sasaki, T.; Eguchi, S.; Ishii, T., Reactions of isoprenoids. IX. Ritter reaction of 5,5-dimethyl-1-vinylbicyclo[2.1.1]hexane. *The Journal of Organic Chemistry* **1970,** *35* (7), 2257-2263.

105.   Meerwein, H.; Laasch, P.; Mersch, R.; Nentwig, J., *Chem. Ber* **1956,** *89*, 224.

106.   Stephen R. Bolsover, J. S. H., Elizabeth A. Shephard, Hugh A. White, Claudia G. Wiedemann, *Cell Biology: A Short Course, 2nd Edition*. **2004**; 552.

107.   GM., C., *The Cell: A Molecular Approach. 2nd edition.* **2000**.

108.   Reamer, R. A.; Brenner, D. G.; Shepard, K. L., Imino-bridged heterocycles. VI . An unusual bridge structure resulting from an attempted ritter reaction in the benzo[5,6]cyclohepta[1,2-c]pyridine system. *Journal of Heterocyclic Chemistry* **1986,** *23* (3), 961-962.

109.   Lamanec, T. R.; Bender, D. R.; DeMarco, A. M.; Karady, S.; Reamer, R. A.; Weinstock, L. M., .alpha.-Effect nucleophiles: a novel and convenient method for the synthesis of dibenzo[a,d]cycloheptenimines. *The Journal of Organic Chemistry* **1988,** *53* (8), 1768-1774.

110.   Samaniego, W. N.; Baldessari, A.; Ponce, M. A.; Rodriguez, J. B.; Gros, E. G.; Caram, J. A.; Marschoff, C. M., Ritter reaction on terpenoids. III. Stereospecific preparation of bicyclic [3.3.1] substituted piperidines. *Tetrahedron Letters* **1994,** *35* (38), 6967-6970.

111.   Rodriguez, J. B.; Gros, E. G.; Caram, J. A.; Marschoff, C. M., Ritter reaction on terpenoids. IV. Remarkable tendency to produce 3-aza-bicyclo[3.3.1]non-2-ene systems from mono and sesquiterpenes. *Tetrahedron Letters* **1995,** *36* (43), 7825-7828.

112.   Hassner, A.; Morgan, T. K.; McLaughlin, A. R., Stereochemistry. 71. Transannular reactions of substituted bicyclo[3.3.1]nonane-3-endo-carbonitriles: synthesis of bifunctional 4-azahomoadamantanes. *The Journal of Organic Chemistry* **1979,** *44* (12), 1999-2004.

113.   Bishop, R.; Hawkins, S. C.; Ibana, I. C., Ritter reactions. 3. A simple entry into the 3-azatricyclo[5.3.1.0^{4,9}]undecane system. *J. Org. Chem.* **1988,** *53* (2), 427-30.

114. Bong, I. C. C.; Ung, A. T.; Craig, D. C.; Scudder, M. L.; Bishop, R., Ritter reactions. V. Further investigation of the 3-azatricyclo[5.3.1.0^{4,9}]undec-2-ene system. *Aust. J. Chem.* **1989,** *42* (11), 1929-37.

115. Ung, A. T.; Williams, S. G.; Angeloski, A.; Ashmore, J.; Kuzhiumparambil, U.; Bhadbhade, M.; Bishop, R., Formation of 3-azabicyclo[3.3.1]non-3-enes: imino amides vs. imino alkenes. *Monatsh Chem* **2014,** *145* (6), 983-992.

116. Ung, A. T.; West, A. N.; Phillips, M. J. A.; Williams, S. G., Synthesis of alkaloid-like compounds via the bridging Ritter reactions II. *Monatsh Chem* **2016**, 1-10.

117. Hemtasin, C.; Ung, A. T.; Kanokmedhakul, S.; Kanokmedhakul, K.; Bishop, R.; Satraruji, T.; Bishop, D., Synthesis of alkaloid-like compounds via the bridging Ritter reaction. *Monatsh. Chem.* **2012,** *143* (6), 955-963.

118. Bishop, R.; Landers, A., Photochemical Formation of [3, 3, 2] Propellanes from 1, 5-Dimethylenecycloalkanes. *Australian Journal of Chemistry* **1979,** *32* (12), 2675-2679.

119. Osyanin, V. A.; Ivleva, E. A.; Klimochkin, Y. N., 2-(2-hydroxyphenyl)-2-adamantanol in Ritter reaction. *Russian Journal of Organic Chemistry* **2011,** *47* (11), 1686-1689.

120. Smith, M. B.; March, J., *March's advanced organic chemistry: reactions, mechanisms, and structure*. John Wiley & Sons: **2007**.

121. Hemtasin, C.; Ung, A. T.; Kanokmedhakul, S.; Kanokmedhakul, K.; Bishop, R.; Satraruji, T.; Bishop, D., Synthesis of alkaloid-like compounds via the bridging Ritter reaction. *Monatsh Chem* **2012,** *143* (6), 955-963.

122. Acheson, R. M., Reactions of acetylenecarboxylic acids and their esters with nitrogen-containing heterocyclic compounds. *Advan. Heterocyclic Chem. (A. R. Katritzky, editor. Academic Press, New York, N.Y.)* **1963,** *1*, 125-65.

123. Acheson, R. M.; Elmore, N. F., Reactions of acetylenecarboxylic esters with nitrogen-containing heterocycles. *Adv. Heterocycl. Chem.* **1978,** *23*, 263-482.

124. Govindachari, T. R.; Chinnasamy, P.; Rajeswari, S.; Chandrasekaran, S.; Premila, M. S.; Natarajan, S.; Nagarajan, K.; Pai, B. R., Some recent work on Schiff bases, imines and iminium salts in synthetic heterocyclic chemistry - a review. *Heterocycles* **1984,** *22* (3), 585-655.

125. Murphy, S.; Taylor, W.; Vadasz, A., The reactions of aromatic Schiff bases with dimethyl acetylenedicarboxylate. I. Reaction in an organic solvent. *Australian Journal of Chemistry* **1982,** *35* (6), 1215-1225.

126. Taylor, W.; Vadasz, A., The reactions of aromatic Schiff bases with dimethyl acetylenedicarboxylate. II. Reaction in the presence of water. *Australian Journal of Chemistry* **1982,** *35* (6), 1227-1230.

127. Roth, R. J.; Acton, N., A facile semisynthesis of the antimalarial drug Qinghaosu. *Journal of Chemical Education* **1991,** *68* (7), 612.

128. Delpech, B.; Qui, K. H., Convenient two-step synthesis of substituted 1-azaadamantanes from. alpha.-pinene. *The Journal of Organic Chemistry* **1978,** *43* (25), 4898-4900.

129. Stevens, R. V.; Kenney, P. M., Studies on the stereochemistry of nucleophilic additions to tetrahydropyridinium salts. Expeditious stereospecific total syntheses of (+)-makomakine, (+)-aristoteline, and (+/-)-hobartine. *Journal of the Chemical Society, Chemical Communications* **1983,** (7), 384-386.

130. Kikelj, D.; Kidrič, J.; Pristovšek, P.; Pečar, S.; Urleb, U.; Krbavčič, A.; Hönig, H., Preparation of diastereomerically pure immunologically active carbocyclic nor-muramyldipeptide analogues. *Tetrahedron* **1992,** *48* (28), 5915-5932.

131. Matsumura, T.; Akiba, M.; Arai, S.; Nakagawa, M.; Nishida, A., Synthetic study of manzamine B: synthesis of the tricyclic central core by an asymmetric Diels–Alder and RCM strategy. *Tetrahedron Letters* **2007,** *48* (7), 1265-1268.

132. Cohen, N. C.; Blaney, J. M.; Humblet, C.; Gund, P.; Barry, D. C., Molecular modeling software and methods for medicinal chemistry. *Journal of medicinal chemistry* **1990,** *33* (3), 883-894.

133. Bickerton, G. R.; Paolini, G. V.; Besnard, J.; Muresan, S.; Hopkins, A. L., Quantifying the chemical beauty of drugs. *Nat Chem* **2012,** *4* (2), 90-98.

134. Kolb, V. M., Biomimicry as a basis for drug discovery. *Progress in drug research. Fortschritte der Arzneimittelforschung. Progres des recherches pharmaceutiques* **1998,** *51*, 185-217.

135. Aebi, A.; Barton, D. H. R.; Burgstahler, A. W.; Lindsey, A. S., Sesquiterpenoids. Part V. The stereochemistry of the tricyclic derivatives of caryophyllene. *Journal of the Chemical Society (Resumed)* **1954,** 4659-4665.

136. Lutz, A. W.; Reid, E. B., Clovene and [small beta]-caryophyllene alcohol. *Journal of the Chemical Society (Resumed)* **1954,** 2265-2274.

137. Barton, D. H. R.; Nickon, A., Sesquiterpenoids. Part VI. The absolute configuration of caryophyllene. *Journal of the Chemical Society (Resumed)* **1954,** 4665-4669.

138. Corey, E. J.; Mitra, R. B.; Uda, H., Total Synthesis of d,l-Caryophyllene and d,l-Isocaryophyllene. *Journal of the American Chemical Society* **1964,** *86* (3), 485-492.

139. Barton, D. H. R.; Lindsey, A. S., 663. Sesquiterpenoids. Part I. Evidence for a nine-membered ring in caryophyllene. *Journal of the Chemical Society (Resumed)* **1951**, 2988-2991.

140. Aebi, A.; Barton, D. H. R.; Lindsey, A. S., 622. Sesquiterpenoids. Part III. The stereochemistry of caryophyllene. *Journal of the Chemical Society (Resumed)* **1953**, 3124-3129.

141. Suginome, H.; Kondoh, T.; Gogonea, C.; Singh, V.; Goto, H.; Osawa, E., Photoinduced molecular transformations. Part 155. General synthesis of macrocyclic ketones based

on a ring expansion involving a selective scission of alkoxyl radicals, its application to a new synthesis of (+/-)-isocaryophyllene and (+/-)-caryophyllene, and a conformational analysis of the two sesquiterpenes and the radical intermediate in the synthesis by MM3 calculations. *Journal of the Chemical Society, Perkin Transactions 1* **1995,** (1), 69-81.

142. Bertrand, M.; Gras, J. L., Synthese totale du (+)-isocaryophyllene. *Tetrahedron* **1974,** *30* (6), 793-796.

143. Mc Murry, J. E.; Miller, D. D., Synthesis of isocaryophyllene by titanium-induced keto ester cyclization. *Tetrahedron Letters* **1983,** *24* (18), 1885-1888.

144. Ohtsuka, Y.; Niitsuma, S.; Tadokoro, H.; Hayashi, T.; Oishi, T., Medium-ring ketone synthesis. Total syntheses of (+)-isocaryophyllene and (+)-caryophyllene. *The Journal of Organic Chemistry* **1984,** *49* (13), 2326-2332.

145. Legault, J.; Pichette, A., Potentiating effect of beta-caryophyllene on anticancer activity of alpha-humulene, isocaryophyllene and paclitaxel. *The Journal of pharmacy and pharmacology* **2007,** *59* (12), 1643-7.

146. Fitjer, L.; Malich, A.; Paschke, C.; Kluge, S.; Gerke, R.; Rissom, B.; Weiser, J.; Noltemeyer, M., Rearrangement of (-)-.beta.-Caryophyllene. A Product Analysis and Force Field Study. *Journal of the American Chemical Society* **1995,** *117* (36), 9180-9189.

147. Kazuo, Y.; Yoshio, H., The Sesquiterpenes of Ginseng. *Bulletin of the Chemical Society of Japan* **1975,** *48* (7), 2078-2080.

148. Gollnick, K.; Schade, G.; Cameron, A. F.; Hannaway, C.; Robertson, J. M., The structure of a hydrocarbon, 2,6,10,10-tetramethyltricyclo[7,2,0,02,7]undec-5-ene, obtained from caryophyllene dihydrochloride: X-ray analysis of the dibromo-

derivative. *Journal of the Chemical Society D: Chemical Communications* **1971,** (1), 46-46.

149.   Henderson, G. G.; McCrone, R. O. O.; Robertson, J. M., CLXXVIII.-The chemistry of the caryophyllene series. Part II. Clovene and isoclovene. *Journal of the Chemical Society (Resumed)* **1929**, 1368-1372.

150.   G. Collado, I.; R. Hanson, J.; J. Macias-Sanchez, A., Recent advances in the chemistry of caryophyllene. *Natural Product Reports* **1998,** *15* (2), 187-204.

151.   Yarovaya, O.; Korchagina, D.; Rybalova, T.; Gatilov, Y.; Polovinka, M.; Barkhash, V., Reactions of caryophyllene, isocaryophyllene, and their epoxy derivatives with acetonitrile under ritter reaction conditions. *Russian Journal of Organic Chemistry* **2004,** *40* (11), 1593-1598.

152.   Fomenko, V. V.; Korchagina, D. V.; Salakhutdinov, N. F.; Barkhash, V. A., Alkylation of Phenols by Caryophyllene on Acid Aluminosilicate Catalysts. *Helvetica Chimica Acta* **2001,** *84* (11), 3477-3487.

153.   Yarovaya, O. I.; Korchagina, D. V.; Salomatina, O. V.; Polovinka, M. P.; Barkhash, V. A., Acid-Catalyzed Reactions of 2,3-Epoxy Derivatives of Citral with Alcohols. *Russian Journal of Organic Chemistry* **2003,** *39* (7), 985-991.

154.   Volcho, K. P.; Yarovaya, O. I.; Kurbakova, S. Y.; Korchagina, D. V.; Barkhash, V. A.; Salakhutdinov, N. F., Synthesis of epoxy dinitriles from citral and their acid-catalyzed transformations. *Russian Journal of Organic Chemistry* **2007,** *43* (4), 511-517.

155.   Salomatina, O. V.; Yarovaya, O. I.; Korchagina, D. V.; Gatilov, Y. V.; Barkhash, V. A., Acid-catalyzed transformations of diepoxy derivatives of terpinolene. *Russian Journal of Organic Chemistry* **2011,** *47* (10), 1479-1486.

156. Boyd, G. V., 4.18 - Oxazoles and their Benzo Derivatives A2 - Katritzky, Alan R. In *Comprehensive Heterocyclic Chemistry*, Rees, C. W., Ed. Pergamon: Oxford, **1984**; 177-233.

157. Yarovaya, O. I.; Korchagina, D. V.; Salomatina, O. V.; Polovinka, M. P.; Barkhash, V. A., Synthesis of heterocyclic compounds in acid-catalysed reactions of citral epoxides. *Mendeleev Communications* **2003,** *13* (1), 27-28.

158. Nisnevich, G.; Korchagina, D.; Makalskii, V.; Dubovenko, Z. V.; Barkhash, V., Molecular-rearrangements of 4,5-epoxides of caryophyllene and isocaryophyllene in superacidic media. Zhurnal Organicheskoi Khimi **1993,** *29* (3), 524-541.

159. Guillena, G.; J. Ramón, D.; Yus, M., Hydrogen Autotransfer in the N-Alkylation of Amines and Related Compounds using Alcohols and Amines as Electrophiles. *Chemical Reviews* **2010,** *110* (3), 1611-1641.

160. National Cancer Institute, B. M., USA: Developmental Therapeutics Program.

161. Stack, V. T., Toxicity of α,β-Unsaturated Carbonyl Compounds to Microorganisms. *Industrial & Engineering Chemistry* **1957,** *49* (5), 913-917.

162. Schultz, T. W.; Yarbrough, J. W., Trends in structure-toxicity relationships for carbonyl-containing alpha,beta-unsaturated compounds. *SAR and QSAR in environmental research* **2004,** *15* (2), 139-46.

163. Elmore, S., Apoptosis: a review of programmed cell death. *Toxicol Pathol* **2007,** *35* (4), 495-516.

164. National Cancer Institute, Division of Cancer Treatment and Diagnosis. https://dtp.cancer.gov/discovery_development/nci-60/methodology.htm (accessed 10/03/2017).

165. Bioassay Laboratory, National Center for Genetic Engineering and Biotechnology (BIOTEC), 113 Thailand Science Park, Phahonyothin Road, Khlong Nueng, Khlong

Luang, Pathum Thani 12120 THAILAND

http://www.biotec.or.th/bioassay/index.php/bioassay-service (accessed 10/03/2017).

166.   O'Brien, J.; Wilson, I.; Orton, T.; Pognan, F., Investigation of the Alamar Blue (resazurin) fluorescent dye for the assessment of mammalian cell cytotoxicity. *Eur J Biochem* **2000,** *267* (17), 5421-6.